MACHINE VISION BASED GRAIN HANDLING SYSTEM

A Thesis

Submitted to the Faculty of Graduate Studies

The University of Manitoba

in partial fulfilment of the requirements for the degree of

Doctor of Philosophy

by

Neeraj Singh Visen

Department of Bisosytems Engineering

University of Manitoba

Winnipeg, Canada

R3T 5V6

0-612-79907-7

THE UNIVERSITY OF MANITOBA

FACULTY OF GRADUATE STUDIES

*****

COPYRIGHT PERMISSION PAGE

MACHINE VISION BASED GRAIN HANDLING SYSTEM

BY

NEERAJ SINGH VISEN

A Thesis/Practicum submitted to the Faculty of Graduate Studies of The University

of Manitoba in partial fulfillment of the requirements of the degree

of

Doctor of Philosophy

ABSTRACT

A line scan and an area scan cameras were used to acquire images of five grain types namely barley, Canada Western Amber Durum (CWAD) wheat, Canada Western Red Spring (CWRS) wheat, oats, and rye from across the various growing regions in the Western Canadian prairies. Images were acquired by placing individual kernels in a non-touching manner in the camera's field of view and by packing them as a bulk sample in a petri dish. Software was developed using C++ on the windows platform to analyze images and extract 51 morphological, 123 color, and 56 textural features. Grain identification was tried using images of individual and bulk kernels.

Classification of individual kernels was done using morphological, color, textural, and all the features combined together, whereas, for bulk samples, classification was tried using color, textural, and both the features combined. The top 20 features from each of morphological, color, and textural sets were selected and classification was carried out using the combined 60. Using the top 10 features of each set, classification was carried out using the combined 30 features. Three types of classifiers, namely back propagation network, non-parametric, and specialist probabilistic neural network, were used for classification purposes. An mean classification accuracy of 96.9, 94.3, 95, and 95.5% were obtained for individual kernel images when the top 20 morphological, color, and textural features were used for grain classification using the back propagation network (BPN), non-parametric, specialist probabilistic neural network (SPNN), and modified SPNN classifiers, respectively. For bulk sample images, classification accuracies close to 100% were obtained using top 20 color and top 20 textural features.

A dual conveyor belt system was designed and fabricated to present the grain samples to the line scan camera in a non-touching manner on a continuous basis. A vibratory hopper was used to feed the grain to the primary conveyor belt. Use of the vibratory hopper and differential belt speed resulted in over 93% instances of single kernels. A comparison of seven size features extracted from images of single grain kernels obtained from area and line scan cameras revealed that there was no variability in size features.

ACKNOWLEDGMENTS

I take this opportunity to sincerely thank my advisor, Dr. D.S. Jayas, whose guidance, encouragement, and affection has had a major influence throughout my research. His positive attitude and words of comfort always inspired me to go further. I don't have enough words to thank him.

I'm grateful to Dr. N.D.G. White, Dr. S.J. Symons, and Dr. B.L. Dronzek for their valuable suggestions and for serving on my advisory committee.

I'm thankful to Messrs. Dale Bourns, Jerry Woods, Matt McDonald, and Jack Putnam who helped me with experimental ideas and who saw the project through to completion.

This project was funded by the Natural Sciences and Engineering Research Council of Canada (NSERC). I wish to thank NSERC and University of Manitoba Graduate Fellowship for financial support. I am grateful to the Industry Services Division of the Canadian Grain Commission for their assistance in sample acquisition. I would like to thank Li Wang, Jitendra Paliwal, and Chitra Karunakaran, for their assistance in alggorithm development.

Finally, I lack words of gratitude for my parents, my wife Preeti, and my son Neelansh, whose love and affection have always been with me. Their sacrifices are invaluable. The love and care of my sisters and their families has always been my strength.

TABLE OF CONTENTS

LIST OF TABLES

LIST OF FIGURES

LIST OF SYMBOLS

AC	Alternating Current
ASC	Area Scan Camera
BPN	Back Propagation Network
CCU	Camera Control Unit
CPS	Canada Prairie Spring
CWAD	Canada Western Amber Durum
CWRS	Canada Western Red Spring
DCF	Digitizer Configuration Files
FOV	Field of View
GLCM	Gray Level Co-occurrence Matrix
GLRM	Gray Level Run-length Matrix
GRNN	General Regression Neural Network
HRS	Hard Red Spring
HRW	Hard Red Winter
LSC	Line Scan Camera
LVQ	Learning Vector Quantization
MVS	Machine Vision Systems
PC	Personal Computer
PNN	Probabilistic Neural Network
SAS	Statistical Analysis System
SPNN	Specialist Probabilistic Neural Network
SWS	Soft White Spring
SWW	Soft White Winter

1. INTRODUCTION

Canada is one of the leading grain producing countries in the world. The agricultural sector of Canada contributes 3% to gross domestic product and employs nearly 2 million people. It occupies about 7% of Canada's land area of which the prairie provinces of Alberta, Saskatchewan, and Manitoba account for 80 percent of total farmland (Canada Grains Council 1994). The soil conditions and short growing season make Canadian farmland suitable for growing high quality red spring wheat, durum, barley, canola, and flaxseed. The total grain and oil seeds production exceeds 55 million tonnes per year (Canada Grains Council 1994). About 30% of these grains are distributed in the domestic market, whereas the rest is exported through a grain collection and distribution system. Typically, grain is delivered to primary elevators (grain handling facilities) in farm trucks from where it is transferred by railcars to terminal elevators for export, mainly by ships. Before the grain can be exported, it undergoes a number of handling operations. In the first step, the grain is received at the terminal elevator where the railcars are inspected for the contents and then emptied into a receiving pit and moved to specific receiving bins. The grain samples from the receiving pits are inspected for test weight, varietal purity, soundness, foreign material, insect infestation, and vitreousness by grain inspectors and graded accordingly (Luo et al. 1999a). The grain is then cleaned and binned before loading into ships for export.

During grain handling operations, information on grain type and grain quality is required at all the stages before the next course of operation can be determined and performed. In the present system, grain type and quality is rapidly assessed by visual inspection. This evaluation process is, however, subjective and is limited by experience and expertise of the individual inspector. The decision making capabilities of a grain inspector can be seriously affected by his physical condition such as fatigue and eyesight; mental state caused by biases and work pressure; and working conditions such as improper lighting, climate, etc.

For efficient functioning of any grain handling system, fast and accurate flow of information is essential. Machine vision systems (MVS) serve as an effective alternative to the existing system of manual monitoring of grain samples at every step. Machine vision system refers to an automated system comprised of cameras/image sensors and microcomputers to perform routine tasks supplementing the human eye and brain. Machine vision systems have been successfully tested and implemented in various industries for tasks such as detecting, measuring, grading, sorting, counting, and packaging objects based on certain pre-defined criteria. Availability of cheap and fast dedicated hardware has enabled real-time processing using MVS, thereby making them compatible with other automated tasks in an industrial setup to work round the clock with little or no human intervention. Use of MVS in the agri-food industry is limited but there are several possibilities in a grain handling facility where such systems can be used.

An MVS can be installed in the receiving yard of a terminal elevator where it is necessary to rapidly identify the contents of the rail car so that grain is identified before unloading in the receiving pit and moved to an appropriate receiving bin. Such a system can work in conjunction with a robotic arm (to unlock and lock the rail cars and hopper openings) and a sampling system (to collect the grain sample and present it to the MVS) to fully automate the process of identifying the contents of the rail car by grain type. This information can then be relayed to the train engine to position the rail car to the receiving pit for unloading. Since a rail car consists of just one grain type, any MVS with classification accuracy higher than 80% can serve the purpose.

Another potential application of MVS is in identification of grain type, dockage, and foreign materials for grain grading and cleaning operations. Such a system can be used to collect information of grain type to decide the type of cleaning device and operating parameters such as rate of grain flow and speed of the cleaner. The information of grain purity, before and after it goes through cleaning operations, can be used to provide feedback to grain cleaners to make necessary modifications to improve the throughput and increase the recovery of salvageable grain.

The application of machine vision to determine the quality of grain has a considerable potential to increase the global competitiveness of Canadian grain because it can make the quality of export grain more consistent and reliable. At the terminal elevator, MVS can be employed to monitor the quality of grain during the blending operations while it is loaded on ships for export. If the grain does not meet buyers' specifications, it can be mixed with under-cleaned or over-cleaned grain, as the case may be, to bring the grain quality as close as possible to the tolerance limit.

To make any technology commercially viable or acceptable for industrial use, it is important that it is fast, efficient, reliable, uncomplicated, widely applicable and easily upgradable. Merely fast acquisition and processing of images would not be sufficient unless it was backed by efficient algorithms that work on optimized features for identification of grain kernels. It is also important to design a system that is uncomplicated and can be operated by a user of average intellect. Since most of the industrial units deal with a wide range of products of varying shapes, sizes, and visual features, it becomes imperative to develop a system that can handle all the items. Neural network based pattern recognition techniques can be used for grain identification as they have potential for solving problems where some inputs and corresponding output values are known but the relationship between the inputs and outputs is not well understood (Luo et al.1999b). Such networks can simultaneously handle large number of input features and output patterns, and can approximate the *a posteriori* distribution of patterns during training through learning and adaptation. Since computer technology is changing at an unprecedented rate, it is necessary to design a system that is modular in nature so that individual components can be altered without affecting or having to modify the rest of the system.

A detailed literature search revealed that some work has been done in the field of grain identification using machine vision and application of neural networks for pattern recognition. From the discussion with industrial sources and after keeping the above mentioned design considerations in mind, a research project was conceived at Department of Biosystems Engineering, University of Manitoba. The long term objectives of the research program were:

1. to develop a machine vision based system for rapid identification of grain types from images of bulk samples

2. to develop and optimize algorithms for qualitative and quantitative assessment of individual grain kernels from digital images for grain cleaning operations, and

3. to evaluate the potential of soft X-ray images for identification of low level of insect

infestations.

Given the vastness of the scope of the project, a team of graduate students was assigned to individual sub-tasks to achieve the overall objective. The objectives of my thesis were formulated to design a system that would meet the demands of the industry by integrating the available techniques with some novel solutions. For this research, the MVS was tested for functionality of individual units/components which can later be incorporated at the industrial level by designing dedicated hardware-based components. The main objectives of this thesis were to:

1. design a dual conveyor belt system to present physically separated grain samples to a line scan camera to identify samples of Canada Western Red Spring (CWRS) wheat, Canada Western Amber Durum (CWAD) wheat, barley, oats, and rye;
2. determine the textural and color features that can be used for rapid identification of different cereal grains from images of bulk samples;
3. develop and optimize algorithms for discrimination of various types of grains by extracting the morphological-, textural-, and color-based features using images of single kernels;
4. compare the morphological features obtained using the line scan and area scan cameras; and
5. investigate the performance of neural network and statistical classifiers for real-time identification of cereal grains in an industrial setup.

2. LITERATURE REVIEW

2.1 Background

Machine vision systems have found their way from scientific research to practical industrial applications because of advances in electronics and the computer industry. Its application can be found in broad areas of production, inspection, process guidance, and scientific research for newer technologies such as virtual reality. Commercial image analysis systems are already in use in industries such as automotive, manufacturing, processing, and electronics (Ballard and Brown 1982; Haralick and Shapiro 1992).

The application of machine vision technique to the grain industry is a recent development. Applying image processing techniques to the agri-food industry pose some special problems. The main obstacle in developing machine vision based systems for applications in the agri-food industry is the variations in size, shape, color, and texture of these biological entities (Tillet 1990, Kranzler 1985, Sarkar 1986). The initial efforts were made as early as 1980 to use image analysis systems in the agri-food industry to perform simple tasks such as inspecting and sorting (Shaw 1990). The early systems were comprised of low resolution (128 x 128 pixels) monochrome or binary image acquisition devices and used simple image processing techniques (Tillet 1991). Researchers have also focused on aspects other than algorithm development for machine vision. Such works include illumination systems for computer vision (Paulsen and McClure 1986; Brown and Timm 1992), camera arrangement and calibration (Humburg and Srinivasan 1994, Crowe et al. 1997), and automated sample presentation systems(Casady and Paulsen 1988, Jayas et al. 1999). Color image processing systems emerged in agri-food industry in the early 90s due to advances in solid-state color imaging sensors as well as availability of low-cost high-speed microcomputers.

2.2 Application of Machine Vision in the Agri-Food Industry

Machine vision systems have a great potential of application in the agri-food industry. A number of studies have been done to develop MVSs that can be implemented in an industrial setup for real- time applications. Several researchers (Barker et al. 1992a, 1992b, 1992c, 1992d; Crowe et al. 1997; Draper and Travis 1984; Keefe and Draper 1986, 1988; Lai et al. 1986; Majumdar et al. 1996, 1999, 2000a, 2000b, 2000c, 2000d; Myers and Edsall 1989; Neuman et al. 1987; Paliwal et al. 1999; Sapirstein and Bushuk 1989; Sapirstein et al. 1987; Symons and Fulcher 1988a, 1988b; Zayas et al. 1985, 1986, 1989) applied digital image analysis and pattern recognition to derive characteristics that can be used for objective grading of cereal grains.

Wigger et al. (1988) applied machine vision techniques to detect and classify fungal-damaged soybeans. Intensity and ratio of red to blue, red to green, and green to blue were taken as input features. They obtained over 98% accuracy in classifying individual healthy soybeans, however, those showing symptoms of infection were classified with 77 to 91% accuracy. An MVS was developed by Miller and Delwiche (1989) to inspect and grade peaches. Peach color was compared to standard peach maturity colors. The MVS classification accuracy was 54% in test samples and was within one color standard in 88% of the tests. Precetti and Krutz (1993a; 1993b; 1993c) developed a personal computer (PC)-based real-time MVS to perform corn husk deduction measurements. Corn to husk surface ratio was calculated by segmenting the images of corn cobs with husks into five different color classes, i.e., background, dried husk, green husk, red cob, and yellow kernels. The MVS measurements were within 1% variation, whereas manual measurements yielded a variation of approximately 4%.

The common image processing techniques used in the machine vision systems for the quality evaluation of agricultural products have been described by Karunanaran et al. (2002). Algorithms for extracting the size, shape, and color features, shape and color moments, Fourier descriptors, and textural features using co-occurrence and run length matrices for the color and gray scale images of objects were discussed in detail. A program was developed for extracting 230 features from color images for cereal grain classification and the accuracy of results was tested using user-defined images of known shapes, colors, and texture.

Algorithms were developed by Visen et al. (2001) to solve the problem of identification and segmentation of occluding groups of grain kernels in a grain sample image. The first algorithm characterized each object in a binary image of a grain sample as either an isolated kernel or a group of occluding kernels by determining the degree of overlap between each object in the input image and its inertial equivalent ellipse. If the degree of overlap was significant, the algorithm characterized the object as an isolated kernel. Otherwise, the algorithm marked the object as a group of touching kernels to be processed by the second algorithm. The second algorithm separated individual grain kernels in binary images of touching kernels. Segmentation lines between nodal points (points where the individual kernel boundaries intersect) were drawn by the algorithm. Nodal points were determined by evaluating the curvature along the boundary and selecting those points at which the curvature fell below a threshold. In situations where more than two nodal points were found, a 'nearest-neighbor criterion' was used to draw the segmentation lines. The algorithm performed with 99% reliability on images containing touching kernels of barley, HRS wheat, and rye. The reliability was considerably lower for images containing kernels with rough boundaries. The morphological features of segmented images were calculated and compared to the results from previous studies.

2.3 Classification Features

Most of the MVSs perform identification and classification tasks based on few input features and a classifier. The classifier is developed using some classification criterion based on input features. A number of researchers have tried various combinations of different input features and classification criterion to develop an MVS to meet their specific needs. Since biological products demonstrate natural variation in shape, size, and color, an MVS must be sufficiently flexible and robust to cope with this variability. A combination of morphological, color, textural (spatial distribution of color) features of the images can be used to develop a machine vision system. A detailed review of MVS systems in agriculture has been done by Jayas et al. (2000) and Karunakaran et al. (2002).

2.3.1 Morphological Features Application of image processing techniques using morphological features has been reported since the early 1970s. Shape of a grain kernel was first estimated by Segerlind and Weinberg (1972) using a Fourier series expansion of the radial distance from the centroid to the periphery of kernels. The image of a grain kernel was obtained by tracing the profile on a grid paper. The error in separation of oats from barley, and wheat from rye based on extracted shape features was 1%. The class (namely, hard red spring (HRS) wheat, hard red winter (HRW) wheat, amber durum, soft white spring (SWS) wheat, soft white winter (SWW) wheat, Canada prairie spring (CPS) wheat, and utility wheat) discrimination for wheat was partially successful with error ranging from 11 to 25%.

Using a recursive learning algorithm and pattern recognition techniques, Brogan and Edison (1974) were able to classify barley, wheat, oats, rye, soybeans, and corn with an overall accuracy of 98%. Pattern recognition alone, however, cannot be recommended for classifying agricultural products due to large annual and regional variability in a grain type and due to significant overlap in morphological features among different grain types.

Draper and Travis (1984) developed a low cost computer based system for analysis and recognition of shape of seed and vegetative structures. The images were acquired from reflected or transmitted light. Travis and Draper (1985) used this system for identification of seeds of cereal grains, fodder plants, and oil and fibre vegetables. They reported success in distinguishing most of the weed species from each other and crop species from their major contaminants.

Kernel morphology was used by Neuman et al. (1987) to objectively classify the Canadian wheat cultivars. Their sample consisted of 576 kernels (sound and uniform) of pedigreed seed of 14 wheat cultivars for analysis. The silhouette images of whole wheat kernels were captured in 'plan' (top) view using transmitted light to determine spatial size and shape parameters and Fourier descriptors of kernels. CWAD and HRS wheat kernels were most easily differentiated groups while there was considerable overlap between HRW and SWS wheat classes. Classification results for discriminating varieties within classes were inconclusive with correct classifications ranging from 15 to 96%.

Zayas et al. (1990) performed image analysis in conjunction with statistical pattern recognition techniques to discriminate whole corn from broken corn kernels. The classifier was developed using multivariate discriminant analysis. A total of 12 morphological features were used as input, of which, five were basic features and remaining seven were derived from them. After using different optical settings, they were able to achieve 100% classification for brokens and 98% for whole corn kernels. The shortcoming of the study was that it was carried out on 210 observations which is a very small sample size. The study needed to be conducted on more images including samples from varying growing locations and growing years.

Howarth et al. (1992) used machine vision to perform curvature analysis on images of carrots to estimate their tip shape. The curvature profile was developed using Freeman chain code. The curvature profile was then reduced using a non-linear least squares technique to six parameters which were used to describe the carrot tip. These parameters were used to develop a Bayesian classifier which separated carrot tips into five classes. When tested on 250 carrots, they achieved a classification accuracy of 86%. The researchers used an area scan camera to acquire images of carrots on the conveyor belt. The illumination consisted of two 200W incandescent lamps. Use of this system could introduce motion blur if the belt was moving at a fast speed and thus make a sharp tip to look blunt or even sharper depending on the orientation of carrot tip with respect to the direction of movement of the conveyor belt. To overcome this problem, a line scan camera or a strobe light with an area scan camera can be used.

A semi-automatic image analyzer was constructed by Keefe (1992) for classification of wheat grains. It determined 69 features for analysis, of which 33 features for each grain were obtained directly while the rest were derived parameters obtained using the 33 primary features. Most of the parameters used were not disclosed because of proprietary nature of research due to commercial interests. Twenty varieties of U.K. wheat were tested using the instrument. To acquire images, each kernel was placed manually in a fixed orientation. For a sample size of 50 grains, the total time taken from receiving the kernel to having the data ready for statistical analysis was approximately 5 min. The overall identification error was 32.9 to 65.8%.

Using features such as ray (i.e., radial distance from the centroid) parameters, slice and aspect ratio parameters, Fourier descriptors, and Chebychev coefficient for characterizing and discriminating among kernels of eight Australian wheat cultivars, Barker et al. (1992a, 1992b, 1992c, 1992d) obtained an overall classification error from 35 to 48%. Their method did not have any practical applicability because of the high error rate and the complex nature of the features used for classification.

Vooren et al. (1992) investigated the applicability of image analysis for variety testing of mushrooms (*Agaricus bisporus* (Lange) Imbach). Images of 230 mushrooms were recorded under controlled lighting conditions and image analysis techniques were used to increase the number of morphological characteristics that could be physically measured. The measurements of length, width, and a range of shape descriptors, determined by means of image analysis, were statistically analyzed. Image analysis exhibited a significant improvement over previous methods which used only manual assessments.

Applicability of machine vision for shape analysis in leaf and plant identification was investigated by Guyer et al. (1993) by combining the areas of feature extraction, pattern recognition and techniques of scene interpretation by humans. An algorithm was implemented to extract shape features using information gathered from critical points along object borders such as the location of angles along the border and local maxima and minima from the plant or leaf centroid. A total of 13 'high level' input features were calculated from 17 morphological features. The classifier was developed by creating two sets of rules using low level and high level features. Using a 40 image data set, they obtained a classification accuracy of 69%. The poor classification was a result of complex input features and classifiers. The classification technique is not suitable for practical application because it required adding more and more rules for specific cases to improve classification accuracy.

Simonton and Pease (1993) developed a technique to identify key features of ornamental cuttings and provided complete classification and interconnection of the major plant parts (e.g. main stem, petioles, and leaf blades). They segmented a plant image into objects which could then be classified according to geometric data. Their classification algorithm was independent of the orientation and relied exclusively on the morphological content of a binary image. A high average percentage of total image pixels (96.6%) were classified correctly in 80 sample images tested. However, sources of error for certain mis-classifications revealed limitations of this technique. Branching or fork-based segmentation left gaps in the geometric data required for satisfactory classification. Also, plant parts which overlapped or occluded other parts cause conflicting geometric data which resulted in classification errors. This problem can be resolved using morphological operators such as erosion and dilation to separate touching objects. Color features can also be used along with morphological features to improve classification accuracy.

A completely new set of grading factors was suggested by Sapirstein and Kohler (1995) to objectively grade wheat. This was based on variability of size, shape, and reflectance features of kernels in a sample. Such system could be easily administered by machine vision based grading. Export samples of CWRS wheat grades 1, 2, and 3 were successfully classified using the mean and variance of the features as quantitative classification variables. For incoming grain samples, however, only grades 1 and 3 could be successfully discriminated from each other.

Image processing techniques have been applied in fisheries for size and species grading of fish. Strachan and Nesvadba (1990) used three methods of discrimination: invariant moments, optimization of the mismatch, and shape descriptors and reported a classification accuracy of 73, 63, and 90%, respectively. The optimization process was computationally intensive and not feasible for commercial application. The other methods were faster and more accurate, however, and were tested on seven types of species only. Ying et al. (1996) developed algorithms to detect the orientation of a catfish and to identify its head, tail, pectoral, ventral, and dorsal fins. The algorithms were invariant to translation, rotation, and scaling. Edge detection and labeling and tracking algorithms were applied to locate the boundary of a catfish and a 2-stage, model-based, catfish segmentation algorithm was proposed to locate each part.

The feasibility of grading pistachio nuts into four grades of large, medium, small, and unsplit using a machine vision system was investigated by Ghazanfari et al. (1998). The silhouette images of individual pistachio nuts were analyzed and area and Fourier descriptors were calculated. Although a total of 15 harmonics were calculated, only seven harmonics were sufficient to separate split nuts from unsplit nuts. Of the seven selected Fourier descriptors, five were from the higher order harmonics which has information of subtle variations and is more suitable for separating unsplit from split nuts. Area was then used to grade them into large, medium, and small categories. An average classification accuracy of 87.1% was obtained for the four grades when using a decision-tree classifier, whereas neural network analysis resulted in a classification accuracy of 94.8%.

The length, width, area, and perimeter of 21 different grain types (cereals, oilseeds, pulse seeds, and speciality seeds), collected from several growing regions in Canada, were determined using machine vision (Paliwal et al. 1998). For each grain type, 100 kernels were selected randomly from a bulk sample and their color images were taken using an area scan camera. These images were converted into binary form and the physical properties were measured using a machine vision algorithm and compared to results from some of the studies done in the past.

2.3.2 Color Features Color is an important visual attribute of grain used in grain inspection and grading. The use of color increases the information content for grain image analysis. Degrading factors such as grass-green, fungal damage, bin-burnt, and mildewed can be expressed as discoloration. Maturity level and varietal differences for several grain types can be easily classified using color information. Most of the previous research, however, has been focused on using morphological features to characterize different grains and their varieties. Not much work has been done so far to design and calibrate illumination systems for color grain image analysis (Luo et al. 1997). The main reason behind this lack in research perhaps is that color information extracted from images is usually variable and unreliable due to the illumination variations that exist in common light sources. Color image processing requires sophisticated hardware and high computational power which can be a deterrent.

Neuman et al. (1989a, 1989b) developed a color digital image processing workstation to objectively evaluate the color of individual cereal grains and other objects identified within a digital image. Color attributes of cultivars belonging to different wheat classes were examined. The mean reflectance value of R, G, and B pixels was used to perform discriminant analysis. The average correct classification ranged from 34 to 90%. The classification accuracy could be increased by using a high resolution camera and incorporating textural features into the classifier.

Zhang et al. (1994) used color images for identification of wild buckwheat using neural network and statistical classifiers. The six color parameters used were made less sensitive to illumination by computing them as ratios of color intensities. They reported over 96% classification accuracy for training data and only 60% accuracy for testing data. They emphasized more on proper selection of training data to improve the classification accuracy, whereas this appears to be a case of overtraining of neural networks. The network possibly learned the training data and over-fitted the solution but failed to generalize when a sample from an independent data set was presented to it.

Patel et al. (1996) used a computer imaging system to detect egg defects using gray level images of grade A eggs, eggs with blood spots, and eggs with dirt stains. Histograms based on the number of pixels at each gray level intensity were generated from the images and used to train neural network models. The neural network models, when applied on an independent set, had a classification accuracy of 85.6 and 80.0% for detecting blood spots and dirt stains, respectively.

Color classification of french fries was done by Panigrahi and Marsh (1996) to classify a cooked french fry as light, normal, or dark. Image histograms were extracted in different color coordinates. Classification accuracy of 90 and 93.8% was achieved using BPN and learning vector quantization (LVQ) network, respectively. The complexity of LVQ network required further evaluation before any practical application.

A set of morphological and color features was used by Luo et al. (1999a, 1999b) to classify cereal grains from western Canadian growing regions. They used statistical and neural network based classifiers and obtained average classification accuracies of 99.0, 96.9, 98.2, 99.0, and 98.2 for barley, CWAD wheat, CWRS wheat, oats, and rye, respectively. The classification accuracies obtained by a combined model of morphological and color features were higher than those obtained by using just one feature set.

Shahin and Symons (1999) used a machine vision system for color classification of lentils using neural network and statistical classifiers. The statistical classifier was developed using linear discriminant analysis. The images were taken using a flat bed scanner and histogram based color segmentation was used to separate damaged (dark brown) and peeled (yellow) lentils. An overall prediction accuracy of 91 and 90% were obtained using linear discriminant analysis and neural networks, respectively. The system was very slow as is took 20 s to take an image and 3 s to analyze and classify. Such a system can not be used for online monitoring of grain samples. Moreover, the images were acquired by spreading lentils over a scanner bed which can result in scratches and accumulation of dust on the surface of the scanner.

El-Faki et al. (2000) used a color machine vision system to detect weeds using color features. The classifier was based on the differences in color of the stems of weeds and the desired crop. Low sensitivity of color features to canopy overlap, leaf orientation, camera focusing, and wind effects made it a more practical choice over morphology and texture based methods. Using discriminant analysis, they obtained a classification accuracy of 54.9 and 62.2% for soyabean and wheat, respectively. They found the statistical classifier to outperform the neural network classifier.

2.3.3 Textural Features Texture is an important characteristic for the analysis of many types of images. Although it is present in almost all spatial images taken in different spectral ranges, a precise definition of texture does not exist. Texture is treated as an attribute representing the spatial arrangement of the gray levels of the pixels in a region. It is sometimes also defined as a descriptor providing a measure of properties such as smoothness, coarseness, and regularity (Gonzalez and Woods 1992). The term texture generally refers to repetition of basic texture elements called texels. The texel contains several pixels, whose placement could be periodic, quasi-periodic or random. Natural textures are generally random, whereas artificial textures are often deterministic or periodic. Texture may be coarse, fine, smooth, granulated, rippled, regular, irregular, or linear. It can be quantitatively described using co-occurrence and run length matrices. A number of researchers (Majumdar et al. 1996; Hayes and Han 1993; Al-Janobi and Kranzler 1994;

Sapirstein et al. 1994) have used textural features in machine vision and image processing related applications.

Wilhoit et al. (1990) investigated the feasibility of using a digital image processing system for selecting mature broccoli heads. Images were obtained under controlled lighting conditions of 48 broccoli plants with a wide range of head sizes. Images were used to develop and test a model based on the gray level run length method of textural analysis. The model exhibited an exponential relationship between head area and the numerical texture measure and had a standard error of head area prediction of ±10%. The results indicated that the model has good capability for classifying broccoli heads into immature and harvestable sizes.

Han and Hayes (1990) developed image classification algorithms using color information to estimate the percent soil cover. The color information was obtained using band-pass optical filters with a black-and-white imaging system. The optimum wavelength pair which best characterized the color difference between soil and crop canopy was 550 nm and 700 nm. Two classification algorithms, one with the linear discrimination method and the other with the nearest neighbor method, were compared with a manual, photographic grid method and a textural image classification method. Both algorithms measured percent soil cover quickly and accurately. The linear discrimination algorithm performed best in all aspects provided that the image is linearly separable in terms of color. The textural classification method was recommended when a color difference is not evident. They reported that their image classification algorithm was faster and more accurate than humans and did not require an expensive color imaging system, however, it had a minimum limit for spatial resolution.

Textural features along with neural networks were used by Murase et al. (1994) to monitor plant growth. Features such as contrast, homogeneity, and local homogeneity were extracted from video images of populations of growing plants and fed to a three layer neural network. The size of plant leaf was determined from the output of the network. They found that textural features of plants varied with their growth stage and that a neural network could be used to relate the varying textural features to the plant growth stage.

Langford et al. (1990) performed computerized identification of pollen grains by textural analysis. They used digitized images from a scanning electron microscope for 192 samples of exine texture covering one-tenth of the total pollen area. The textural features were calculated from co-occurrence matrix of gray levels and used as input to the classification program. The classifier was constructed using a linear discriminant function to find the optimum linear direction in multi-variate space to separate feature vectors from two classes. They achieved over 94% classification accuracy using a leave-one-out scheme and a variable selection procedure. The selection of a variable using stepdisc analysis and the use of other textural features such as run length matrix features may further increase the classification accuracy.

Shearer et al. (1994) developed a maturity classification algorithm for the analysis of line scan images of broccoli plants using a one dimensional co-occurrence texture analysis. Eleven texture features were derived from the normalized co-occurrence matrices. Discriminant analysis techniques were used to classify individual observations into one of the three groups, i.e., immature, mature, and over-mature. They tested classification accuracy for 480 observations from three broccoli cultivars using gray level images of size 512 by 512 pixels. Gray level reduction technique was used to reduce an 8 bit image to a 7 bit image through a 1 bit image. The maximum accuracies achieved were 90 and 83.1% for individual and multiple cultivars, respectively, at 64 gray levels. Since the co-occurrence matrix was developed using 0° and 180° directions only, the results were dependent on orientation of the object. To overcome this, the matrix would have been calculated for all the eight directions.

Majumdar et al. (1996) used different lens combinations to acquire images of barley, CWRS wheat, CWAD wheat, and rye at various resolutions and to classify the grain kernels based on textural analysis. They determined the gray level co-occurrence matrix (GLCM) and the gray level run length matrix (GLRM) for pixels in all directions. The features were extracted for R, G, and B bands, and different combinations of R, G, and B bands. They obtained a classification accuracy of over 96% for all grains using the red band only, and over 94% using a '3R+2G+1B' color band combination at 0.20 mm spatial resolution. This study was further extended by including oats and rye kernels into the grain set (Majumdar and Jayas 2000d). Using the 15 most significant features in the texture model, the classification accuracies of barley, CWAD wheat, CWRS wheat, oats, and rye were 100.0, 98.2, 85.2, 100.0, and 76.3%, respectively, when tested on an independent data set

2.4 Application of Multi-layer Neural Network Classifiers in MVS

Neural network classifiers have been successfully implemented for various quality inspection and grading tasks of different agricultural products. For a detailed review of literature on techniques of image analysis of agricultural products with reference to use of neural network classifiers for decision making, refer to the journal paper titled "Multi-layer Neural Networks for Image Analysis of Agricultural Products" by Jayas et al. (2000).

2.4.1 Evaluation of neural network architectures for cereal grain classification using morphological features This research was aimed at evaluating the most commonly used neural network architectures for cereal grain classification using the frequently used morphological features as inputs. An evaluation of the classification accuracy of nine different neural network architectures was done to classify five different kinds of cereal grains namely, HRS wheat, CWAD wheat, barley, oats, and rye. To evaluate the classification accuracy of the different neural network architectures, color images of 7500 kernels (1500 kernels of each grain type) were taken. For each kernel, eight morphological features namely, area, perimeter, length of major axis, length of minor axis, elongation, roundness, Feret diameter, and compactness were extracted and used as input to the neural networks. The networks were trained using 70% of the kernels and 20% of the kernels were used for validation of each grain type. Testing of the trained network was done on the remaining 10% of the kernels as well as the whole data set. The relative importance of the input features was also compared and the features that contributed the least to the classification, were eliminated to decrease the complexity of the networks. The best results were obtained using a 4-layer back-propagation network with each layer connected to an immediately previous layer. The classification accuracies were in excess of 97% for HRS wheat, CWAD wheat, and oats. The classification accuracies for barley and rye were about 88%. The network required only four input features namely, Feret diameter, area, minor axis length, and compactness for classification. A general-regression neural network architecture was found to be the least suitable for grain classification (Paliwal et al. 2001).

2.4.2 Specialist Neural Networks for Cereal Grain Classification It was hypothesized that robust specialist networks can be designed using a combination of simple networks having similar or different network architectures. To test this hypothesis, the classification accuracies of four simple network architectures (namely, back propagation network (BPN), Ward network, general regression neural network (GRNN), and probabilistic neural network (PNN)) were compared with the accuracies given by specialist networks. Each specialist network was designed using a combination of five simple networks, each specializing in classifying one grain type. The grain types used in this study were CWRS wheat, CWAD wheat, barley, oats, and rye. To evaluate the classification accuracy of the different neural network architectures, high resolution color images of 5000 kernels (1000 kernels of each grain type) were taken. For each kernel, eight morphological features (namely, area, perimeter, length of major axis, length of minor axis, elongation, roundness, Feret diameter, and compactness) and four color features (namely, mean, median, mode, and standard deviation of the gray level values of the objects in the image) were extracted and used as input to the neural networks. Best classification accuracies (98.7%, 99.3%, 96.7%, 98.4%, and 96.9% for barley, CWRS wheat, CWAD wheat, oats, and rye, respectively) were obtained using specialist PNN (Visen et al. 2002).

3. MATERIALS AND METHODS

3.1 Grain Samples

The grain samples used in this study were collected from six locations in Manitoba, 10 locations in Saskatchewan, and seven locations in Alberta. The Industry Services Division of the Canadian Grain Commission (Winnipeg, MB) provided the grain samples which were collected at terminal elevators from incoming railcars and from samples of graded grain being loaded into the ships for export. The choice of locations was based on climatic subdivisions of the Canadian Prairies (Putnam and Putnam 1970). The selected locations represent five sample locations from the humid prairie, five locations from the semi-arid region, six locations from the sub-humid prairie, and seven locations from the sub-boreal region (figure 3.1). Grain samples were collected for barley (20 locations), CWAD wheat (19 locations), CWRS wheat (22 locations), oats (16 locations), and rye (14 locations).

3.2 Sample Presentation Equipment

3.2.1. Area Scan Camera The grain samples were presented to the area scan camera in a non-touching manner using a pair of tweezers. The samples were manually put on a black non-reflective card and carefully arranged so that none of the kernels was fully or partially out of the field of view (FOV)of the camera.

3.2.2 Line Scan Camera For the purpose of presenting the grain samples in a non-touching manner to the line scan camera, a differential conveyor belt speed based sample presentation apparatus was designed and fabricated. Figure 3.2 shows the schematic design of the sample presentation system with the setup of a line scan camera.

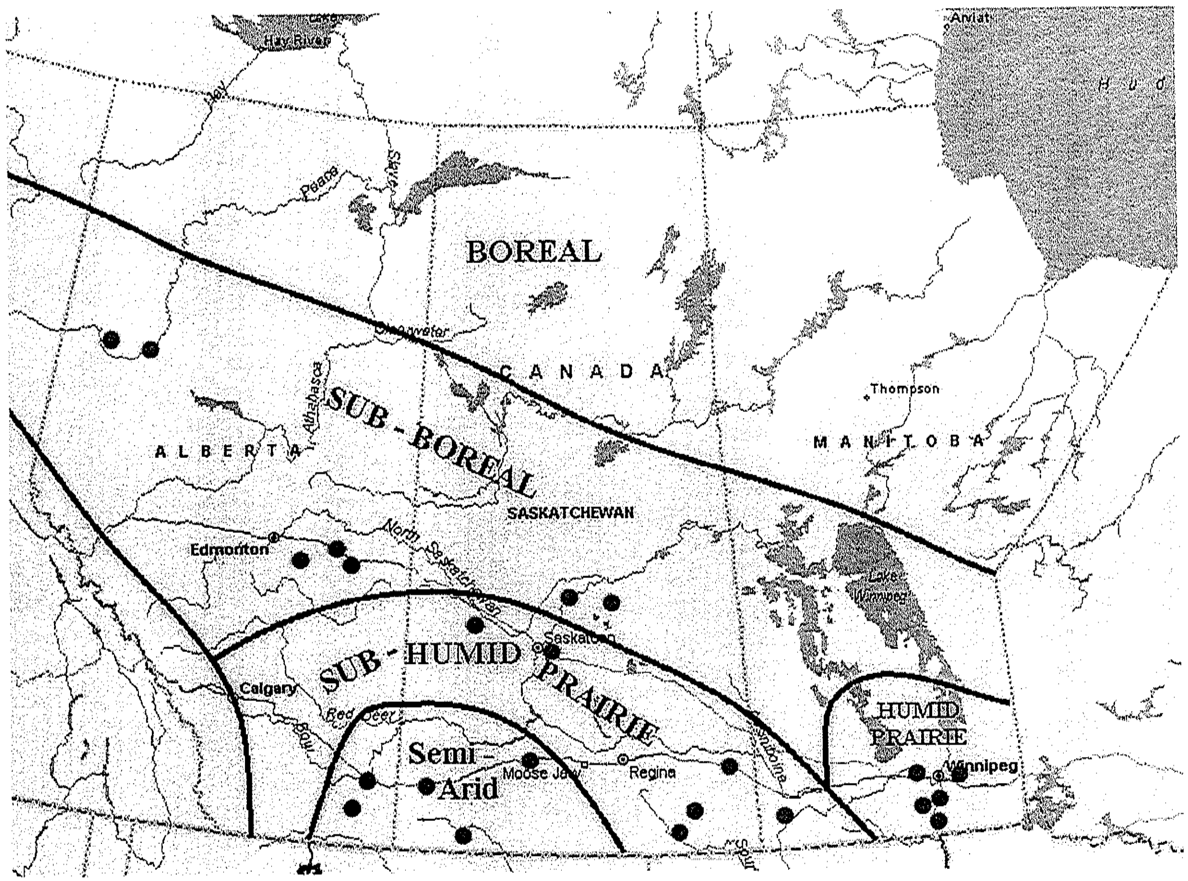

Figure 3.1 Various growing locations in Canadian prairies from where the grain samples were collected (Putnam and Putnam 1970).

Grain was dropped on to the feeder by gravity from the hopper at a rate of 60g/min (Crowe et al. 1997) from a height of 50 mm to obtain some separation at the time of dropping the grain kernels. The feeder was attached to a vibratory motor (15A, Eriez Manufacturing Co., Erie, PA) whose amplitude could be adjusted my changing the RPM from 1000 to 10 000 to achieve further separation of grain kernels.

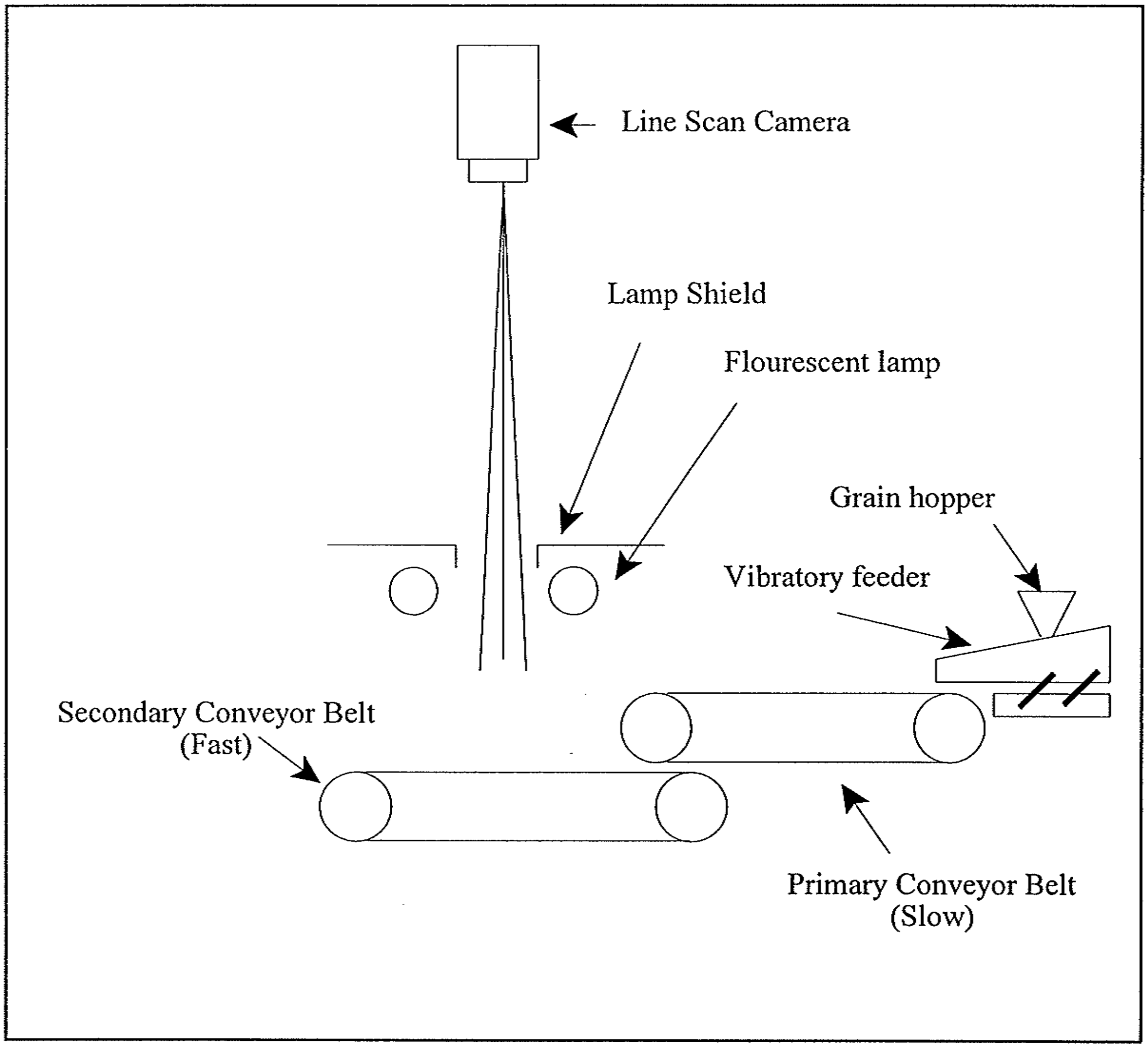

Figure 3.2 Schematic showing the line scan camera and conveyor belt.

The conveyor belts were driven by a 115 W motor (Robbins and Myers, Cheshire, CT). To guide the flow of grain kernels so that they drop on the primary conveyor belt, the feeder was inclined at an angle of 15 degrees from the horizontal. The grain then dropped from the primary belt on to the secondary belt which ran at double the speed of the primary belt. The differential speed resulted in separation of any leftover touching kernels.

3.3 Image Acquisition

For this research, two different types of image acquisition systems were used. An area scan camera (ASC) was used to take images of single grain kernels and bulk samples of different grain types. These images were used to form a database of extracted kernel features of different grain types. A line scan camera (LSC) was used for taking images of grain kernels moving on the conveyor belt. This system, in future, can be integrated with a hardware-based, image processing system for real time, online image acquisition and classification purposes. The results from images of bulk samples would assist in rapidly determining the grain type of a given sample whereas images of single kernels can further provide information about various qualitative and quantitative features of individual kernels in a given sample.

3.3.1. Illumination Standardization

Programs developed by Luo et al. (1999a) were used for illumination standardization and imaging system tuning. The illumination level was standardized using a Kodak white card with 90% reflectance (E152-7795, Eastman Kodak Co., Rochester, NY) as a white reference. The image of the white card was acquired over a small central area of 50 x 50 pixels, and the mean gray level values of the R, G, and B bands were computed and used as the illumination level indicators. The iris control of the camera was manually adjusted to perform white balance until all three values (R, G, and B) were 250 ± 1. The line scan camera had a hardware-based illumination standardization capability. Color calibration was done by first coring the lens to produce completely dark conditions followed by placing a Kodak white card in the field of view. The in-built calibration system adjusted the gains such that values of all the pixels from R, G, and B sensors were 250 ± 1.

3.3.2. Area scan camera

3.3.2.1 Hardware The hardware for ASC consists of a 3-chip CCD color camera (DXC-3000A, Sony, Japan) (Figure 3.3) with a zoom lens of 10-120 mm focal length (VCL-1012BY), close-up lens set (72 mm, Tiffen, Hauppauge, NY), a camera control unit (CCU-M3, Sony, Japan), a personal computer (PIII 450 MHz), color frame grabbing board (Matrox Meteor-II multi-channel, Matrox Electronic Systems Ltd., Montreal, PQ), and a diffuse illumination chamber. The camera control unit (CCU) provided optional controls and image enhancement features such as iris control, brightness, contrast, color balance, white balance, signal gain etc. The automatic gain control on CCU was disabled and camera was set to manual mode for focus and aperture settings. The camera was mounted over the illumination chamber on a copy stand (m3, Bencher Inc., Chicago, IL), which provided easy vertical movement to fine tune the position of the camera with respect to grain kernels. The 72 mm close-up lens was used to achieve a spatial resolution of 0.060mm/pixel in horizontal and vertical directions.

The imaging hardware was controlled using the Meteor Lite software which was installed on the PC. The NTSC composite color signal from the camera was converted by the camera control unit at a speed of 30 frames per s into three parallel analog RGB video signals and a sync signal. The signal was fed to the frame grabbing board using the multi-channel input connectors. The live video was displayed on the computer monitor and the frame was frozen, when desired, using the computer keyboard. The frame grabber installed in the PC digitized the RGB analog video signals of the frozen frame into three 8-bit 640 x 480 digital images. These three images were overlaid to display as a color image on the monitor and then saved in a tiff format image for storage and analysis.

3.3.2.2 Software The image acquisition was done using the Meteor Lite software library that was provided along with the frame grabber. Frame grabber settings for the meteor multi-channel boards are stored in so called digitizer configuration files (DCF). They can be created and edited using the Matrox Intellicam utility. The DCF file was created using the area scan camera specification (Appendix A.1) which included:

Norm of the input signal: The video norm determines the number of rows per frame, the number of frames per s, and the duration of the active portion of a video line.

H-Res Total: It gives the total number of pixels in the active portion of a video line, according to the video norm and the pixel clock setting. This number is relevant for determining the physical width of a pixel in the frame buffer.

V-Res Total: It gives the number of lines per frame according to the video norm of the input signal.

Pixel clock or sampling rate: It determines H-Res Total.

3.3.2.3 Light source Lighting is the critical component of all machine vision applications. Any study dealing with color and textural analysis would be futile unless a system that uniformly distributes light over the FOV is used to illuminate the objects to be imaged. For this study, in order to minimize the variation in the light intensity in the FOV, a semi-spherical bowl-shaped light diffuser of 390 mm diameter was used. The light diffuser was made of steel and the inner side of the bowl was painted white and smoked with magnesium oxide. A circular flourescent light source of 305 mm diameter, 32-W circular lamp (FC12T9/CW, Philips, Singapore) (Figure 3.4) with a rated voltage of 120 V was placed around the sample which was then covered with the bowl to reflect the light inwards. This method of lighting created a large area of uniform illumination which eliminated shadows and greatly minimizes the effects of specular reflections. Luo et al. (1997) evaluated several sources and methods of illumination and reported that this system was most stable with time. It was least sensitive to variations in voltage and produced uniform illumination over large FOV and hence recommended it to be used with the area scan camera.

The power supply to the light source was provided via a voltage regulator (CVS, Sola Canada Inc., Toronto, ON) rated at ±0.5 V to ensure a constant voltage throughout an imaging session, which generally lasted around 2 h at a time. The overall voltage was adjusted by the variac. To eliminate flicker from flourescent light source and ensure constant light intensity, a high-frequency precision illumination lamp controller (FX0648-2/120, Mercron, Richardson, TX) fitted with a photodiode light sensor was used. It converted the input of 120V and 60Hz of alternating current (AC) power supply to 165 V AC and 60kHz, thereby removing flicker and increasing the light intensity. The light controller stabilized the light of the flourescent lamps to within 0.25% of the selected intensity using a real-time light feed-back system.

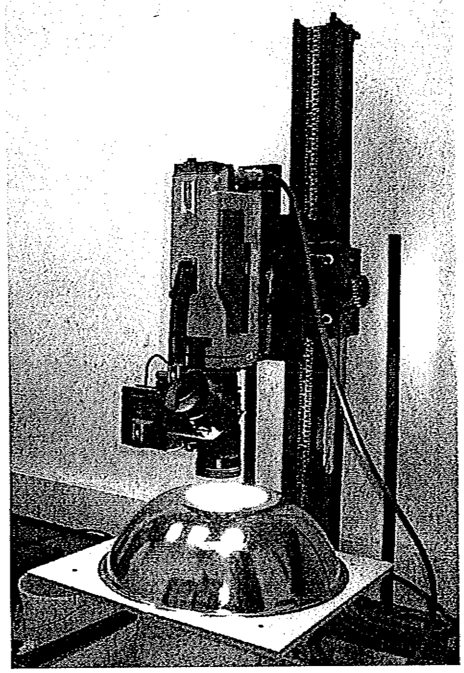

Figure 3.3 Area scan camera setup.

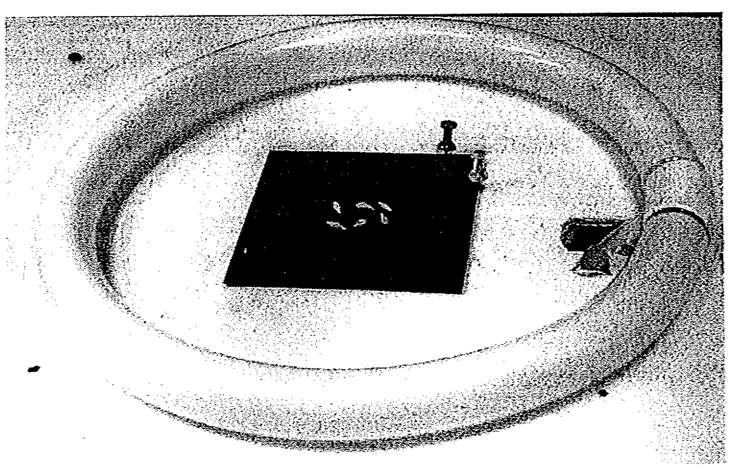

Figure 3.4 Illumination setup for area scan camera.

3.3.2.4 Frame capture For this study, two types of images were acquired - single kernel and bulk sample images (Figure 3.5). The single kernel images consisted of physically separated grain kernels placed on a non-reflective black card, whereas bulk sample images consisted of freely packed kernels of a particular grain type in a petri dish. The image acquisition system was powered on 30 min before each imaging session to stabilize the flourescent lamps, photo diode, CCD sensors, and any other electro-optical device. Although the relative position of the camera lens from the object was fixed, each imaging session was started by imaging a Canadian 10 cent coin, which has a known diameter of 17.96 mm. This ensured that all the session had the same spatial resolution and this image could be later used as a reference image for spatial calibration.

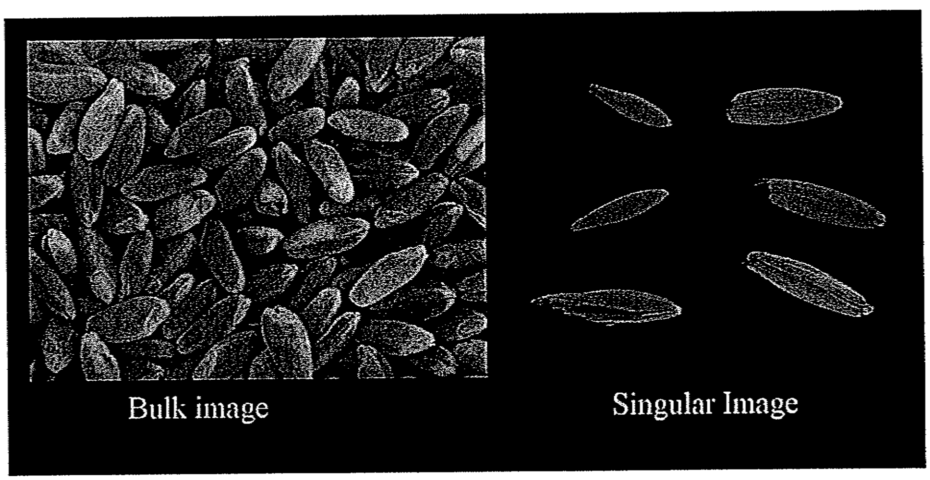

Figure 3.5 A sample of single kernel and bulk sample images.

The grain sample to be imaged as single kernel images was obtained by pouring about 500 g of grain into a large plastic bag and shaking it to mix the grain thoroughly. Approximately 1000 grain kernels were taken out from the plastic bag using a scoop. These were then spread out in a plate and six kernels were randomly picked at a time and placed in the FOV of the camera in a non-touching manner with the help of tweezers. A total of 600 kernels were imaged (100 images) for each growing region in one session. After imaging, the grain kernels were sealed in a plastic bag, labeled with relevant information, and stored for future reference.

The grain sample for bulk sample images was obtained by pouring 2 kg of grain kernels into a large plastic bag and shaking it to mix the grain thoroughly. The grain was then slowly poured into the petri dish until it was completely filled. The excess grain was gently shaken off the petri dish such that the top level of grain was almost horizontal and matched up to the rim of the petri dish. A total of 20 images were taken for each growing region. After imaging, the grain kernels were sealed in a plastic bag, labeled with relevant information, and stored for future reference.

3.3.3 Line scan camera

3.3.3.1 Hardware The line scan assembly consisted of dual conveyor belt system (Spewak 1995), line scan camera (Model Trillium TR 2K, Dalsa, Waterloo, ON) (Figure 3.6), power supply(PS3-DP9-115, Vision 1, Bozeman, MT), PC (PIII 450 MHz), color frame grabbing board (Model Viper-Digital, Coreco Inc., St. Laurent, PQ), and a flourescent light source. The line scan camera was mounted on copy stand (Super repro, The Vitec Group plc, Suffolk, UK) above the center of the secondary conveyor belt such that the line of sensors was perpendicular to the direction of motion of the conveyor belt. The camera was fitted with a macro lens (SP 90 mm, Tamron Inc., Commack, NY) of 90 mm focal length using a cannon FD mount adapter. The frame grabber board supplied control information to the camera and monitored the speed of the conveyor belt via the output from the rotary shaft encoder (M21AA, Dynamics Research Corporation, Andover, MA).

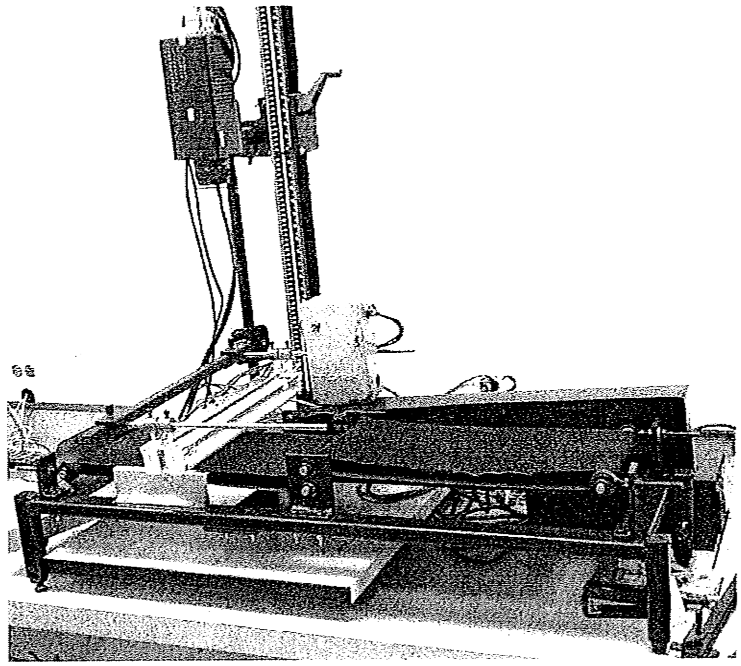

Figure 3.6 Line scan camera setup.

The camera uses a precisely-aligned beam-splitting prism with interference filters to separate R, G, and B inputs from a common optical axis with high transmission efficiency. This common optical axis approach provides higher fidelity images than interdigitated color imagers, where R, G, and B sensors placed next to each other in a single row, and trilinear imagers, where three rows of sensors - one for each color band, are placed adjacent to each other. Use of interdigitated or trilinear approach creates misalignment of pixel data and mis-registration of color data that must be corrected when the color channels are recombined during post-processing, thereby increasing complexities, computational requirements, and chances of erroneous data.

3.3.3.2 Software The line scan camera was controlled by ASCII communications protocol which allowed configuring and programming all camera functions through the recommended standard RS-232 serial interface. Software and image processing library (Sapera 4.0, Coreco Inc., St. Laurent, PQ) allowed control of all aspects of image acquisition and display. The Coreco camera (.cca) and Coreco video (.cvi) files (Appendix A.2 and A.3) were developed using Cam Expert software. The .cca file contains all the acquisition parameters that describe the camera's video signal characteristics and operation modes such as video format, resolution, synchronization source and timing, channels/taps configuration, modes supported by the camera, and related parameters. The .cvi extension contains all the acquisition parameters relating to the frame grabber board such as buffer size, buffer type, external sync, strobe, internal frame/ line trigger enabling, DC restoration, contrast, saturation, hue, brightness, etc.

3.3.3.3 Light source The optical axis of the camera across the width of the belt was uniformly illuminated by two 15 W flourescent lamps (F15T8, General Electric Company, New York, NY) that were 25 mm in diameter and 457 mm long. The lamps were positioned on opposite sides of the sensed region. The power source for the lamps (Model FX0648-2/120, Mercron, Richardson, TX) incorporated a photo-diode light sensor in a feedback loop, similar to the area scan system, and provided a uniform level of illumination under varying conditions.

3.3.2.4 Frame capture The illumination and camera were turned on 30 min prior to capturing frames and the motors or conveyor belt and vibratory hopper were switched on 10 min in advance. The image of a Canadian 10 cent coin was taken for performing spatial calibrations. The grain samples to be imaged were obtained by pouring around 500 g of samples in a large plastic bag. The samples were then poured into the vibratory feeder to drop kernels on the belt at a uniform rate. The rpm of the vibratory motor and opening of the feeder was adjusted to attain grain flow with the least occurrences of touching kernels. The grain coming off the secondary conveyor belt was collected in a 4 L capacity plastic bucket. After imaging, the grain kernels were sealed in a plastic bag, labeled with relevant information, and stored for future reference.

3.4 Executing Image Processing Code

A program was written in visual C++ incorporating the algorithms developed for feature extraction from color images of grain kernels. The first draft was developed by Li Wang which was later modified, debugged, optimized, and validated with the help of J. Paliwal and C. Karunakaran (Karunakaran et al. 2002). The executable file of the compiled source code is available upon request from Dr. D.S. Jayas.

3.4.1 Command line syntax The program was executed by taking certain user inputs in the command statement at dos prompt. In default mode, the program ran on single kernel images and computed 51 morphological, 123 color, and 56 textural features. The command line syntax for the default mode was:

exe_filename imagelist_filename output_filename

where exe_filename was the name of the executable file obtained after compiling the C++ code, imagelist_filename was the name of the text file containing the path and filename of the image files to be processed, and output_filename referred to the desired output filename that would contain all the features computed by the program. The same program, however, could be run on bulk sample images by specifying a fourth parameter in command line as follows:

exe_filename imagelist_filename output_filename B

where the first three parameters are the same as described above and the fourth parameter 'B' or 'b' stands for bulk sample images. Use of any character other than B or b as a fourth parameter would make the program run in default mode. The program calculated 123 color and 56 textural features for bulk sample images. No morphological features were computed because the whole image was treated as one object and the boundary of the image was treated as the object boundary. Morphological, color, and textural features computed by the program are listed in Appendix B.

3.4.2 Image list The program performed batch image analysis by reading the list of path and image filename to be processed from a text file. The program could process image files stored on the local computer or on any computer connected by internet. The following four lines show sample entries in the image list file:

C:\WINDOWS\Desktop\Imaging\Images\red.tif

G:\CWRS98\w1___001.tif

P:\Grain Samples\Graded\Barley98\b1___001.tif

\\Net67\C\Durum98\d_fai006.tif

where C:\ and G:\ are local drives, P:\ is a mapped network drive of a remote computer connected via internet, and \\Net67 is a drive on the local area network accessed by network neighborhood.

The image list operations were made fail-safe by incorporating these details:

- files that did not exist were skipped and the program jumped to the next line of image list file,
- blank spaces/tabs before first character in a line in image list file were skipped in reading,
- blank lines in the image list file were skipped in reading, and
- any line starting with a double forward slash (//) were skipped.

The last feature was introduced to allow intentional skipping of desired files without having the need to delete the entries from image list file.

3.4.3 Skipped list The program was checked for memory leakage and optimized so that it could process over 1000 image files in one session without running out of memory resources. Since thousands of kernels were processed, the output file became very large and it became impossible to determine which files were skipped during the batch operation. To facilitate this, a routine was written that created a file called skipped.txt which contained those entries from the image list file that were skipped. The skipping could occur in the following situations:

- incorrect file name in image list file (file does not exist),
- line in image list file starting with a double forward slash,
- incorrect format of image file,
- corrupt tiff file, and
- first pixel in the image being an object pixel (first pixel is required to be a background pixel to allow region growing for the segmentation operation).

3.4.4 Output list The output of the program was written to a text file specified by the command line parameter output_filename. The output file consisted of a list of image features with all features of a kernel written in one row starting with kernel number in the first column followed by image file name, area, perimeter, and so on. The following four lines show the first five outputs for image file b3___051.tif:

1	d:\Grain Samples\Graded\Barley98\b3___051.tif	6068	390.298	74.6726
2	d:\Grain Samples\Graded\Barley98\b3___051.tif	5289	326.266	67.7791
3	d:\Grain Samples\Graded\Barley98\b3___051.tif	5493	334.330	70.859
4	d:\Grain Samples\Graded\Barley98\b3___051.tif	5559	331.056	66.7533

The output file consisted of the kernel number and image file name to facilitate back tracking to the image from which a particular feature was calculated.

3.5 Inside the Image Processing Code

The image processing code can be divided into two parts: data extraction for feature calculation and feature calculation itself. This section goes through the code in order in which the commands were executed to extract object data and calculate the features. The list of features and their formulas can be found in Appendix B and Karunakaran et al. (2002), respectively.

3.5.1 Starting the program The command line syntax and other relevant details have been covered in section 3.4.

3.5.2 Reading an image file The name and path of the image file to be processed was read from the imagelist_filename file. The file header was read to make sure that the file being opened was a TIF format file. The horizontal and vertical dimensions of the image were determined and stored and later used to reserve memory space for different operations. To store R, G, and B values of all the pixels, a pointer was created for each color that stored information in a sequence about pixels, starting from the top left corner and proceeding rowwise, until the end of the file was reached.

3.5.3 Thresholding Gray scale image data was generated using the R, G, and B pixel values and an adaptive thresholding technique (Karunakaran et al. 2002) was applied on these data to determine a preliminary threshold value. After experimenting with images of different grain types, an empirical relation was developed between the threshold value calculated and the threshold value used. If the threshold value was over 40, it was reduced by 20 to obtain the final threshold value, whereas if it was already below 40, a threshold of 20 was used. This technique enabled segmentation of dark grain kernels while getting the maximum object area of normal-color grains. Thresholding operation was not performed on bulk sample images because the entire image was treated as one object.

3.5.4 Corner pixel check The first pixel, i.e. the top left most, is required to be a background pixel to allow region growing for the segmentation operation in single kernel images. A check was run before proceeding to the segmentation routine to determine whether the corner pixel belonged to an object or to the background. If it belonged to an object, the image was skipped because no objects could be extracted, otherwise the program proceeded to the segmentation algorithm.

3.5.5 Segmentation This algorithm required a threshold value as an input to the function. An index image was created in this operation that contained values for pixel positions depending on what it represented in the actual image, such as background, object, perimeter, centroid, etc. At the first step of segmentation, the pixels having a gray level value higher than the threshold were given the value of 1 and the rest were assigned a value of 0 in the index image. For bulk sample images, all pixels in the index image were assigned a value corresponding to object number 1.

3.5.5.1 Background removal A list was formed of all the pixels in the index image and region growing was carried out by matching the value of neighboring pixels, starting with the top left pixel, until all the pixels in the list that were inter-connected and belonged to the background were used. The used pixels were assigned a value of -1 in the index image and the unused pixels of the list retained their value of 0 or 1. This resulted in 'hole-filling' of the objects because any pixel with a value other than -1 belonged to an object. A 'hole' is a small dark region within an object that is assigned a background pixel value because of falling below the threshold.

3.5.5.2 Kernel extraction The index image was scanned until it encountered the first object pixel. Region growing was carried out and pixels of the first object were assigned a value of 100 in the index image. The successive objects were assigned values in increments of 100.

3.5.5.3 Noise removal While imaging grain kernels, unwanted material such as small dust particles and chaff can be a part of the image. These may get counted as desired objects and later give erroneous results. To prevent this, it is important to remove these object from the image. The area of extracted kernels was determined by counting the number of pixels belonging to that object. If the pixel count was less than 400, the pixel values of that object were changed to -1 in the index image, making them a part of the background. This part thus also calculated the feature - area of objects.

3.5.6 Boundary extraction The kernel boundary was determined by finding values of pixels adjacent to object pixels in the index image using a 4-connect technique. If any of the four neighboring pixels had a value of -1 (background), the pixel's value in the index image was incremented by 1 in the index image. This resulted in all the perimeter pixels having a value of 101, 201, 301, etc. for objects 1, 2, and 3, respectively. The perimeter length was calculated using the Euclidean distance principle by finding direction of the adjacent perimeter pixel. If the adjacent pixel could be found by the 4-connect method, 0.5 was added to the pixel length, whereas if the adjacent pixel could not be found by 4-connect but was located using 8-connect, 0.707 was added to the perimeter length. Since each pixel has two adjacent pixels, any of the three possible values (1, 1.207, and 1.414) per pixel were determined.

3.5.7 Center of mass and radius The x and y coordinates for center of mass of objects were calculated by averaging the x and y coordinate values, respectively, of all the object pixels. The radius routine used center of mass values to determine mean, minimum, and maximum radius values.

3.5.8 Major axis length It was calculated by finding the maximum distance between two points on the perimeter that were diametrically opposite with respect to the center of mass. The feature was stored along with coordinate values of extreme points to determine minor axis length.

3.5.9 Minor axis length This routine used major axis and center of mass coordinates as input to the function. Minor axis length was calculated by finding the maximum distance between two points on the perimeter that were diametrically opposite with respect to the center of mass and formed a right angle with major axis.

3.5.10 Fourier descriptors Fourier descriptors are mathematical transformations that represent the shape of the object in a frequency domain. The lower frequency descriptors contain information about the general shape, and the higher frequency descriptors contain information about smaller/finer details. Two types of Fourier descriptors were calculated in this study: radial length transform and perimeter coordinate transform. A set of 128 radial lengths and their perimeter coordinates, calculated at an increment of $2\pi/128$ angle starting at major axis, was used as an input to determine 20 descriptors each for radial and boundary transform. The radial descriptors were normalized by dividing the values with the 0^{th} descriptor, which is the same as mean radius. The boundary descriptors were normalized by dividing by the 1^{st} descriptor because dividing by the 0^{th} descriptor, which is same as the centroid coordinates, would make the descriptors dependent on translation.

3.5.11 Shape moments Hu's invariant moments were calculated to determine shape characteristics of grain kernels. This routine required centroid coordinates as input to the function. The moments were calculated by determining the distance of the object pixel from its centroid.

3.5.12 Color moments The same technique of shape moments was extended to color data to calculate color moments for R, G, and B color bands. The distances of the object pixel from its centroid were multiplied by the R, G, and B pixel value when calculating the respective color moments.

3.5.13 Color means, ranges, and variances The statistical features were obtained using the color data from R, G, and B bands of the image. The routine to calculate variance required mean as an input to the function.

3.5.14 HSI means and ranges The HSI features were calculated by first converting the RGB data into HSI data using the standard conversion formulae.

3.5.15 Histogram features The histogram features contained the information about the number of pixels falling in a particular gray scale range. Since the color images were of 24 bit size, each color could have 256 possible values ranging from 0 to 255. Having 256 features for each color band would result in an excessive number of features and result in many color levels with no pixel in them. Information from such a histogram is easier to interpret visually rather than quantitatively. To overcome this, the histogram range was reduced to 32 levels by dividing the pixel values by 8.

3.5.16 Textural features Calculation of textural features is a computationally intensive process because the dimension of matrices that need to be solved are a direct consequence of the number of gray levels in the image. An image with n gray levels requires solving of an $n \times n$ co-occurrence matrix and an $n \times r$ run length matrix where r is the run length. A preliminary study was carried out to determine the effect of reduced-gray-level textural features on classification accuracy of grain kernels. This would help to select the best reduced-gray-level data and reduce the complexity of calculations in the final selected features set. The levels of R, G, and B bands and gray scale (0.80R+0.16G+0.04B) were reduced from 256 to 128, 64, 32, 16, and 8 and the textural features extracted from each case, including 256 levels, were used for classification, and the results were compared. The results indicated that a 32 level image was most suited for textural analysis.

The program was made flexible by introducing two variables, 'gray level divisor' and 'gray levels' which could be defined at the beginning of the program. The 'gray levels' variable specified the number of reduced gray levels and 'gray level divisor' specified the number that was needed to divide the gray level data ranging from 0 to 255 to convert it to reduced-gray-level data ranging from 0 to the reduced gray level. The textural features were calculated by determining co-occurrence and run length matrices for a 32 color level image for R, G, B, and gray scale data. An example of change in texture with reduction in gray level is shown in Figure 3.7.

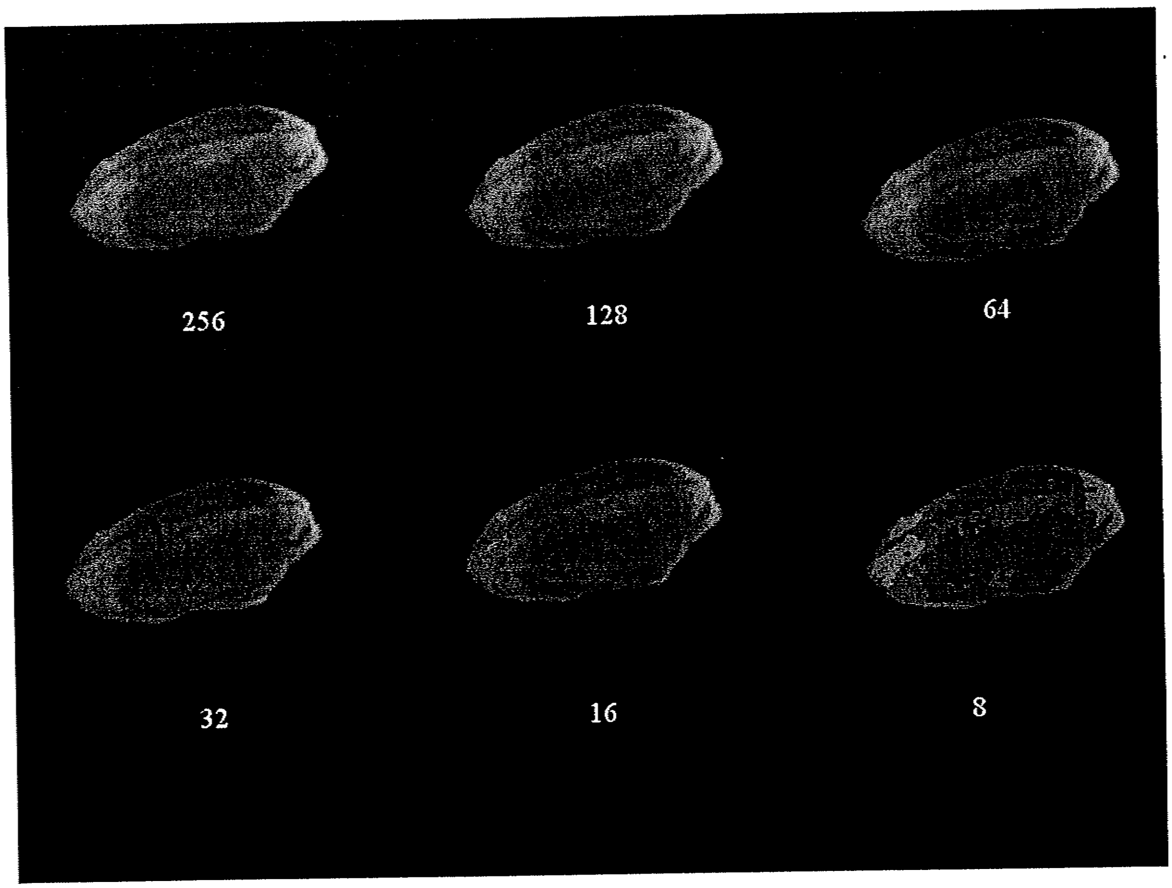

Figure 3.7 Change in texture of a CWRS wheat kernel due to reduction in the number of gray levels used in an image from 256 to 8.

3.6 Data for Analysis

The data for analysis was generated from single kernel and bulk sample images. The data from single kernel images consisted of morphological, color, and textural features, whereas data from bulk sample images consisted of color and textural features. Output class data were added to it depending on the type of analysis being performed. The statistical method required just one output class having five different values for five different types of grains. The BPN had five output classes with a value of 0 and 1. The output class representing the actual grain type was assigned a value of 1 and the remaining four classes were assigned a value of 0. The specialist probabilistic neural network (SPNN) had two output classes having a value of 0 and 1. The output class representing the actual grain type was assigned a value of 1 and the class representing the remaining grain types was assigned a value of 0.

3.6.1 Single image data A database of morphological, color, and textural features was created for each of barley, CWAD wheat, CWRS wheat, oats, and rye using 7500 kernels of each grain type, selected randomly from the different growing regions. Because of limited production of grains, not all grain types were available at all locations, however, they were uniformly distributed across the growing regions (figure 3.1). To determine the best suited morphological, color, and textural features for a particular grain, the data set was divided into three subsets, one each for morphology, color, and texture for each grain type. For each grain type, each of these three subsets were further divided into five data sets containing information of 1500 kernels. One data set from each grain type was merged together to create five data sets called production data sets which were used to perform cross validation of neural network and statistical classification results. Similar data sets were also created without splitting data into morphological, color, and textural features sets to perform analysis using all the features. After determining the top 20 and the top 10 most suited morphological, color, and textural features, the combined 60 and the combined 30 features sets were created that were similar to the all features data set except that they had limited number of morphological, color, and textural features.

3.6.2 Bulk sample image data To determine the top 10 and the top 20 most-suited features for bulk sample image analysis, a data set was created for each of color and textural features using 1000 images each of barley, CWAD wheat, CWRS wheat, oats, and rye. These data sets were split into five subsets for cross validation analysis. After determining the top 10 and the top 20 features, the color and textural data were merged to perform the analysis using all features, the combined 20 features, and the combined 40 features. The data were created only for BPN because preliminary analysis of data for single kernel images showed that BPN outperformed non-parametric statistical classifiers. No data were prepared for specialist network because classification accuracies of BPN gave satisfactory results.

3.7 Neural Network Architectures

The neural network architectures were developed using a commercial software called NeuroShell. For this research, two types of neural network architectures were developed: BPN and specialist probabilistic neural networks (SPNN).

3.7.1 Back propagation networks The BPN was presented with input patterns and it produced five outputs corresponding to each grain type. The output class was determined by comparing the five outputs which ranged from 0 to 1. The unknown kernel was assigned to the class having the highest output.

3.7.2 Specialist probabilistic neural networks This network was a combination of five sub-networks (barley specialist network, CWAD wheat specialist network, CWRS wheat specialist network, oats specialist network, and rye specialist network). Each of the specialist sub-network had 12 inputs and two output categories. A sub-network specializing in a particular grain type, say barley, was trained using the data which consisted of two classes of output patterns - barley and 'the rest'. In essence, each of the specialist sub-networks was trained to categorize an unknown object belonging to its class by assigning it a value between 0 and 1. A value of 1 meant that the unknown object belonged to that class, herein barley, and 0 meant that the object belonged to any of the other classes *i.e.*, CWAD wheat, CWRS wheat, oats, or rye. The final outcome was determined by comparing the output of all the specialist sub-networks and the one having the highest value was declared the winner. The unknown grain type was assigned the class corresponding to that of the winner.

The success of PNN networks is dependent upon the smoothing factor. NeuroShell uses a calibration procedure to decide which smoothing factor is best for the given problem. The calibration procedure used for this study is called genetic adaptive. It uses a genetic algorithm to find appropriate individual smoothing factors for each input as well as an overall smoothing factor.

Training for PNN using the genetic adaptive option took place in two parts. The first part trained the network with the data in the training set. The second part used calibration to test a whole range of smoothing factors, trying to optimize a combination that works best on the test set with the network created in the first part. Completion of this step is treated as the elapsing of one generation. Training was completed when 20 generations elapsed without any improvement in networks performance. At the end of training, the individual smoothing factors were used as a sensitivity analysis tool to determine relative importance that input had to the model.

3.8 Statistical Classifier The non-parametric statistical classifier was developed using a commercial software called Statistical Analysis System (SAS) Release 8.2 (SAS Institute Inc., NC) under Windows NT 4.0 operating system on a PIII 450 MHz PC. Discriminant analysis was carried out by writing a program in the SAS environment and non-parametric tests were carried out for five features sets. Since the value of features ranged considerably, the input data were standardized using 'PROC Standard' routine.

To determine relative importance of an input feature for classification, stepdisc analysis was carried out using 'PROC STEPDISC'. The STEPDISC procedure performed a stepwise discriminant analysis to select a subset of the quantitative variables for use in discriminating among the classes. The STEPDISC procedure used forward selection, i.e., the program started with all variables and selected the variables in descending order of contribution.

4. RESULTS AND DISCUSSION

4.1 Execution of Code

All image processing and data analyses were carried out on a Pentium III PC with 512 MB of random access memory (RAM) running under Windows NT 4.0 operating system. A color image of 640 by 480 pixels containing six grain kernels required 43 s of central processing unit (CPU) time for analysis before results were written to a text file. More than 40 s of CPU time were spent in the segmentation operation and calculation of 230 features took an additional 3 s. For images of bulk samples, since no segmentation operation had to be performed, processing of the image took less time as compared to single kernel images. The program took 4.5 s to process a bulk color image of 640 by 480 pixels.

4.2 Selection of Reduced Gray Level

A 24 bit color image is made up of R, G, and B band images, each having 256 levels of that particular color. As a result, the total number of colors in a 24 bit image are over 16 million. To perform textural analysis, the color image is either converted into a single 8 bit gray level image having 256 shades of gray ranging from black to white or the color image is split into three 8-bit gray level images, each corresponding to R, G, and B color band components of the color image. Since having 256 color levels in textural analysis considerably increases computational requirements, a preliminary study was carried out to investigate the effect of reduced gray level on textural-features-based classification accuracies. The gray levels were reduced to 128, 64, 32,16, and 8 for R, G, B, and gray images and the classification accuracies were compared to those obtained using 256 color level images (Appendix C).

Textural features were extracted for 600 kernels of each of the five grain types and a 4-layer BPN was used to develop a neural network classifier. The neural network consisted of 56 inputs, 30 neurons in each of the two hidden layers, and five outputs. The network used logistic scaling and activation functions at input and processing levels, respectively. Training and testing was done on 30 and 20% of the data, respectively and the entire process was repeated three times using different training and testing data sets. The network was trained for 1000 epochs and was then applied on a production data set consisting of 1500 kernels (i.e. 300 for each grain type). The summarized results of textural analysis are shown in Figure 4.1.

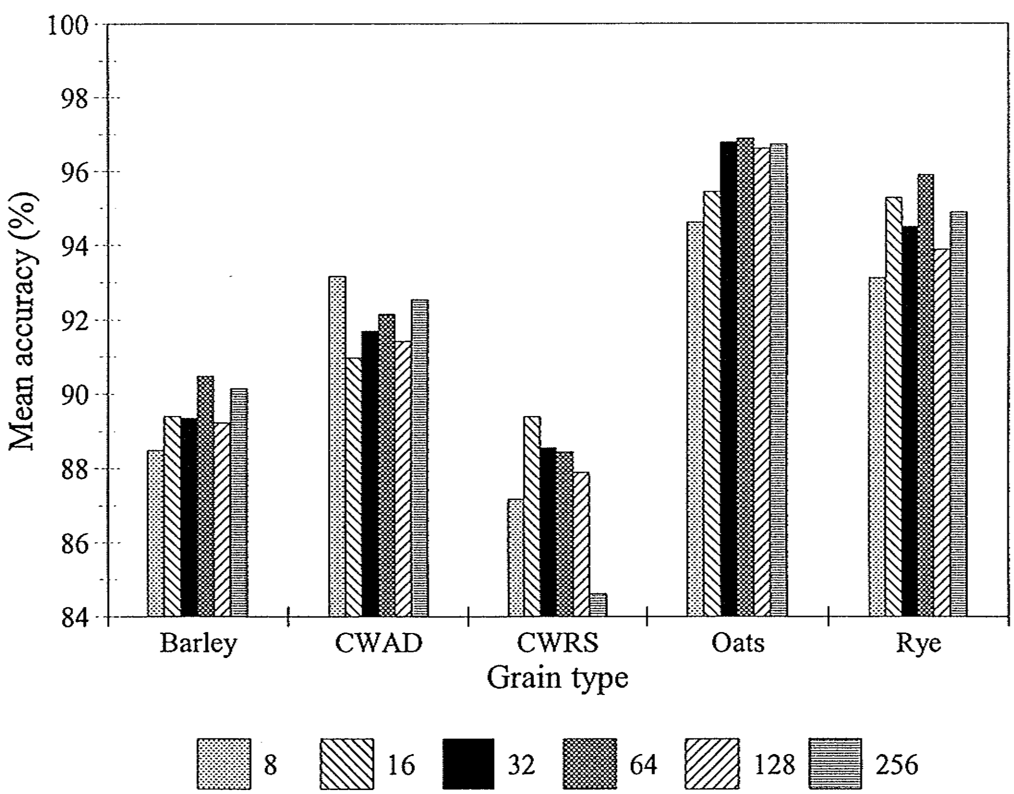

Figure 4.1 Classification accuracies of cereal grains at different gray levels.

There does not seem to be much variation in classification accuracy with the increase of number of gray levels (Figure 4.1 and Appendix C.1). The worst results were obtained for CWRS wheat using 256 gray levels, whereas eight gray levels gave the worst results for barley, oats, and rye. The number of gray levels selected was 32 because it reduced computational requirements as compared to 64, 128, and 256 gray levels and still had sufficient texture as compared to 8 and 16 gray levels. An example of change in texture with reduction in gray levels is shown in Figure 3.5. Majumdar and Jayas (2000c) also reported use of 32 gray levels as the best choice for textural analysis.

4.3 Grain Type Identification using Bulk sample images

A classification study was carried out for five different types of features sets. The first two sets consisted of 123 color and 56 textural features, respectively. The third set consisted of all the color and textural features combined, i.e., a total of 179 features. The fourth and fifth sets were a subset of the third set. They consisted of the top 10 and top 20 color and textural features each combined, thus having a total of 20 and 40 features, respectively. The top 10 and top 20 color and textural features were determined from studies using the first two sets.

4.3.1 Analysis using color features The features set used consisted of 123 color features. A four layer BPN was used to develop a classifier. It consisted of 123 input nodes, 39 nodes in each of the two hidden layers, and five output nodes, one for each grain type. The network used logistic scaling and activation functions at input and processing levels, respectively. Training and testing was done on 200 images (i.e. 50 images of each grain type) each, and the entire process was repeated five times using different training and testing data sets. The network was trained for 1000 epochs and was then applied on the production data set consisting of 1000 images. The summarized results of color analysis are shown in Table 4.1.

Table 4.1 Classification accuracies of cereal grains from bulk sample images obtained using a BPN classifier with color features as inputs.

	Classification accuracy for five trials, %					
	1	**2**	**3**	**4**	**5**	**Mean**
Barley	97.5	98.5	99.5	100	99	98.9
CWAD	100	100	100	100	100	100
CWRS	100	100	100	100	100	100
Oats	99	99.5	99	99	96.5	98.6
Rye	100	99.5	99.5	100	99.5	99.7

The classification accuracy was very high and consistent throughout the five trials just using the color features (Table 4.1). The contribution factor of each input feature was calculated by the network, and the average contribution of these features over five trails was used to determine the top 20 color features. Table 4.2 gives the top 20 features ranked in order of their decreasing contribution to the classification process. The contribution list shows that most of the color features come from the red band of the bulk sample images. Further studies can be carried out using a monochrome camera with a red filter to acquire just the red band data and investigate classification accuracies. Using just one color band for image acquisition and classification will increase the processing speed and greatly reduce the hardware cost.

Table 4.2 The top 20 color and textural features based on their respective contribution towards classification accuracy for cereal grains while using a BPN classifier.

	Features set	
Rank	**Color**	**Textural**
1	Red histogram range 2	Red GLRM short run
2	Red histogram range 3	Blue GLCM cluster shade
3	Red histogram range 1	Gray GLRM short run
4	Green histogram range 1	Blue GLRM short run
5	Hue mean	Green GLCM cluster shade
6	Red histogram range 4	Green GLCM correlation
7	Saturation mean	Green GLRM short run
8	Green variance	Green GLCM variance
9	Blue histogram range 2	Blue GLCM variance
10	Red range	Red GLCM mean
11	Blue histogram range 1	Green GLCM mean
12	Red histogram range 17	Red GLCM inertia
13	Blue histogram range 3	Blue GLCM mean
14	Red histogram range 14	Red GLCM uniformity
15	Red variance	Blue GLRM long run
16	Red mean	Green GLCM uniformity
17	Red histogram range 16	Red GLCM correlation
18	Red histogram range 19	Blue GLCM correlation
19	Red histogram range 5	Red GLRM entropy
20	Red histogram range 15	Blue GLCM entropy

4.3.2 Analysis using textural features The features set used consisted of 56 textural features. A four layer BPN was used to develop a classifier. It consisted of 56 input nodes, 22 nodes in both hidden layers and five output nodes, one for each grain type. The network used logistic scaling and activation functions at input and processing levels, respectively. Training and testing were done on 200 images (i.e. 50 images of each grain type) each, and the entire process was repeated five times using different training and testing data sets. The network was trained for 1000 epochs and was then applied on the production data set consisting of 1000 images. The summarized results of textural analysis are shown in Table 4.3.

Table 4.3 Classification accuracies of cereal grains from bulk sample images obtained using a BPN classifier with textural features as inputs.

	Classification accuracy for five trials, %					
	1	**2**	**3**	**4**	**5**	**Mean**
Barley	100	100	100	100	100	100
CWAD	100	100	100	100	100	100
CWRS	100	100	100	100	100	100
Oats	99.5	100	100	99.5	99	99.6
Rye	100	100	100	100	99.5	99.9

Similar to classification accuracies obtained using color features, the classification accuracies were very high and consistent using textural features (Table 4.3). Table 4.2 gives the top 20 features ranked in order of their decreasing contribution to the classification process.

4.3.3 Analysis using all features The features set used consisted of 123 color and 56 textural features. A four layer BPN was used to develop a classifier. It consisted of 179 input nodes, 53 nodes in both hidden layers and five output nodes, one for each grain type. The summarized results of the textural analysis are shown in Table 4.4.

Table 4.4 Classification accuracies of cereal grains from bulk sample images obtained using a BPN classifier with all features as inputs.

	Classification accuracy for five trials, %					
	1	**2**	**3**	**4**	**5**	**Mean**
Barley	100	100	99.5	100	100	99.9
CWAD	100	100	100	100	100	100
CWRS	100	100	100	100	100	100
Oats	100	100	100	100	99	99.8
Rye	100	100	100	100	99.5	99.9

The classification accuracy, as expected, was very high for all the grain types. Table 4.5 lists the top 40 features based on their respective contribution towards classification accuracy. It can be seen that both color and textural features appear in the list and are equally important towards classification of bulk sample images. Further analysis was carried out using the combined 40 (top 20 color plus top 20 textural from table 4.2) and the combined 20 (top 10 color plus top 10 textural from table 4.2) features sets to determine the change in classification accuracies after reducing the input features.

Table 4.5 The top 40 features from the all features set based on their respective contribution towards classification accuracy for cereal grains in bulk sample images while using a BPN classifier.

Rank	Features	Rank	Features
1	Red histogram range 3	21	Blue GLCM cluster shade
2	Gray GLRM short run	22	Red GLCM mean
3	Blue GLRM short run	23	Green GLRM long run
4	Red histogram range 1	24	Blue histogram range 2
5	Red GLRM short run	25	Red histogram range 14
6	Red histogram range 2	26	Blue mean
7	Green GLRM short run	27	Red histogram range 20
8	Hue mean	28	Red histogram range 21
9	Green GLCM inertia	29	Blue GLRM long run
10	Gray GLRM color non-uniformity	30	Blue GLCM entropy
11	Red histogram range 4	31	Green GLCM uniformity
12	Blue GLRM color non-uniformity	32	Green histogram range 1
13	Red GLRM long run	33	Red moment 1
14	Red GLRM color non-uniformity	34	Red GLCM uniformity
15	Red mean	35	Blue GLCM uniformity
16	Saturation mean	36	Hue range
17	Red GLCM inertia	37	Gray GLRM long run
18	Gray GLRM entropy	38	Red histogram range 19
19	Gray GLCM mean	39	Gray GLCM homogeneity
20	Blue GLRM runpercent	40	Blue GLCM correlation

4.3.4 Analysis using the combined 40 features set The features set used consisted of the top 20 color and the top 20 textural features. A four layer BPN was used to develop a classifier. It consisted of 40 input nodes, 18 nodes in both hidden layers and five output nodes, one for each grain type. The network used logistic scaling and activation functions at input and processing levels, respectively. Training and testing was done on 200 images (i.e. 50 images of each grain type) each, and the entire process was repeated five times using different training and testing data sets. The network was trained for 1000 epochs and was then applied on the production data set consisting of 1000 images (i.e. 200 images of each grain type). The summarized results of the textural analysis are shown in Table 4.6.

Table 4.6 Classification accuracies of cereal grains from bulk sample images obtained using a BPN classifier with the combined 40 features as input.

	Classification accuracy for five trials, %					
	1	**2**	**3**	**4**	**5**	**Mean**
Barley	100	100	100	100	100	100
CWAD	100	100	100	100	100	100
CWRS	100	100	100	100	100	100
Oats	100	100	99.5	99.5	100	99.8
Rye	100	100	100	100	100	100

Since the accuracy was very high, number of inputs was further reduced to 10 each from color and textural features sets.

4.3.5 Analysis using the combined 20 features set The features set used consisted of the top 10 color and the top 10 textural features. A four layer BPN was used to develop a classifier. It consisted of 20 input nodes, 14 nodes in both hidden layers and five output nodes, one for each grain type. The network used logistic scaling and activation functions at input and processing levels, respectively. Training and testing were done on 200 images (i.e. 50 images of each grain type) each, and the entire process was repeated five times using different training and testing data sets. The network was trained for 1000 epochs and was then applied on the production data set consisting of 1000 images (i.e. 200 images of each grain type). The summarized results of textural analysis are shown in Table 4.7.

Table 4.7 Classification accuracies of cereal grains from bulk sample images obtained using a BPN classifier with the combined 20 features as input.

	Classification accuracy for five trials, %					
	1	**2**	**3**	**4**	**5**	**Mean**
Barley	100	100	99	100	100	99.8
CWAD	100	100	100	100	100	100
CWRS	100	100	100	100	100	100
Oats	99.5	99.5	99.5	98	95	98.3
Rye	100	100	100	100	100	100

Even though the number of inputs was greatly reduced, the classification accuracies still remained high for all the grain types.

4.3.6 Summary of bulk analysis The classification accuracies obtained using different input features sets are shown in Figure 4.2. Color alone cannot be used for classification of bulk sample images. Best results were obtained using the combined 40 features set. Other than oats, all the grain types can be classified with close to 100% classification accuracy using just the combined 20 features set. Majumdar and Jayas (1999) reported classification accuracies close to 100% using images of bulk samples. The results from this study can be used for rapid identification of grain types when they arrive in rail cars at the terminal elevators. A grain sample can be collected in a tray and the bulk sample image can be acquired of the grain heap. The information from MVS can then be used to match the information from the rail company before dumping the grains into the pit for proper binning. Since this classification technique does not require time consuming image processing routines such at segmentation and Fourier descriptors, it can readily be implemented using commercial imaging libraries with DSP boards for real time operations.

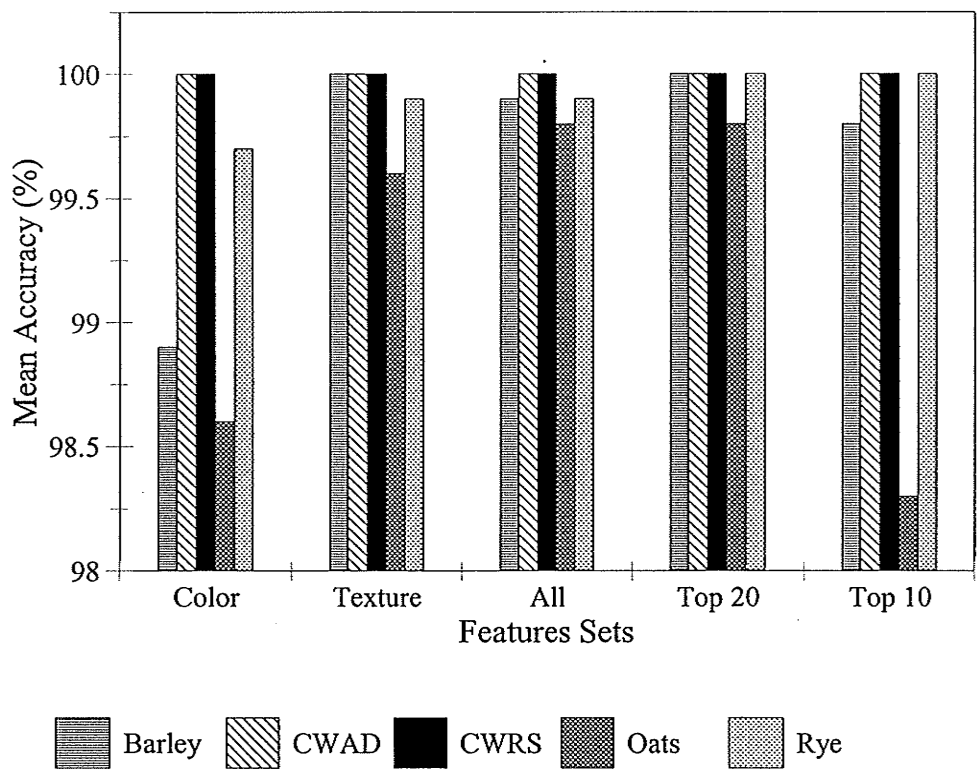

Figure 4.2 Classification accuracies of cereal grains using different input features sets.

4.4 Grain Type Identification in Single kernel images

The classification study was carried out for six different types of features sets. The first three sets consisted of 51 morphological, 123 color and 56 textural features, respectively. The third set consisted of all the morphological, color and textural features combined, i.e., a total of 230 features. The fourth and fifth sets were a subset of the third set. They consisted of the top 10 and the top 20 morphological, color and textural features combined, thus having a total of 30 and 60 features respectively. The top 10 and top 20 features were determined from studies using the first three sets.

Three types of classifiers, namely BPN, non-parametric statistical, and specialist PNN were used to classify the cereal grains and the classification accuracies obtained using each method were compared for all six different features sets. Analysis using BPN and the non-parametric statistical classifier was carried out five times, whereas that using specialist PNN was done three times only because of excessively long durations (over 72 h) required to carry out one replicate.

4.4.1 Analysis using morphological features

4.4.1.1 BPN classifier A four layer BPN was used to develop a classifier. It consisted of 51 input nodes, 58 nodes in both hidden layers and five output nodes, one for each grain type. The network used logistic scaling and activation functions at input and processing levels, respectively. Training and testing was done on 7500 grain kernels (1500 of each grain type) and the entire process was repeated five times using different training and testing data sets. The network was trained for 1000 epochs and was then applied on the production data set consisting of 22500 kernels. The network took approximately 11.5 h to train. The summarized results of the morphological analysis are shown in Table 4.8.

Except for CWAD wheat and rye, the mean classification accuracy for all the grain types was over 95%. Low classification accuracies can be attributed to large variations in shape and size of CWAD wheat grain kernels. Most of the CWAD wheat kernels were misclassified as rye and CWRS wheat kernels (Appendix D, Table D.1). This could be due to immature CWAD wheat grain kernels which are closer to CWRS wheat grain kernels in shape and size whereas the mature CWAD wheat kernels are closer to rye kernels in shape. Vice versa, rye was mainly classified as CWAD wheat kernels. Majumdar and Jayas (2000a) reported misclassification due to close morphological resemblance between CWAD and CWRS wheats.

Table 4.8 Classification accuracies of cereal grains from single kernel images obtained using a BPN classifier with morphological features as inputs.

	Classification accuracy for five trials, %					
	1	**2**	**3**	**4**	**5**	**Mean**
Barley	95.9	96.0	97.0	96.3	97.2	96.5
CWAD	90.3	88.0	90.0	88.7	90.0	89.4
CWRS	98.7	99.2	98.9	98.0	96.6	98.3
Oats	93.4	94.2	97.2	95.9	94.4	95.0
Rye	92.4	92.7	92.3	93.8	92.8	92.8

Table 4.9 gives the top 20 features ranked in order of their decreasing contribution to the classification process. Perimeter, followed by mean radius and area, are the most important feature when using a BPN. Size, however, alone is not sufficient. Shape features such as Fourier descriptors and Hu's invariant moments also feature high in the ranking for contribution towards classification.

Table 4.9 The top 20 morphological, color, and textural features based on their respective contribution towards classification accuracy for cereal grains in single kernel images while using a BPN classifier.

	Features set		
Rank	**Morphological**	**Color**	**Textural**
1	Perimeter	Red moment 1	Green GLCM mean
2	Mean radius	Red moment 2	Green GLCM cluster shade
3	Area	Green moment 2	Green GLRM runpercent
4	Boundary FD 2	Blue histogram range 1	Green GLCM variance
5	Minor axis length	Red moment 3	Blue GLCM mean
6	Boundary FD 18	Blue moment 1	Green GLCM correlation
7	Radial FD 2	Hue mean	Green GLRM long run
8	Radial FD 3	Blue variance	Blue GLRM color non-uniformity
9	Shape moment 3	Saturation mean	Green GLCM entropy
10	Boundary FD 5	Blue mean	Green GLRM short run

. . . continued . . .

. . . continued Table 4.9 . . .

Rank	Features set		
	Morphological	**Color**	**Textural**
11	Boundary FD 17	Red histogram range 9	Green GLRM run length non-uniformity
12	Shape moment 4	Green variance	Blue GLCM correlation
13	Radial FD 5	Red variance	Blue GLRM short run
14	Minimum radius	Blue range	Red GLCM homogeneity
15	Major axis length	Red histogram range 10	Blue GLCM variance
16	Boundary FD 20	Green histogram range 1	Red GLCM variance
17	Boundary FD 1	Green moment 1	Gray GLRM run length non-uniformity
18	Boundary FD 3	Red range	Blue GLRM runpercent
19	Maximum radius	Green range	Red GLRM run length non-uniformity
20	Boundary FD 12	Red histogram range 11	Blue GLRM run length non-uniformity

4.4.1.2 Non-parametric statistical classifier The statistical classifier was developed using SAS software. It consisted of 51 inputs and one output class. The output class had five values, one for each grain type. The classification accuracies obtained are shown in Table 4.10. The confusion matrix (Appendix D, Table D.2) reveals that, similar to BPN, CWAD wheat was misclassified as rye and vise versa. More than 5% of oats were incorrectly classified as rye kernels.

Table 4.10 Classification accuracies of cereal grains from single kernel images obtained using a non-parametric statistical classifier with morphological features as inputs.

	Classification accuracy for five trials, %					
	1	2	3	4	5	Mean
Barley	93.8	94.1	92.0	92.4	93.5	93.2
CWAD	91.4	91.0	90.8	90.0	90.1	90.7
CWRS	96.2	97.4	97.5	97.0	96.8	97.0
Oats	89.4	90.1	94.4	92.1	90.9	91.4
Rye	89.6	90.6	92.0	91.9	92.7	91.4

Similar to BPN, CWRS wheat had the highest and CWAD wheat had the lowest classification accuracy. Table 4.11 lists the top 20 input features in descending order of their contribution for classification when using a non-parametric statistical classifier. Interestingly, not only are there some new features in the top 20 list as compared to BPN, the rankings have also changed. This is due to very different approaches that BPN and non-parametric statistical classifiers have for grain classification. Shape feature are higher up in the ranking than size features, thus both types of features are equally important.

Table 4.11 The top 20 morphological, color, and textural features based on their respective contribution towards classification accuracy for cereal grains in single kernel images while using a non-parametric statistical classifier.

	Features set		
Rank	**Morphological**	**Color**	**Textural**
1	Minor axis length	Red moment 2	Red GLRM entropy
2	Boundary FD 18	Saturation mean	Green GLRM long run
3	Radial FD 2	Green mean	Red GLRM color non-uniformity
4	Radial FD 7	Red moment 1	Green GLRM run length non-uniformity
5	Shape moment 2	Red mean	Green GLCM inertia
6	Major axis length	Green range	Blue GLCM mean
7	Shape moment 1	Blue range	Green GLCM variance
8	Area	Blue histogram range 1	Red GLRM runpercent
9	Boundary FD 6	Red variance	Blue GLRM color non-uniformity
10	Maximum radius	Red moment 3	Red GLCM variance

. . . continued . . .

. . . continued Table 4.11 . . .

	Features set		
Rank	**Morphological**	**Color**	**Textural**
11	Radial FD 3	Red histogram range 22	Red GLCM homogeneity
12	Perimeter	Blue histogram range 4	Blue GLRM entropy
13	Boundary FD 3	Green variance	Blue GLCM variance
14	Radial FD 4	Green moment 2	Red GLRM run length non-uniformity
15	Boundary FD 17	Green moment 1	Green GLRM runpercent
16	Shape moment 3	Blue variance	Green GLRM short run
17	Minimum radius	Red moment 4	Blue GLRM short run
18	Boundary FD 9	Blue histogram range 8	Green GLCM mean
19	Boundary FD 2	Red histogram range 6	Green GLRM entropy
20	Boundary FD 10	Blue histogram range 5	Red GLCM mean

4.4.1.3 Specialist PNN classifier A specialist PNN used to develop a classifier consisted of 5 sub-networks, each of which specialized in one grain type. Each of the sub-networks consisted of 51 input nodes, 7500 nodes in the hidden layer and two output nodes. The network used logistic scaling at the input level. The training was stopped if the minimum error value of the network remained unchanged for 20 training generations. The trained network was then applied on the production data set consisting of 22500 kernels. The network took less than a minute to train, however, the calibration procedure can take anywhere from 24 h to 72 h for a network of this size. The summarized results of morphological analysis are shown in Table 4.12 and the confusion matrix is listed in Appendix D, Table D.3.

Table 4.12 Classification accuracies of cereal grains from single kernel images obtained using a specialist PNN classifier with morphological features as inputs.

	Classification accuracy for three trials, %			
	1	**2**	**3**	**Mean**
Barley	86.4	88.0	89.4	87.9
CWAD	79.2	83.5	82.2	81.6
CWRS	95.5	96.3	96.0	95.9
Oats	89.7	92.6	90.1	90.8
Rye	89.3	86.0	87.6	87.6

The classification accuracies were low for all the grain types except for CWRS wheat. Table 4.13 lists the top 20 input features in descending order of their contribution for classification when using a specialist PNN classifier.

Table 4.13 The top 20 morphological features based on their respective contribution towards classification accuracy for cereal grains in single kernel images while using a specialist PNN classifier.

	Grain Type				
Rank	**Barley**	**CWAD**	**CWRS**	**Oats**	**Rye**
1	Boundary FD 6	Shape moment 4	Radial FD 4	Boundary FD 2	Minor axis length
2	Minimum radius	Maximum radius	Boundary FD 18	Boundary FD 14	Radial FD 16
3	Radial FD 2	Perimeter	Area	Perimeter	Major axis length
4	Minor axis length	Mean radius	Shape moment 4	Boundary FD 8	Radial FD 3
5	Boundary FD 16	Radial FD 5	Radial FD 2	Area	Boundary FD 3
6	Shape moment 4	Boundary FD 14	Perimeter	Radial FD 2	Boundary FD 14
7	Boundary FD 2	Area	Radial FD 6	Radial FD 5	Boundary FD 2
8	Radial FD 6	Boundary FD 17	Mean radius	Maximum radius	Radial FD 14
9	Boundary FD 13	Radial FD 6	Boundary FD 17	Boundary FD 20	Boundary FD 6
10	Boundary FD 1	Radial FD 4	Major axis length	Boundary FD 16	Radial FD 13

. . . continued . . .

. . . continued Table 4.13 . . .

	Grain type				
Rank	**Barley**	**CWAD**	**CWRS**	**Oats**	**Rye**
11	Boundary FD 20	Boundary FD 4	Maximum radius	Major axis length	Perimeter
12	Radial FD 3	Boundary FD 2	Boundary FD 4	Boundary FD 13	Boundary FD 10
13	Radial FD 5	Radial FD 14	Radial FD 5	Mean radius	Shape moment 4
14	Boundary FD 14	Radial FD 2	Boundary FD 14	Boundary FD 11	Boundary FD 1
15	Radial FD 18	Radial FD 8	Boundary FD 13	Boundary FD 12	Radial FD 7
16	Radial FD 8	Boundary FD 16	Boundary FD 19	Boundary FD 9	Radial FD 12
17	Radial FD 14	Radial FD 3	Radial FD 14	Boundary FD 17	Boundary FD 19
18	Shape moment 1	Radial FD 16	Radial FD 3	Minimum radius	Boundary FD 4
19	Perimeter	Boundary FD 18	Shape moment 3	Boundary FD 4	Boundary FD 8
20	Radial FD 13	Radial FD 11	Radial FD 1	Radial FD 9	Boundary FD 7

For a given grain type, different features have different contribution towards differentiating that particular grain type from other grain types. The performance of different classifiers, when only morphological features are used as inputs, is shown in Figure 4.3. The classification accuracies are the highest using the BPN.

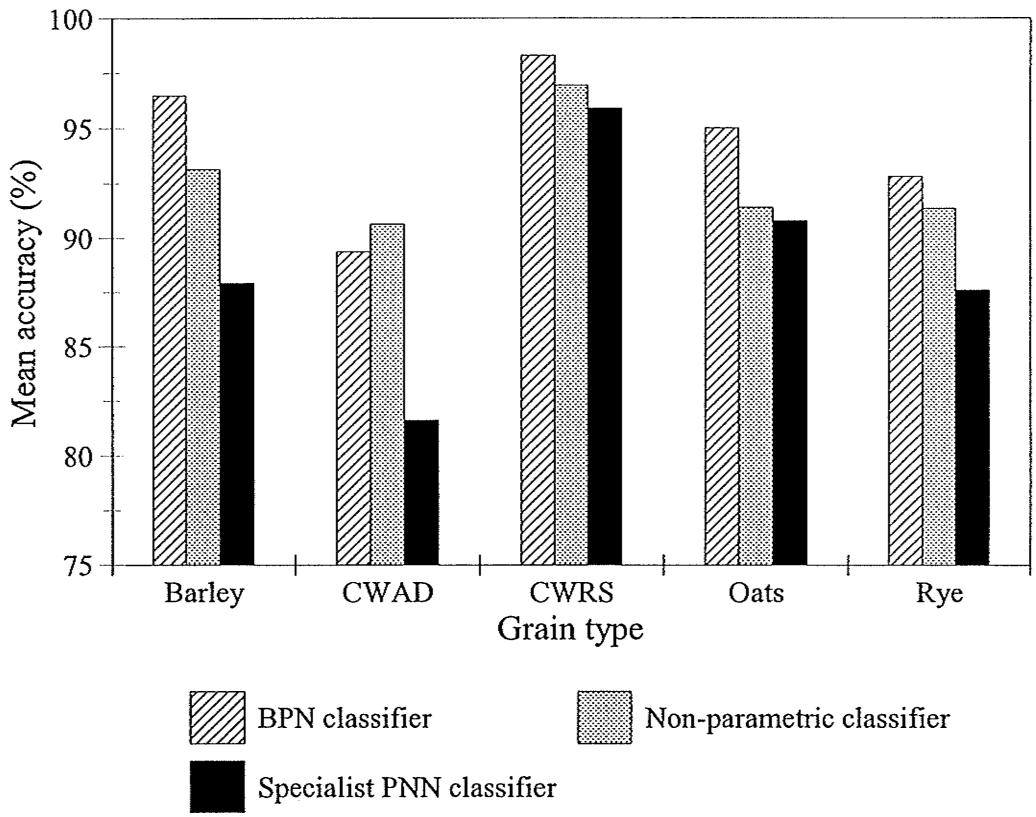

Figure 4.3 Comparison of classification accuracies of the BPN, non-parametric, and specialist PNN classifier with morphological features as inputs.

4.4.2 Analysis using color features

4.4.2.1 BPN classifier A four layer BPN was used to develop a classifier. It consisted of 123 input nodes, 76 nodes in both hidden layers and five output nodes, one for each grain type. The network took 64 h to complete training using 7500 kernels in training and testing sets. The network was trained for 1000 epochs and was then applied on the production data set consisting of 22500 kernels. The summarized results of color analysis are shown in Table 4.14.

Table 4.14 Classification accuracies of cereal grains from single kernel images obtained using a BPN classifier with color features as inputs.

	Classification accuracy for five trials, %					
	1	**2**	**3**	**4**	**5**	**Mean**
Barley	94.0	93.1	95.1	92.5	94.2	93.8
CWAD	90.5	92.2	93.4	95.2	93.3	92.9
CWRS	99.1	98.5	99.4	99.3	98.7	99.0
Oats	92.4	93.8	94.1	93.4	90.8	92.9
Rye	95.4	94.8	95.4	91.8	94.9	94.5

The classification accuracies were high for all the grain types with CWRS wheat getting near perfect results. The confusion matrix (Appendix D, Table D.4) reveals that barley was misclassified as CWAD wheat and oats, CWAD wheat was misclassified as barley and CWRS wheat, oats was misclassifed as barley and rye, and rye was misclassified as CWAD wheat and oats. The top 20 features ranked according to their contributions are listed in Table 4.9. Similar to previous study by Luo et al. (1999a), it was found that the histogram features contributed very little to the classification process. It can be seen that the red color band plays an important role in classification. Three of the top five features are from the red band. Also, Hu's moments appear in four of the top five features making it an important feature for classification purposes.

4.4.2.2 Non-parametric statistical classifier The statistical classifier was developed using SAS software. It consisted of 123 inputs and one output class. The output class had five values, one for each grain type. The classification accuracies obtained are shown in Table 4.15.

Table 4.15 Classification accuracies of cereal grains from single kernel images obtained using a non-parametric statistical classifier with color features as inputs.

	Classification accuracy for five trials, %					
	1	**2**	**3**	**4**	**5**	**Mean**
Barley	71.5	66.1	65.8	80.7	73.5	71.5
CWAD	81.1	80.6	81.7	73.4	78.5	79.1
CWRS	93.6	90.3	90.9	93.0	93.7	92.3
Oats	60.7	68.1	74.5	67.2	63.5	66.8
Rye	87.7	91.2	91.4	81.8	86.7	87.8

The non-parametric statistical classifier, in comparison to BPN, performed the entire training and classification very fast, however, the classification accuracies obtained from it were very low. Other than CWRS wheat, no grain type had classification accuracy over 90%. Looking at the confusion matrix (Appendix D, Table D.5), it can be inferred that misclassification for barley, CWAD wheat, and oats was simlar to BPN. Rye, in this case, was mainly misclassified as CWRS wheat. The top 20 color features, based on their contribution for classification, are listed in Table 4.11. Similar to that of the BPN, three of the top five features were from the red band, however, the features and their rankings are quite different from the top 20 color features from the BPN analysis.

4.4.2.3 Specialist PNN classifier A specialist PNN used to develop a classifier consisted of five sub-networks, each consisting of 123 input nodes, 7500 nodes in the hidden layer and two output nodes. The summarized results of color analysis are shown in Table 4.16.

Table 4.16 Classification accuracies of cereal grains from single kernel images obtained using a specialist PNN classifier with color features as inputs.

	Classification accuracy for three trials, %			
	1	**2**	**3**	**Mean**
Barley	87.8	91.7	90.3	89.9
CWAD	81.6	79.2	79.4	80.1
CWRS	94.7	93.8	95.2	94.6
Oats	71.8	80.0	73.0	74.9
Rye	87.6	92.8	89.4	89.9

The classification accuracies were low for all the grain types except CWRS wheat. The confusion matrix (Appendix D, Table D.6) shows that the misclassification trend of all the grain types was similar to the non-parametric statistical classifier confusion matrix. Table 4.17 lists the top 20 input features in descending order of their contribution to classification when using a specialist PNN classifier. The color histogram plays an important role is classifying CWAD wheat and rye kernels, whereas the moment features are more important in classifying CWRS wheat and oats kernels. Barley features both histogram features and moments in the top five features. Rye mainly used the red band, whereas CWAD wheat used data from the blue and the green band. CWRS wheat and oats also showed preference for the red band, whereas barley used all the color bands in the top five features.

Table 4.17 The top 20 color features based on their respective contribution towards classification accuracy for cereal grains in single kernel images while using a specialist PNN classifier.

	Grain Type				
Rank	**Barley**	**CWAD**	**CWRS**	**Oats**	**Rye**
1	Red moment 1	Hue mean	Red moment 1	Red moment 2	Red histogram range 30
2	Blue histogram range 27	Blue histogram range 32	Red moment 2	Hue mean	Red histogram range 17
3	Red histogram range 25	Blue histogram range 1	Blue histogram range 10	Red moment 1	Red histogram range 25
4	Blue histogram range 19	Green histogram range 15	Green moment 2	Green moment 2	Red histogram range 15
5	Blue moment 4	Red histogram range 20	Hue mean	Intensity range	Green histogram range 30
6	Blue variance	Red histogram range 9	Red moment 3	Blue histogram range 28	Blue moment 4
7	Red histogram range 21	Red moment 2	Blue histogram range 17	Blue histogram range 31	Red mean
8	Red histogram range 19	Blue histogram range 25	Blue histogram range 1	Blue histogram range 32	Blue histogram range 28
9	Red histogram range 7	Red moment 1	Red histogram range 23	Red histogram range 5	Red histogram range 19
10	Blue moment 1	Green histogram range 12	Red histogram range 19	Blue moment 1	Red moment 2

. . . continued . . .

. . . continued Table 4.17 . . .

	Grain type				
Rank	**Barley**	**CWAD**	**CWRS**	**Oats**	**Rye**
11	Red histogram range 32	Green moment 1	Green histogram range 18	Red histogram range 10	Red histogram range 21
12	Red histogram range 12	Red histogram range 16	Red histogram range 7	Green histogram range 23	Blue histogram range 13
13	Green moment 4	Blue histogram range 30	Blue histogram range 12	Blue histogram range 27	Green histogram range 28
14	Red histogram range 31	Blue histogram range 23	Green histogram range 2	Blue histogram range 12	Red histogram range 32
15	Red histogram range 10	Red histogram range 11	Green histogram range 28	Saturation mean	Blue moment 2
16	Red histogram range 11	Blue histogram range 3	Red histogram range 9	Blue histogram range 29	Red histogram range 16
17	Green moment 2	Green histogram range 18	Blue histogram range 32	Blue histogram range 24	Red histogram range 18
18	Red moment 3	Saturation mean	Red histogram range 27	Blue histogram range 11	Green moment 1
19	Red histogram range 8	Red histogram range 30	Green histogram range 15	Red histogram range 25	Blue histogram range 29
20	Blue histogram range 6	Green histogram range 30	Red histogram range 31	Blue moment 4	Green histogram range 12

The performance of different classifiers, when only color features are used as inputs, is shown in Figure 4.4.

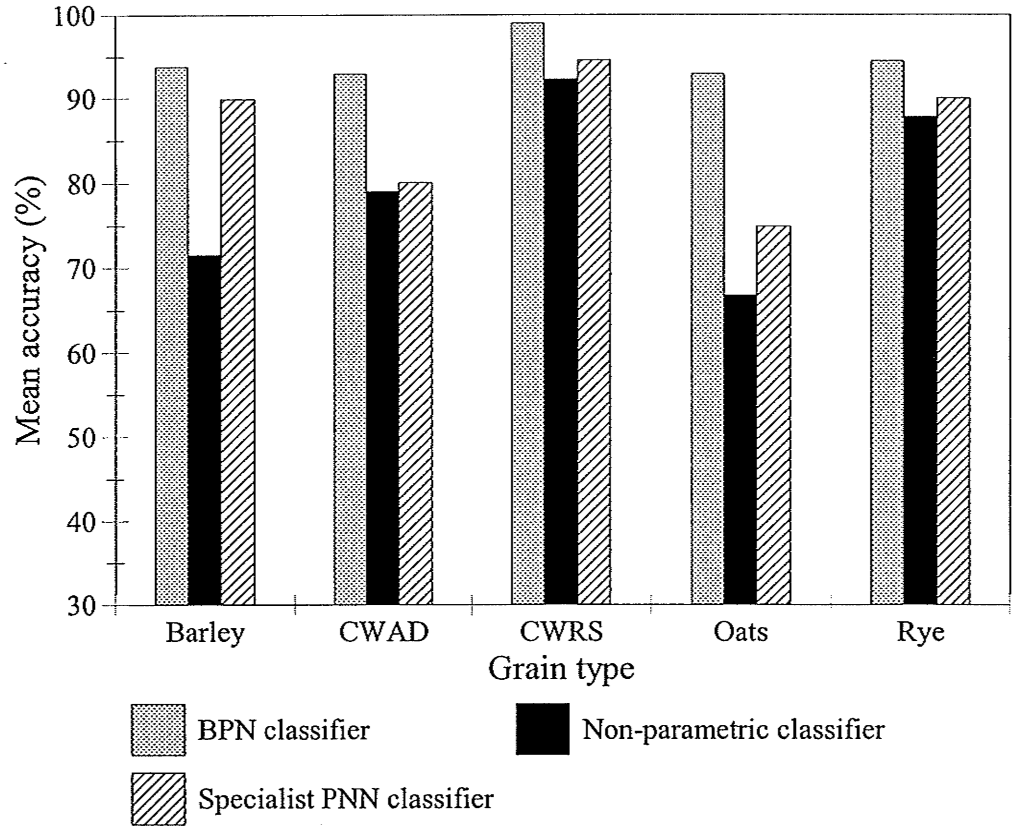

Figure 4.4 Comparison of classification accuracies of the BPN, non-parametric, and specialist PNN classifier with color features as inputs.

The classification accuracy of CWRS wheat was highest no matter what classifier was used. The BPN outperformed specialist PNN and non-parametric statistical classifier. The performance of the specialist network improved compared to that using just the morphological features. The results are consistent with the findings of Luo et al. (1999b) who demonstrated the superiority of neural network classifier over non-parametric classifier while using color features.

4.4.3 Analysis using textural features

4.4.3.1 BPN classifier A 4 layer BPN was used to develop a classifier. It consisted of 56 input nodes, 58 nodes in both hidden layers and five output nodes, one for each grain type. The network took 15 h to complete training using 7500 kernels in training and testing sets. The network was trained for 1000 epochs and was then applied on the production data set consisting of 22500 kernels. The summarized results of textural analysis are shown in Table 4.18.

Table 4.18 Classification accuracies of cereal grains from single kernel images obtained using a BPN classifier with textural features as inputs.

	Classification accuracy for five trials, %					
	1	2	3	4	5	Mean
Barley	93.1	96.3	95.9	93.0	92.8	94.2
CWAD	90.6	92.8	91.8	90.8	91.6	91.5
CWRS	94.1	90.4	96.8	96.8	96.1	94.9
Oats	93.9	91.0	89.0	89.7	90.4	90.8
Rye	96.1	96.0	96.2	93.1	94.4	95.2

The classification accuracies obtained using textural features ranged from 90 to 95%. Best results were for rye, closely followed by CWRS wheat and barley. Accuracies for CWAD wheat and oats were low in comparison to other grains. The CWAD wheat kernels were mainly misclassifed as CWRS wheat kernels, whereas, oats was misclassified as barley (Appendix D, Table D.7). The top 20 features ranked according to their contributions are listed in Table 4.9. For textural analysis, green band played a vital role. Four of the top five textural features were from the green band. Also, co-occurrence matrix features were more important than run length matrix features. Figure 4.5 shows a comparison of classification accuracies using morphological, color, and textural features with a BPN classifier.

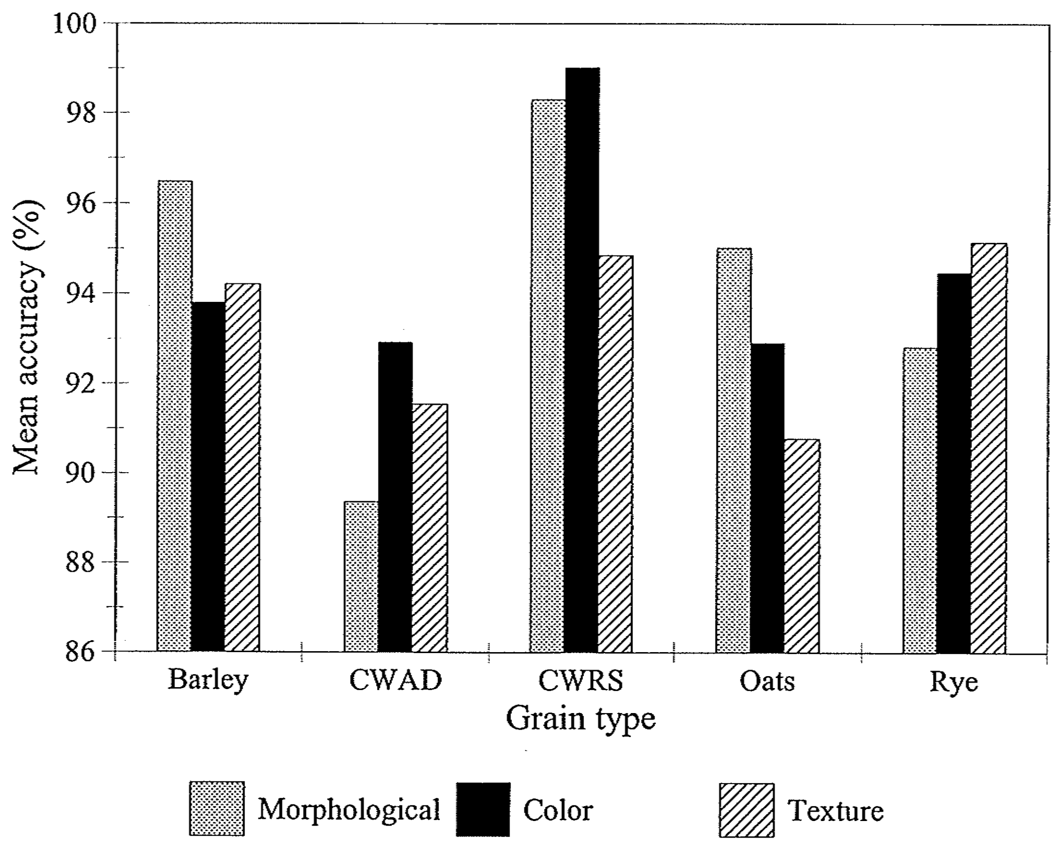

Figure 4.5 Classification accuracies of the BPN classifier using morphological, color and textural features as inputs.

Classification accuracies for grains changed when using a different features set. Barley and oats were best classified using morphological features, whereas CWAD wheat and CWRS wheat were best classified using color features. Texture alone did not produce good results except for rye. Therefore, further trials were conducted by combining textural features with other features sets to increase the classification accuracy.

4.4.3.2 Non-parametric statistical classifier The statistical classifier was developed using SAS software. It consisted of 56 inputs and one output class. The output class had five values, one for each grain type. The classification accuracies obtained are shown in Table 4.19.

Table 4.19 Classification accuracies of cereal grains from single kernel images obtained using a non-parametric statistical classifier with textural features as inputs.

	Classification accuracy for five trials, %					
	1	**2**	**3**	**4**	**5**	**Mean**
Barley	91.7	91.3	90.9	90.8	92.4	91.4
CWAD	92.2	93.2	92.4	92.3	92.5	92.5
CWRS	95.2	96.3	97.0	94.7	94.6	95.6
Oats	89.8	92.2	92.7	90.7	90.0	91.1
Rye	96.9	96.9	96.2	94.4	96.5	96.2

The results for the non-parametric statistical classifier using textural features improved in comparison to color analysis. Classification accuracies for CWRS wheat and rye were over 95%, whereas it remained around 92% for the other three grains. Barley was mainly misclassified as oats, CWAD wheat as CWRS wheat, CWRS wheat as rye, and oats was misclassified as barley (Appendix D, Table D.8). The top 20 textural features, based on their contribution for classification, are listed in Table 4.11. Similar to BPN, three of the top five features were from the green band, however, run length matrix features appeared higher in ranking order as compared to co-occurrence matrix features. Figure 4.6 shows a comparison of classification accuracies using morphological, color, and textural features with a non-parametric statistical classifier. The classification accuracies using morphological and textural features gave accuracies over 90%, however, accuracies using color features were low.

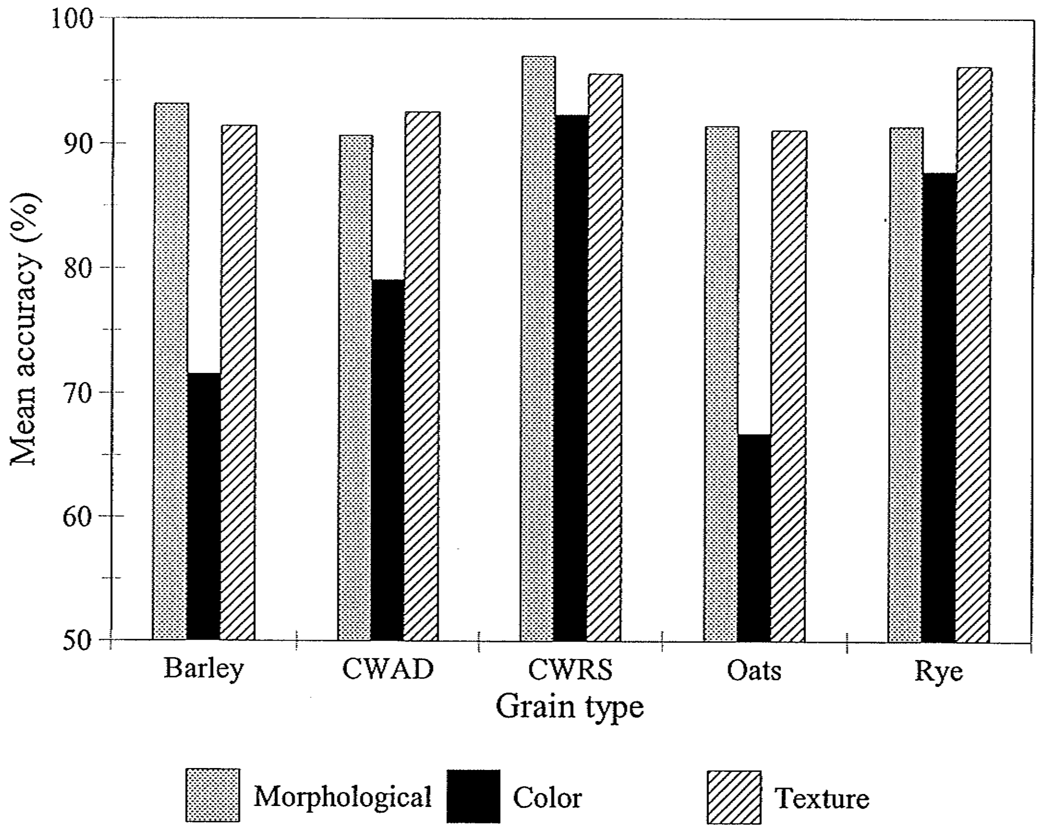

Figure 4.6 Classification accuracies of the statistical classifier using morphological, color and textural features as inputs.

4.4.3.3 Specialist PNN classifier A specialist PNN used to develop a classifier consisted of five sub-networks, each consisting of 56 input nodes, 7500 nodes in the hidden layer and two output nodes. The summarized results of textural analysis are shown in Table 4.20 and the confusion matrix is listed in Appendix D, Table D.9.

The classification accuracies were low for all the grain types with only rye being over 90%. Barley was mainly misclassified as CWAD and CWRS wheat, CWAD wheat was misclassified as CWRS wheat, CWRS wheat was misclassified as rye and CWAD wheat, oats was misclassified as barley and CWAD wheat, and rye was misclassified as CWRS wheat.

Table 4.20 Classification accuracies of cereal grains from single kernel images obtained using a specialist PNN classifier with textural features as inputs.

	Classification accuracy for three trials, %			
	1	**2**	**3**	**Mean**
Barley	86.9	91.3	88.5	88.9
CWAD	80.5	82.5	80.5	81.2
CWRS	88.8	83.6	87.2	86.5
Oats	79.4	79.5	79.4	79.4
Rye	88.7	92.4	89.8	90.3

Table 4.21 lists the top 20 textural features in descending order of their contribution to classification when using a specialist PNN classifier. Of the top 10 features, the run length matrix features appear eight and seven times for barley and CWRS wheat, respectively. For CWAD wheat and rye, co-occurrence matrix features appear eight and seven times, respectively. Barley predominantly uses the green band, whereas CWAD wheat, and oats make use of the blue band data in three of the top five features.

Table 4.21 The top 20 textural features based on their respective contribution towards classification accuracy for cereal grains in single kernel images while using a specialist PNN classifier.

	Grain Type				
Rank	**Barley**	**CWAD**	**CWRS**	**Oats**	**Rye**
1	Green GLRM long run	Blue GLCM homogeneity	Gray GLRM entropy	Blue GLCM variance	Blue GLCM mean
2	Blue GLRM long run	Blue GLRM short run	Gray GLRM run length non-uniformity	Green GLRM short run	Red GLCM mean
3	Green GLCM mean	Blue GLCM variance	Green GLCM correlation	Red GLRM short run	Green GLRM runpercent
4	Green GLRM short run	Red GLRM entropy	Red GLCM correlation	Blue GLCM mean	Green GLRM long run
5	Gray GLRM runpercent	Green GLCM variance	Green GLRM long run	Blue GLCM cluster shade	Blue GLCM variance
6	Green GLRM run length non-uniformity	Gray GLCM inertia	Blue GLRM long run	Green GLRM long run	Green GLCM variance
7	Red GLRM run length non-uniformity	Gray GLCM correlation	Green GLRM short run	Gray GLCM inertia	Red GLCM cluster shade
8	Red GLRM runpercent	Red GLCM cluster shade	Red GLRM long run	Gray GLCM entropy	Gray GLCM cluster shade
9	Gray GLCM variance	Gray GLCM mean	Red GLCM homogeneity	Green GLRM run length non-uniformity	Blue GLCM cluster shade
10	Gray GLRM run length non-uniformity	Blue GLCM entropy	Green GLRM runpercent	Blue GLCM uniformity	Red GLRM long run

. . . continued . . .

. . . continued Table 4.21 . . .

	Grain type				
Rank	**Barley**	**CWAD**	**CWRS**	**Oats**	**Rye**
11	Blue GLCM variance	Blue GLRM long run	Red GLCM variance	Red GLRM long run	Green GLRM short run
12	Blue GLCM correlation	Green GLRM run length non-uniformity	Blue GLRM run length non-uniformity	Blue GLRM run length non-uniformity	Gray GLRM long run
13	Blue GLCM entropy	Blue GLCM mean	Green GLRM run length non-uniformity	Green GLRM entropy	Blue GLRM long run
14	Blue GLRM run length non-uniformity	Red GLCM variance	Blue GLCM mean	Gray GLCM cluster shade	Gray GLCM mean
15	Green GLRM runpercent	Gray GLCM entropy	Blue GLCM variance	Red GLCM variance	Red GLCM inertia
16	Green GLCM cluster shade	Gray GLCM homogeneity	Green GLCM entropy	Gray GLRM long run	Red GLCM correlation
17	Blue GLRM short run	Red GLRM color non-uniformity	Blue GLCM entropy	Red GLCM cluster shade	Green GLCM inertia
18	Gray GLCM cluster shade	Green GLCM correlation	Green GLCM homogeneity	Blue GLCM correlation	Red GLRM runpercent
19	Red GLCM inertia	Gray GLRM entropy	Gray GLCM homogeneity	Blue GLRM long run	Blue GLRM run length non-uniformity
20	Green GLCM uniformity	Red GLRM runpercent	Red GLCM mean	Red GLCM inertia	Blue GLRM short run

The performance of different classifiers, when only textural features are used as inputs, is shown in Figure 4.7.

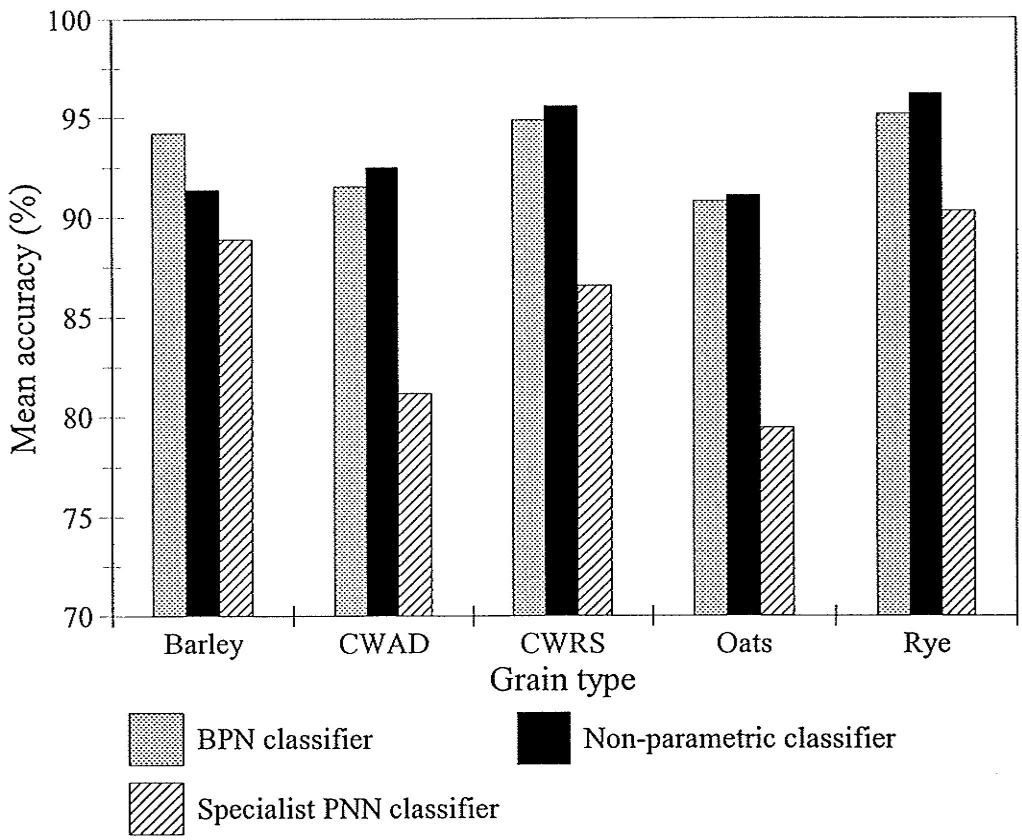

Figure 4.7 Comparison of classification accuracies of the BPN, non-parametric, and specialist PNN classifier with textural features as inputs.

The classification accuracy of BPN and non-parametric statistical classifier were better than those obtained using a specialist PNN classifier. Figure 4.8 shows a comparison of classification accuracies using morphological, color, and textural features with a specialist

PNN classifier.

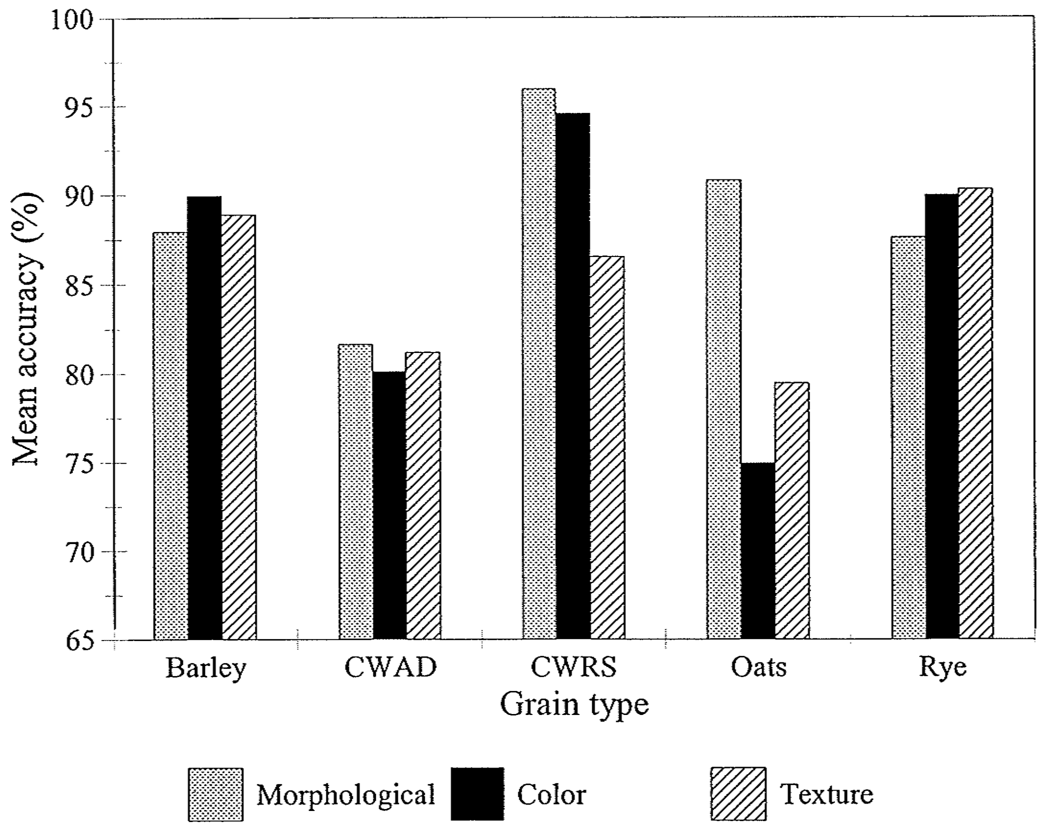

Figure 4.8 Classification accuracies of the specialist PNN classifier using morphological, color and textural features as inputs.

Classification accuracies for barley, CWAD wheat, and rye were in a close range no matter what features set was used. The morphological set gave the best overall results for CWAD wheat, CWRS wheat, and oats.

4.4.4 Analysis using all features

4.4.4.1 BPN classifier A four layer BPN was used to develop a classifier. It consisted of 230 (51 morphological, 123 color, and 56 textural features) inputs, 102 nodes in both the hidden layers and five output nodes, one for each grain type. The network took approximately 75 h to train. The summarized results for all features analysis are shown in Table 4.22.

Table 4.22 Classification accuracies of cereal grains from single kernel images obtained using a BPN classifier with all features as inputs.

	Classification accuracy for five trials, %					
	1	**2**	**3**	**4**	**5**	**Mean**
Barley	97.7	99.0	98.7	98.1	97.6	98.2
CWAD	90.5	91.7	91.9	90.2	90.4	90.9
CWRS	98.3	98.2	98.9	99.2	98.3	98.6
Oats	97.9	98.1	98.8	98.7	98.3	98.4
Rye	99.0	99.6	98.7	98.5	99.2	99.0

Except for CWAD wheat, the classification accuracy for all the grain types was over 98%. Most of the CWAD wheat kernels were mis-classified as CWRS wheat kernels (Appendix D, Table D.10). This could be due to immature CWAD wheat kernels which were closer to CWRS wheat grain kernels in appearance. Inclusion of grain samples from a large number of growing regions and for different growing years resulted in considerable overlap in features of similar looking grain types due to annual and regional variability. Table 4.23 gives the top 20 features ranked in order of their decreasing contribution to the classification process.

Table 4.23 The top 20 features from the all features set based on their respective contribution towards classification accuracy for cereal grains in single kernel images while using a BPN and non-parametric classifier.

	Classifier	
Rank	**Back propagation network**	**Non-parametric**
1	Hue mean	Radial FD 2
2	Minor axis length	Boundary FD 18
3	Boundary FD 2	Radial FD 7
4	Saturation mean	Green GLCM inertia
5	Radial FD 2	Shape moment 2
6	Boundary FD 20	Minor axis length
7	Perimeter	Saturation mean
8	Blue GLRM short run	Green GLCM mean
9	Boundary FD 18	Green range
10	Green GLRM short run	Shape moment 1

. . . continued . . .

. . . continued Table 4.23 . . .

	Classifier	
Rank	**Back propagation network**	**Non-parametric**
11	Gray GLRM short run	Blue GLRM color non-uniformity
12	Boundary FD 3	Green GLRM short run
13	Blue histogram range 1	Blue GLRM entropy
14	Radial FD 5	Radial FD 5
15	Green GLRM runpercent	Green GLCM entropy
16	Green GLRM long run	Shape moment 3
17	Minimum radius	Red GLCM mean
18	Gray GLCM inertia	Red GLRM entropy
19	Boundary FD 16	Green GLRM runpercent
20	Red GLRM short run	Boundary FD 17

The top 20 features using BPN consists of 10 morphological, three color, and seven textural features. Of the three color features, two appear at rank 1 and rank 4 thereby making color an important aspect for grain classification. Although there are a lot of textural features in the top 20 list, their best rank is eight. Run length matrix features contribute more in this model as compared to co-occurrence matrix features.

4.4.4.2 Non-parametric statistical classifier The statistical classifier was developed using SAS software. It consisted of 230 inputs and one output class. The output class had five values, one for each grain type. The classification accuracies obtained are shown in Table 4.24.

Table 4.24 Classification accuracies of cereal grains from single kernel images obtained using a non-parametric statistical classifier with all features as inputs.

	Classification accuracy for five trials, %					
	1	2	3	4	5	Mean
Barley	79.8	93.9	94.8	77.6	79.3	85.1
CWAD	85.0	92.3	92.5	87.7	86.8	88.9
CWRS	99.6	90.1	96.7	99.2	99.1	96.9
Oats	91.8	93.3	98.7	96.0	94.9	95.0
Rye	94.8	97.6	98.8	96.2	94.7	96.4

The non-parametric statistical classifiers gave better results for CWRS wheat, oats, and rye as compared to barley and CWAD wheat, for which the classification accuracies were less than 90%. The barley kernels were misclassified as oats and CWAD wheat kernels were misclassified as CWRS wheat (Appendix D, Table D.11). The all feature model gave better results than those obtained using just one of the morphological, color, or textural features sets. Table 4.23 lists the top 20 input features in descending order of their contribution for classification when using a non-parametric statistical classifier. The top 20 features using non-parametric classifier consists of nine morphological, two color, and nine textural features. Most of the morphological features appear higher in rank making it the most important of the features sets for grain classification using a non-parametric statistical classifier.

4.4.4.3 Specialist PNN classifier A specialist PNN used to develop a classifier consisted of five sub-networks, each of which specialized in one grain type. Each of the sub-networks consisted of 230 input nodes, 7500 nodes in the hidden layer and two output nodes. The network used logistic scaling at the input level. Training and testing was done on 7500 grain kernels (1500 of each grain type) and the entire process was repeated five times using different training and testing data sets. The training was stopped if the minimum error value of the network remained unchanged for 20 training generations. The trained network was then applied on production data set consisting of 22500 kernels. The network took less than a minute to train, however, the calibration procedure took 79 h. The summarized results of all features analysis are shown in Table 4.25. The classification accuracies were over 94% for all the grain types except for CWAD wheat which was misclassified as CWRS wheat for over 10% of the instances (Appendix D, Table D.12).

Table 4.25 Classification accuracies of cereal grains from single kernel images obtained using a specialist PNN classifier with all features as inputs.

	Classification accuracy for three trials, %			
	1	**2**	**3**	**Mean**
Barley	93.9	95.7	95.3	95.0
CWAD	87.3	89.6	87.6	88.2
CWRS	98.6	98.4	98.5	98.5
Oats	94.0	96.2	94.0	94.7
Rye	97.9	98.4	97.7	98.0

The performance of the specialist network improved as compared to that when using just the morphological, color, or textural features set. Table 4.26 lists the top 20 input features in descending order of their contribution for classification when using a specialist PNN classifier. The top three features for barley are from the morphological set making shape an important attribute to distinguish barley from other grain types. Another noticeable feature is the prominence of the blue band in the top 10 features for barley. CWAD wheat makes use of color and textural features from all color bands. Only one morphological feature appears in the top 10 list. The top 10 feature list for CWRS wheat lists only one textural feature. For oats, all the features sets contribute substantially, however, the red band appears most of the time in the list. Rye makes use of the textural features to separate itself from other grain types. The top 10 feature list includes only one morphological feature, whereas textural features appear six times.

Table 4.26 The top 20 features from all features set based on their respective contribution towards classification accuracy for cereal grains in single kernel images while using a specialist PNN classifier.

	Grain Type				
Rank	**Barley**	**CWAD**	**CWRS**	**Oats**	**Rye**
1	Radial FD 2	Saturation mean	Radial FD 2	Gray GLRM short run	Radial FD 6
2	Minor axis length	Hue mean	Hue mean	Boundary FD 2	Gray GLRM short run
3	Boundary FD 16	Red histogram range 24	Major axis length	Blue histogram range 14	Green GLRM long run
4	Blue histogram range 6	Blue histogram range 6	Green GLCM mean	Red histogram range 24	Green histogram range 21
5	Green GLCM homogeneity	Gray GLCM inertia	Boundary FD 20	Blue histogram range 11	Blue histogram range 14
6	Blue histogram range 16	Red GLCM correlation	Radial FD 4	Red moment 1	Red GLCM variance
7	Blue histogram range 7	Green GLRM long run	Red histogram range 1	Red GLRM short run	Green GLRM runpercent
8	Hue range	Green histogram range 6	Blue histogram range 15	Red histogram range 30	Red GLRM short run
9	Gray GLRM entropy	Boundary FD 8	Boundary FD 2	Radial FD 2	Red GLRM long run
10	Blue GLCM cluster shade	Green histogram range 18	Green histogram range 23	Minimum radius	Blue histogram range 26

. . . continued . . .

. . . continued Table 4.26 . . .

Rank	Grain type				
	Barley	**CWAD**	**CWRS**	**Oats**	**Rye**
11	Boundary FD 20	Green GLRM color non-	Green mean	Blue GLRM short run	Red GLCM mean
12	Blue histogram range 24	Radial FD 4	Gray GLRM runpercent	Green histogram range 3	Maximum radius
13	Green histogram range 28	Blue histogram range 26	Green histogram range 30	Boundary FD 11	Radial FD 8
14	Blue histogram range 15	Green histogram range 11	Boundary FD 18	Green histogram range 19	Green GLCM cluster
15	Gray GLCM inertia	Major axis length	Blue histogram range 18	Blue histogram range 30	Red GLCM uniformity
16	Hue mean	Boundary FD 12	Radial FD 19	Blue histogram range 13	Green moment 1
17	Red histogram range 27	Boundary FD 15	Red histogram range 6	Red histogram range 2	Radial FD 1
18	Boundary FD 13	Blue histogram range 18	Red histogram range 28	Blue histogram range 31	Red mean
19	Green histogram range 30	Green histogram range 7	Minimum radius	Green histogram range 24	Blue moment 2
20	Minimum radius	Boundary FD 16	Red variance	Red histogram range 3	Boundary FD 16

The performance of different classifiers, when all features were used as inputs, is shown in Figure 4.9.

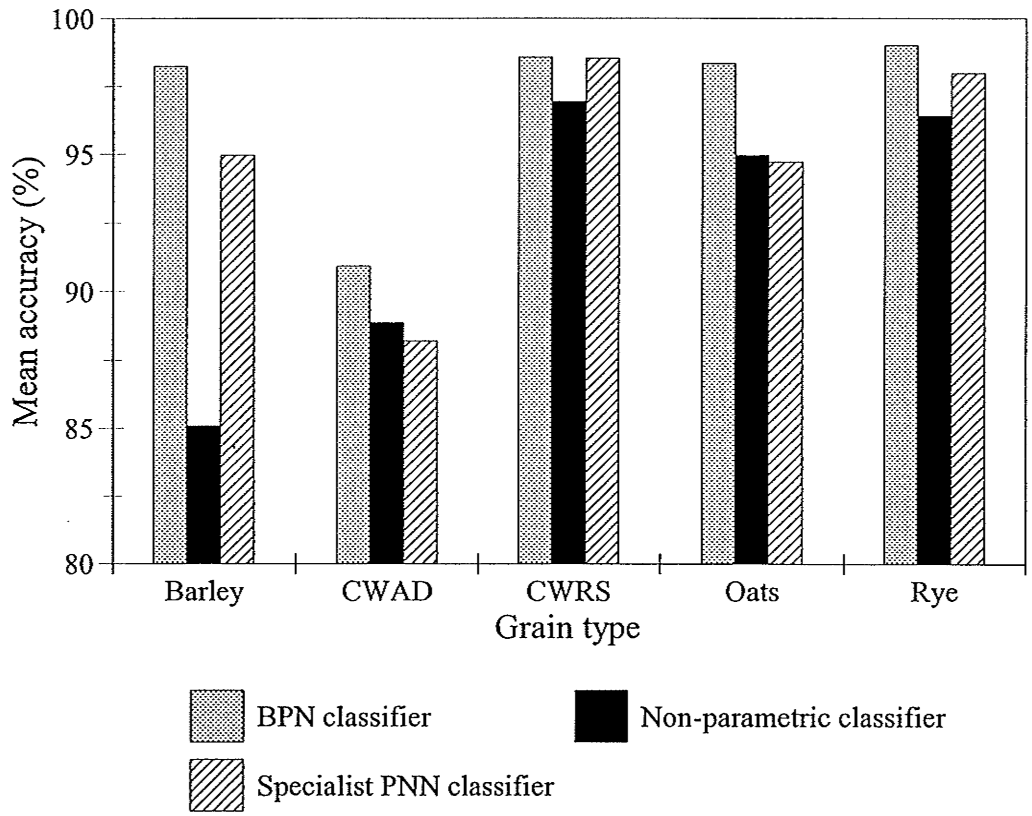

Figure 4.9 Comparison of classification accuracies of the BPN, non-parametric, and specialist PNN classifier with all features as inputs.

The BPN classifier gave the best results for all grain types, followed by the specialist PNN classifier and the non-parametric statistical classifier. Classification accuracies using BPN were in high 90s except for CWAD wheat, for which all the classifiers showed a drop in performace. The specialist PNN classifier shows a trend similar to the BPN, however, the accuracies remained slightly low. For the non-parametric classifier, except for barley, the trend was similar to the other two classifiers for the remaining grain types.

4.4.5 Analysis using the combined 60 features set

4.4.5.1 BPN classifier A four layer BPN was used to develop a classifier. It consisted of 60 (top 20 morphological, top 20 color, and top 20 textural features) inputs, 60 nodes in both hidden layers and five output nodes, one for each grain type. The network used logistic scaling and activation functions at input and processing levels, respectively. Training and testing was done on 7500 grain kernels (1500 of each grain type) and the entire process was repeated five times using different training and testing data sets. The network was trained for 1000 epochs and was then applied on a production data set consisting of 22500 kernels. The network took approximately 28 h to train. The summarized results of the combined 60 features set analysis are shown in Table 4.27.

Table 4.27 Classification accuracies of cereal grains from single kernel images obtained using a BPN classifier with the combined 60 features as input.

	Classification accuracy for five trials, %					
	1	2	3	4	5	Mean
Barley	97.6	98.8	98.0	98.5	97.7	98.1
CWAD	90.2	90.6	91.7	90.5	89.7	90.5
CWRS	98.6	98.9	98.1	98.7	99.0	98.7
Oats	97.6	98.6	99.1	98.6	97.9	98.4
Rye	98.8	99.1	99.0	98.8	98.9	98.9

Except for CWAD wheat, the classification accuracy for all the grain types was over 98%. The confusion matrix shows that in 8.28% instances, CWAD wheat was misclassified as CWRS wheat (Appendix D, Table D.13). The classification accuracies did not change in comparison to all features model even after eliminating a large number of features. This suggests that many of the features extracted were redundant and increased unnecessary complexity in the classifier without actually contributing towards the final output. This redundancy of features was also reported by Luo et al (1999a).

4.4.5.2 Non-parametric statistical classifier The statistical classifier was developed using SAS software. It consisted of 60 inputs and one output class. The output class had five values, one for each grain type. The classification accuracies obtained are shown in Table 4.28.

Table 4.28 Classification accuracies of cereal grains from single kernel images obtained using a non-parametric statistical classifier with the combined 60 features as input.

	Classification accuracy for five trials, %					
	1	**2**	**3**	**4**	**5**	**Mean**
Barley	89.2	96.3	93.8	86.5	85.9	90.4
CWAD	90.2	91.7	88.1	91.0	90.4	90.3
CWRS	99.0	98.4	89.9	99.0	98.9	97.1
Oats	94.5	97.3	96.4	95.2	95.3	95.8
Rye	98.0	98.7	98.0	97.9	97.5	98.0

The non-parametric statistical classifiers gives better results when using the combined 60 features set as compared to all features set. This clearly suggests that the redundant features in the all features set had an adverse affect on the classification accuracies. The overall performance of the classifier improved with accuracies of all grain types being over 90%. For CWRS wheat, oats, and rye, the accuracies were over 95%. Barley was misclassified as oats and CWAD wheat again was misclassified as CWRS wheat in 8.0% of the instances (Appendix D, Table D.14).

4.4.5.3 Specialist PNN classifier A specialist PNN used to develop a classifier consisted of five sub-networks, each of which specialized in one grain type. Each of the sub-networks consisted of 60 input nodes, 7500 nodes in the hidden layer and two output nodes. The network used logistic scaling at the input level. The network took less than a minute to train, however, the calibration procedure took 47 h. The summarized results of the combined 60 features set analysis are shown in Table 4.29.

Table 4.29 Classification accuracies of cereal grains from single kernel images obtained using a specialist PNN classifier with the combined 60 features as input.

	Classification accuracy for three trials, %			
	1	**2**	**3**	**Mean**
Barley	93.1	94.1	94.6	93.9
CWAD	88.2	90.1	88.6	89.0
CWRS	98.5	98.3	98.4	98.4
Oats	96.1	96.5	95.2	95.9
Rye	97.6	97.6	97.5	97.6

The classification accuracies were over 93% for all the grain types except for CWAD wheat which like other classifiers got misclassified as CWRS wheat for 9.8% of the kernels in the production set (Appendix D, Table D.15). The performance of the specialist network did not decrease when compared to the all features model even though the number of features decreased to 60 from 230. Thus, we can conclude that there were a lot of redundant features in the all features set.

The performance of different classifiers, when the combined 60 features were used as inputs, is shown in Figure 4.10. The BPN classifier gives best results for all grain types, whereas the non-parametric statistical classifier performed the worst. Classification accuracies using BPN were in the high 90s except for CWAD wheat, for which all the classifiers showed a drop in performance. The specialist PNN classifier shows a trend similar to the BPN, however, the accuracies remained slightly lower in comparison to the BPN but were better than for the non-parametric classifier.

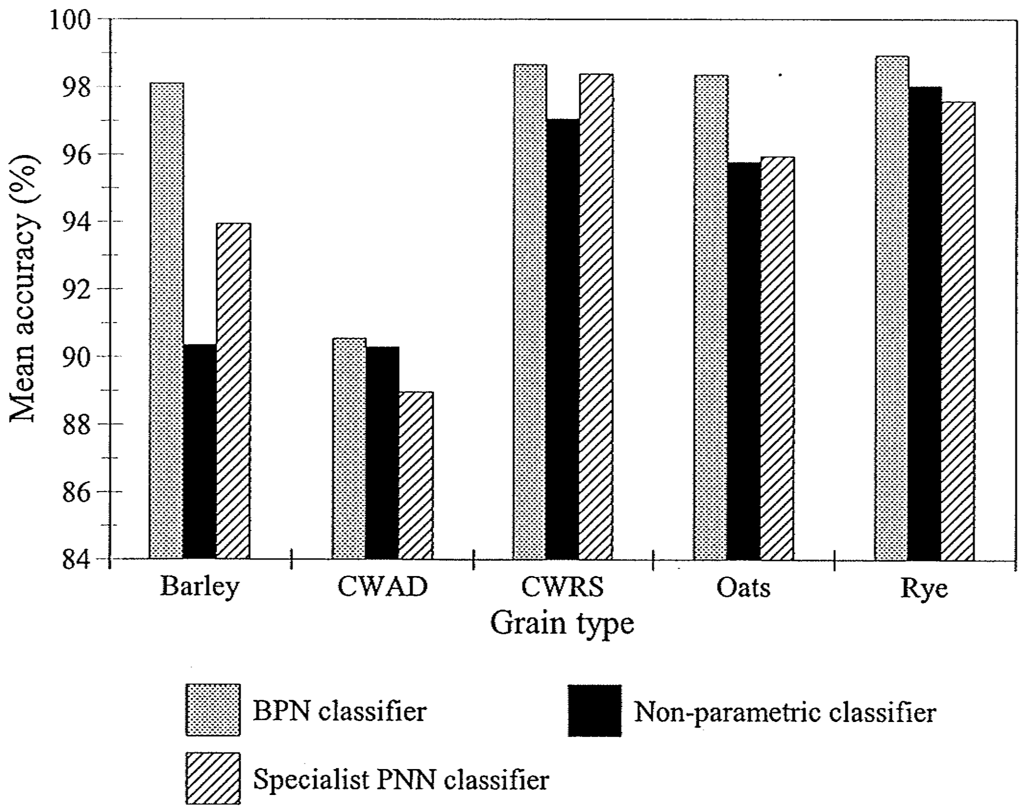

Figure 4.10 Comparison of classification accuracies of the BPN, non-parametric, and specialist PNN classifier with the combined 60 features as inputs.

4.4.6 Analysis using the combined 30 features set

4.4.6.1 BPN classifier A four layer BPN was used to develop a classifier. It consisted of 30 (top 10 morphological, top 10 color, and top 10 textural features) inputs, 52 nodes in both hidden layers and five output nodes, one for each grain type. The network used logistic scaling and activation functions at input and processing levels, respectively. Training and testing were done on 7500 grain kernels (1500 of each grain type) and the entire process was repeated five times using different training and testing data sets. The network was trained for 1000 epochs and was then applied to the production data set consisting of 22500 kernels. The network took approximately 10 h to train. The summarized results for the combined 30 features analysis are shown in Table 4.30.

Table 4.30 Classification accuracies of cereal grains from single kernel images obtained using a BPN classifier with the combined 30 features as input.

	Classification accuracy for five trials, %					
	1	2	3	4	5	Mean
Barley	97.8	98.3	97.3	98.4	97.8	97.9
CWAD	89.3	90.4	91.5	90.0	89.3	90.1
CWRS	98.5	98.8	98.2	98.4	98.5	98.5
Oats	97.2	98.4	98.7	97.3	97.3	97.8
Rye	97.8	98.4	98.2	98.1	97.8	98.0

Except for CWAD wheat, the classification accuracy for all the grain types was over 97%. More than 8% of CWAD wheat kernels were misclassified as CWRS wheat kernels (Appendix D, Table D.16). The classification accuracies slightly decreased for oats and rye as compared to the all features and the combined 60 features model. This suggests that some of the useful features were also dropped when the features set was reduced from 60 to 30 features. Figure 4.11 shows a comparison of the classification accuracies obtained for the combined 30, the combined 60, and all features sets.

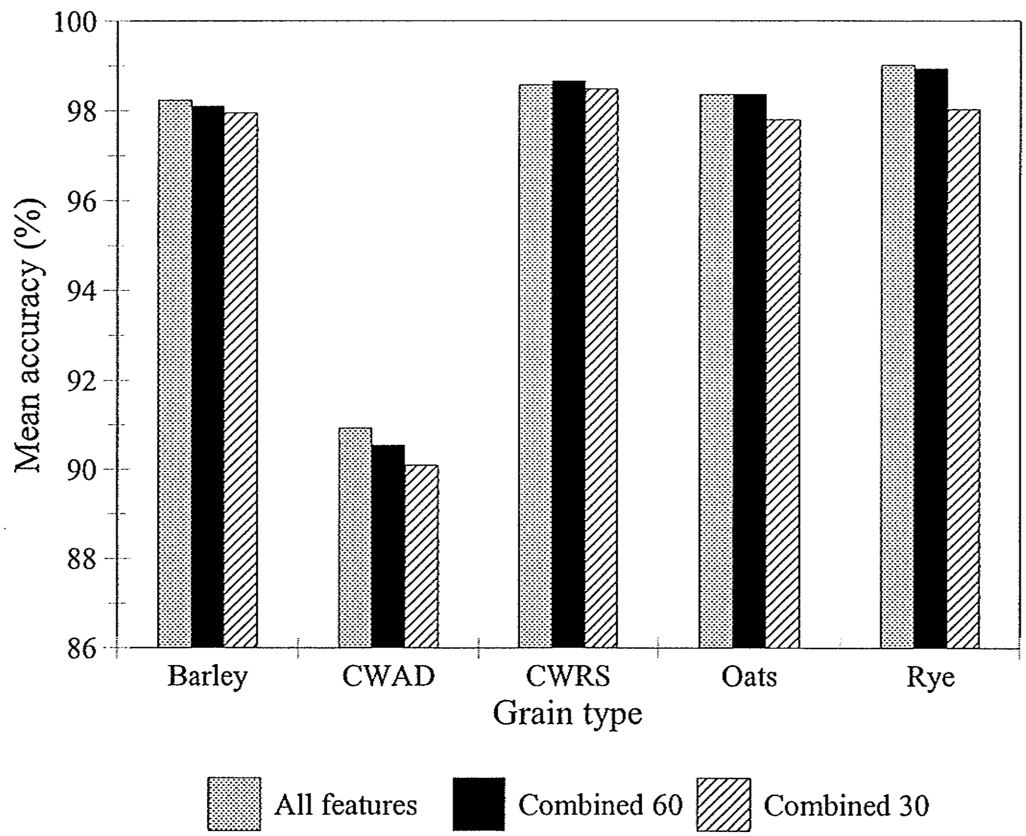

Figure 4.11 Classification accuracies of the BPN classifier using the combined 30, the combined 60, and all features as inputs.

The analysis of variance, however, revealed that the classification accuracies obtained using different classifiers were not significantly different ($P<0.05$) for barley, CWAD wheat, and CWRS wheat. Hence, the classifier using the combined 30 features set can be used for grain classification analysis using a BPN because it greatly reduces the computational time for feature extraction and classification processes without compromising greatly on the classification accuracies for oats and rye.

4.4.6.2 Non-parametric statistical classifier The statistical classifier was developed using SAS software. It consisted of 30 inputs and one output class. The output class had five values, one for each grain type. The classification accuracies obtained are shown in Table 4.31. Classification accuracies remained above 90% for all grain types. For barley and rye, the accuracies were over 95%. Confusion matrix results are shown in Appendix D, (Table D.17).

Table 4.31 Classification accuracies of cereal grains from single kernel images obtained using a non-parametric statistical classifier with the combined 30 features as input.

	Classification accuracy for five trials, %					
	1	2	3	4	5	Mean
Barley	95.5	96.4	94.7	94.9	93.9	95.1
CWAD	89.7	91.8	90.0	90.8	90.7	90.6
CWRS	98.3	98.2	98.2	75.0	98.3	93.6
Oats	93.5	96.0	93.9	96.3	93.7	94.7
Rye	98.0	98.0	97.6	98.7	98.4	98.2

Figure 4.12 shows a comparison of the classification accuracies obtained for the combined 30, the combined 60, and all features sets using a non-parametric classifier. The analysis of variance showed that the classification accuracies of CWAD wheat, oats, and rye were statistically similar ($P<0.05$) for all the three features sets. The classification accuracy for barley was the highest using the combined 30 features model, whereas it gave the worst

results for CWRS wheat. The combined 60 features model gave the best results for CWRS wheat but its accuracy with barley was low. Considering the overall classification accuracy, the combined 30 features set can be used for grain classification analysis using a non-parametric statistical classifier because it gives the best results for all grain types except CWRS wheat, for which its performance is better than that of the combined 60 features model for barley.

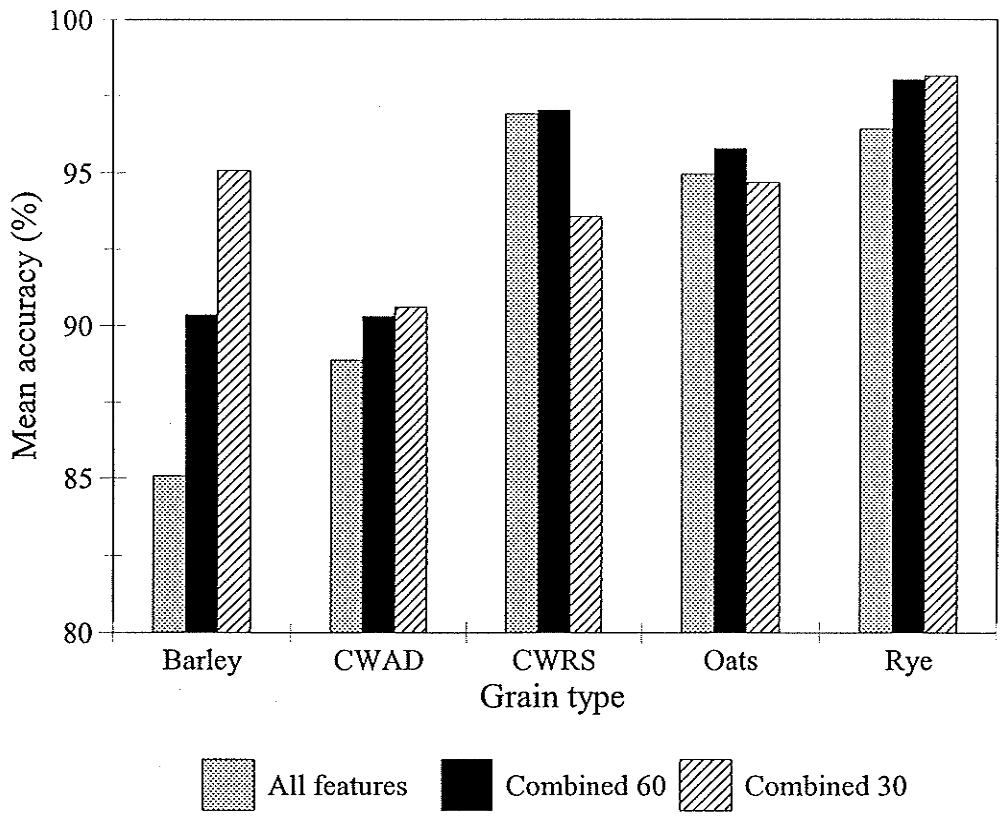

Figure 4.12 Classification accuracies of the non-parametric statistical classifier using the combined 30, the combined 60, and all features sets as inputs.

4.4.6.3 Specialist PNN classifier A specialist PNN used to develop a classifier consisted of five sub-networks, each of which specialized in one grain type. Each of the sub-networks consisted of 30 input nodes, 7500 nodes in the hidden layer and two output nodes. The network took less than a minute to train, however, the calibration procedure took 33 h. The summarized results of the combined 30 features analysis are shown in Table 4.32 and the confusion matrix is shown in Appendix D, Table D.18.

Table 4.32 Classification accuracies of cereal grains from single kernel images obtained using a specialist PNN classifier with the combined 30 features as input.

	Classification accuracy for three trials, %			
	1	2	3	Mean
Barley	92.2	94.0	94.9	93.7
CWAD	87.6	89.2	87.2	88.0
CWRS	98.4	98.3	98.3	98.3
Oats	94.8	96.2	93.4	94.8
Rye	96.6	97.1	96.6	96.8

The classification accuracies were over 93% for all the grain types except for CWAD wheat. Closer examination of the data revealed that most of the misclassified CWAD wheat kernels were classified as CWRS wheat. Figure 4.13 shows a comparison of the classification accuracies obtained using the BPN, non-parametric statistical, and specialist PNN classifiers for the combined 30 features set. The BPN outperformed non-parametric statistical and specialist PNN classifier. It gave the highest classification for all grain types except for CWAD wheat, for which it was second highest. The non-parametric statistical classifier had the best results for CWAD wheat and rye, whereas the specialist PNN had thesame results as the BPN for CWRS wheat. The performance of the non-parametric statistical classifier was better than the specialist PNN classifier for barley, CWAD wheat, and rye, and it matched the results for oats, thereby, making it a better choice of the two classifiers.

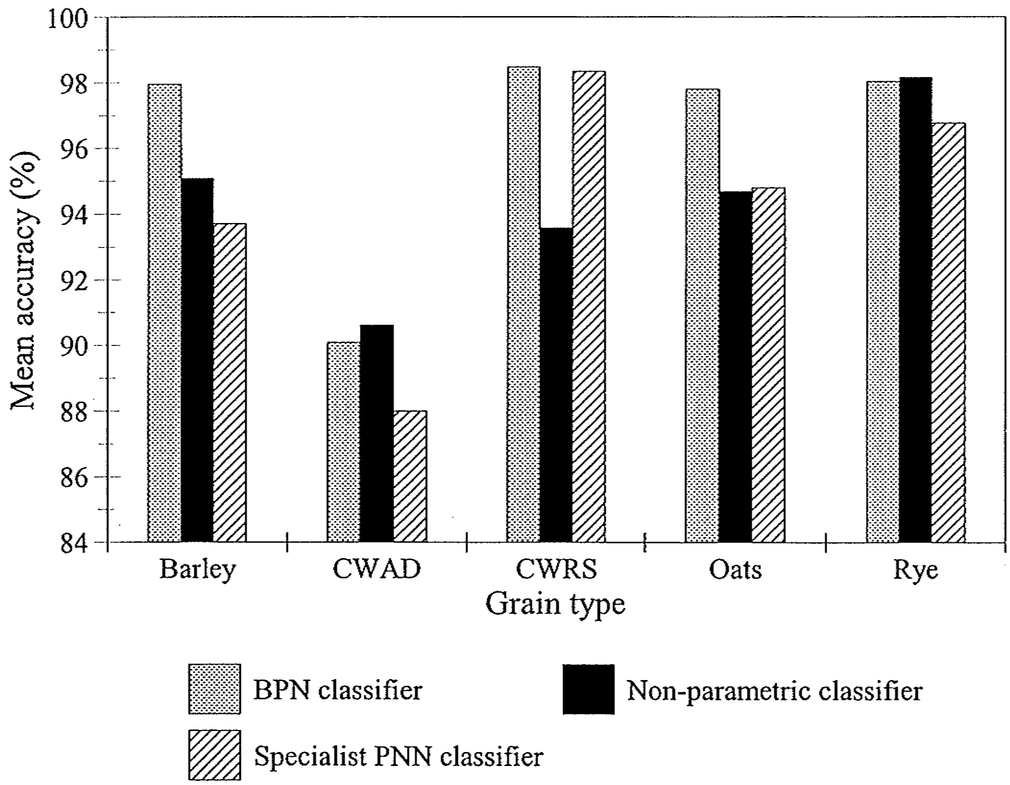

Figure 4.13 Comparison of classification accuracies of the BPN, non-parametric, and specialist PNN classifier with the combined 30 features sets as inputs.

Figure 4.14 shows a comparison of the classification accuracies obtained for the combined 30, the combined 60, and all features sets using a specialist PNN classifier. Further analysis of results using analysis of variance show that the classification accuracies were not statistically different. Therefore, the combined 30 features set is recommended for grain classification when using a specialist PNN classifier.

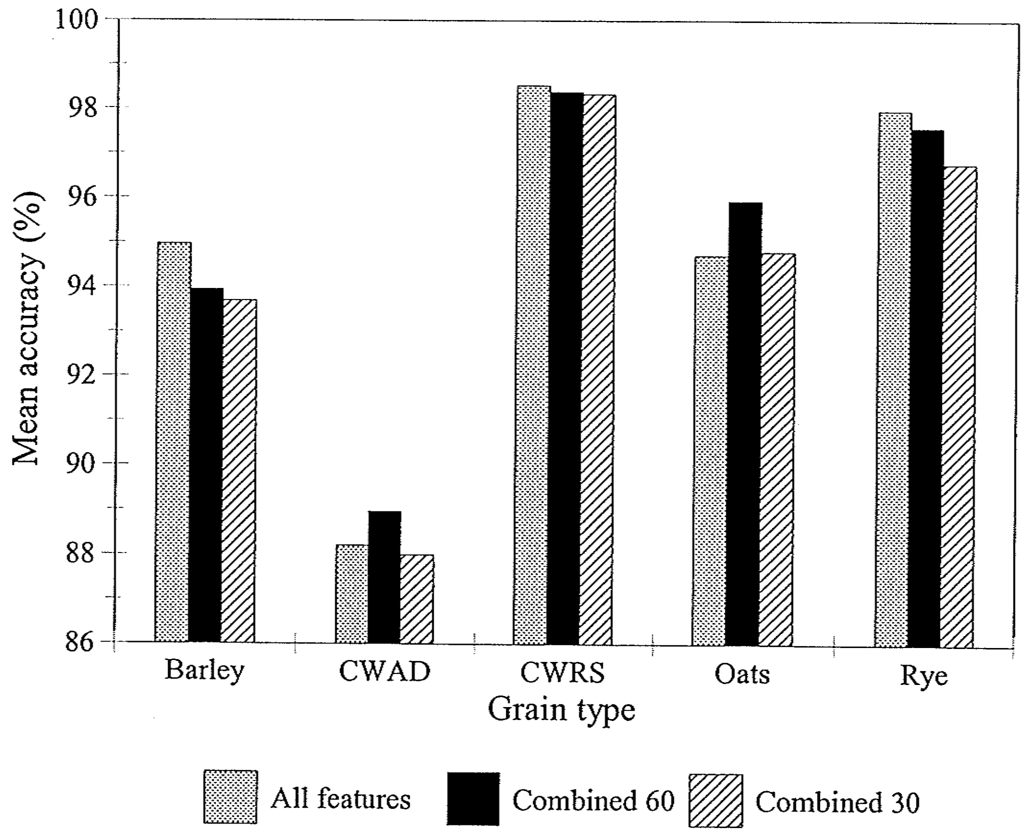

Figure 4.14 Classification accuracies of the specialist PNN classifier using the combined 30, the combined 60, and all features sets as inputs.

4.5 CWAD-CWRS specialist network

Analysis of the BPN, SPNN, and non-parametric statistical classifier showed that for all the instances, CWAD wheat was often misclassified as CWRS wheat. To combat this situation, a CWAD-CWRS specialist network (CCSN) was developed and tested in conjunction with the SPNN network using the combined 60 features. The CCSN had an architecture similar to a specialist sub-network except that it used a total of the best 30 features common to the CWAD combined 60 specialist network, the CWRS combined 60 specialist network, and all the features CCSN. Hence, the network consisted of 30 input, 7500 hidden, and two output nodes. The network was trained using a data set that consisted of just the CWAD and CWRS wheat kernels. So, using a CCSN, a modified SPNN was developed whose functioning is described as follows:

1. In the first step, an unknown grain kernel was presented to the SPNN using the combined 60 features set.

2. If the grain kernel was classified (or misclassified) as barley, oats, or rye, the classification process stopped and the unknown kernel was assigned the class determined by the network.

3. If the grain kernel was classified as CWAD or CWRS wheat, its top 30 features (as determined above) were presented to the CCSN. The output of the CCSN was assigned as the class of the unknown grain kernel. The classification accuracies obtained from modified SPNN are shown in Table 4.33 and the list of features used is shown in Table 4.34.

Table 4.33 Classification accuracies of CWAD and CWRS wheat kernels obtained using a CCSN for grain kernels that were classified as CWAD or CWRS wheat kernels by the combined 60 features set based SPNN.

	Classification accuracy for three trials, %			
	1	**2**	**3**	**Mean**
CWAD	92.0	92.2	92.1	92.1
CWRS	98.1	98.3	98.6	98.3

The confusion matrix of the modified SPNN is shown in Appendix D, Table D.19. The results indicate that the classification accuracies improved significantly ($P<0.05$ for paired t-test) for CWAD wheat but did not improve for CWRS wheat. The reason for that is there was not much scope of improvement for CWRS grain kernels, whereas 9.75% of CWAD kernels were initially misclassified as CWRS wheat (Appendix D, Table D.15).

Table 4.34 The top 30 features used in the modified SPNN that were common to the CWAD specialist network, the CWRS specialist network, and the all features CCSN.

Rank	Features	Rank	Features
1	Radial FD 2	16	Blue histogram range 1
2	Blue histogram range 23	17	Blue GLRM long run
3	Radial FD 5	18	Red GLCM cluster shade
4	Blue histogram range 32	19	Red histogram range 31
5	Hue mean	20	Radial FD 1
6	Saturation mean	21	Red histogram range 7
7	Radial FD 6	22	Blue histogram range 30
8	Boundary FD 2	23	Blue histogram range 10
9	Green GLCM correlation	24	Green moment 1
10	Boundary FD 18	25	Green histogram range 30
11	Red histogram range 23	26	Gray GLCM mean
12	Red moment 1	27	Radial FD 3
13	Red GLCM variance	28	Green GLRM runpercent
14	Red histogram range 9	29	Boundary FD 19
15	Red moment 2	30	Gray GLCM entropy

4.6 Comparison of Area and Line Scan Camera Performances

Single kernel images of 150 barley, CWAD wheat, CWRS wheat, oats, and rye kernels were acquired using an area and a line scan camera and seven size-based morphological features were extracted for images from both the sources. The features set consisted of area, perimeter, major axis, minor axis, minimum radius, maximum radius, and mean radius. Statistical comparison was done to determine the variability in features obtained using two different types of image acquisition systems.

The images from area scan camera were obtained by manually placing the grain kernels in the field of view using a pair of tweezers, whereas the kernels were randomly dropped on to the primary belt of the dual conveyor belt system from the vibratory hopper. The use of vibratory feeder and dual conveyor belt system resulted in over 93% instances of single kernels. The differential belt speed resulted in separation of touching kernels along the direction of the belt movement, however, instances of kernel occlusion remained after kernels fell from the primary to the secondary belt with kernels touching on their sides. The design can be further improved by adding a comb-like object perpendicular to the direction of movement of the primary and/or the secondary conveyor belts and by using a conveyor belt with grooves to increase sidewards separation.

Two types of analysis were carried out for comparison. For the first study, images of 150 kernels were taken using the area scan camera and the same kernels were imaged using a line scan camera. The results from this study are shown in Table 4.35. The features extracted using the area and the line scan cameras were very close to each other. The slight difference (< 1%) in the mean and standard deviation values is because of the different orientations in which the grain kernels rest when placed after moving from one camera's FOV to the other's. Another source of variation can be the different illumination techniques used for the area and the line scan cameras. For the area scan camera, the kernel is illuminated from all sides due to the diffused light from the illumination chamber, whereas, for the area scan camera, the kernel is mainly illuminated from the top. This can result in minor differences in thresholding results for the perimeter pixels. For the second analysis, two random samples, each consisting of 150 kernels were taken. One sample was imaged using the area scan camera whereas the other sample was imaged using the line scan camera. The results from this study are shown in Table 4.36. The statistical results from analysis of variance indicate that the grain kernels in the images acquired using the area and the line scan cameras were similar to each other.

Table 4.35 Size based morphological features of 150 grain kernels from single kernel images of each of the five grain types acquired using an area scan camera (ASC) and a line scan camera (LSC). The kernels were imaged using the ASC and the LSC.

Grain type	Property	Morphological Features													
		Area (pixels)^2		Perimeter (pixels)		Maximum radius (pixels)		Minimum radius (pixels)		Mean radius (pixels)		Major axis length (pixels)		Minor axis length (pixels)	
		ASC	LSC	ASC	LSC	ASC	LSC	ASC	LSC	ASC	LSC	ASC	LSC	ASC	LSC
Barley	Mean	5431.5	5419.7	340.7	339.9	70.4	70.3	26.0	26.0	44.7	44.6	134.0	133.7	55.2	55.1
	S.D.	521.3	520.3	23648.	23.5	5.1	5.0	2.2	2.2	2.4	2.4	10.3	10.3	4.5	4.5
CWAD	Mean	4500.5	4486.9	292.1	291.2	60.3	60.1	22.6	22.5	39.9	39.8	117.8	117.4	47.8	47.6
	S.D.	528.4	525.2	18.7	18.7	4.5	4.5	2.2	2.2	2.5	2.5	8.6	8.5	4.3	4.2
CWRS	Mean	3643.9	3635.5	253.1	252.5	50.5	50.4	22.8	22.8	35.0	35.0	97.7	97.5	47.8	47.7
	S.D.	303.5	303.0	11.1	11.0	3.0	2.9	1.8	1.8	1.4	1.4	5.3	5.2	3.5	3.5
Oats	Mean	5295.8	5282.2	381.0	380.0	81.2	81.0	20.8	20.7	47.8	47.7	155.9	155.5	43.3	43.1
	S.D.	1242.1	1237.4	58.9	58.6	12.0	11.9	2.5	2.5	6.5	6.4	22.0	21.9	5.0	5.0
Rye	Mean	4082.0	4070.2	295.8	294.9	64.2	64.0	20.0	19.9	39.3	39.1	120.7	120.3	42.5	42.4
	S.D.	328.0	324.5	16.8	16.6	4.4	4.3	1.7	1.6	1.8	1.8	7.6	7.6	3.1	3.0

Table 4.36 Size based morphological features of two samples of 150 grain kernels from single kernel images of each of the five grain types acquired using an area scan camera (ASC) and a line scan camera (LSC). Different kernels were imaged using the ASC and the LSC.

Grain type	Property	Morphological Features													
		Area (pixels)^2		Perimeter (pixels)		Maximum radius (pixels)		Minimum radius (pixels)		Mean radius (pixels)		Major axis length (pixels)		Minor axis length (pixels)	
		ASC	LSC	ASC	LSC	ASC	LSC	ASC	LSC	ASC	LSC	ASC	LSC	ASC	LSC
Barley	Mean	5377.0	5419.7	335.5	339.9	70.4	70.3	26.1	26.0	44.4	44.6	132.6	133.7	55.3	55.1
	S.D.	639.3	520.3	28.9	23.5	5.2	5.0	2.4	2.2	2.9	2.4	11.0	10.3	4.6	4.5
	Pr > F	0.83		0.72		0.71		0.84		0.86		0.89		0.92	
CWAD	Mean	4656.5	4586.9	299.8	291.2	61.9	60.1	22.1	22.5	40.7	39.8	121.3	117.5	47.4	47.6
	S.D.	517.6	525.2	16.9	18.6	3.8	4.5	2.1	2.2	2.3	2.5	7.3	8.5	4.0	4.2
	Pr > F	0.28		0.27		0.40		0.21		0.36		0.28		0.37	
CWRS	Mean	3627.9	3635.5	257.6	252.5	50.5	50.4	22.1	22.8	35.0	35.0	97.9	97.4	46.4	47.7
	S.D.	532.9	403.0	19.3	11.0	3.7	2.9	2.6	1.8	2.5	1.4	6.9	5.2	5.0	3.5
	Pr > F	0.32		0.41		0.37		0.40		0.45		0.39		0.49	
Oats	Mean	5196.9	5282.1	379.3	380.0	84.1	81.0	19.5	20.7	48.2	47.7	161.4	155.6	40.8	43.1
	S.D.	1575.4	1237.4	71.3	58.6	15.8	11.9	2.8	2.5	8.2	6.4	29.7	21.9	5.6	5.0
	Pr > F	0.83		0.69		0.56		0.80		0.78		0.66		0.75	
Rye	Mean	3843.6	4070.2	289.1	294.9	63.1	64.0	19.1	19.9	38.3	39.1	118.0	120.4	40.7	42.4
	S.D.	278.4	324.5	16.0	16.6	4.7	4.3	1.5	1.6	1.8	1.8	8.0	7.6	2.9	3.0
	Pr > F	0.23		0.37		0.24		0.33		0.52		0.29		0.25	

5. CONCLUSIONS AND RECOMMENDATIONS

The research work done for this thesis gives a good understanding of image analysis, processing, and classification techniques that can be employed in the grain industry to automate and assist in several grain handling operations. An image database was created for five grain types from various growing locations on the Canadian prairies. The database consists of images of individual grain kernels placed in a non-touching manner in the camera's field of view and of large number of kernels packed together. A computer program was written to extract 230 features (51 morphological, 123 color, and 56 textural) that can be used in different combinations to attain the best classification results. Two different neural network architectures were evaluated and their classification accuracies were compared to a non-parametric statistical classifier.

Based on the preliminary results, the classifiers were modified by training them with optimized features sets to improve the classification accuracies. Mean classification accuracies of 96.9, 94.3, 95.0, and 95.5% were obtained when the combined 60 features were used for grain classification using BPN, non-parametric, SPNN, and the modified SPNN classifiers, respectively. Using the combined 30 features, classification accuracies of 96.4, 94.4, and 94.3 were obtained using BPN, non-parametric, and SPNN classifiers, respectively. Optimized features sets now exist for different types of classifiers and grain types that can be used for classification purposes. It was concluded that all - morphological, color, and textural features play an important role in the grain classification process. An excessive number of these features can have a detrimental effect on the classifier by inducing redundancies and increasing computational time of the classifiers. The results from this study can be used to select input features when developing a new type of classifier. The results also provide a reference for classification accuracies of five grain types obtained by developing a classifier using a large database (over 50 000) of grain kernels.

A novel concept of specialist neural networks was introduced in this study for the purpose of grain classification. These networks specialize in differentiating a particular grain type from another or the rest of the grain types. The downside of these networks is that they are complex and require more memory and computational power, however, they serve as a very effective tool for post-processing of another network's output to improve the overall classification accuracy. These networks can be very useful when there are not a large number of output classes or when it is required to study the characteristics of a particular grain type with respect to the rest of the grain types.

Results of bulk sample image analysis have been very encouraging and this technology can be implemented in the grain industry for real-time determination of grain type after some research using a line scan camera in an actual grain elevator. Classification accuracies close to 100% were obtained for grain type determination using images of bulk samples with the combined 40 features as input. This result is of particular interest because automation of grain handling operations may not require such high classification accuracies. Moreover, since the bulk sample image analysis does not require time consuming image processing operations such as adaptive thresholding, background removal, and kernel extraction, computational requirements are not as severe as single kernel image analysis. The only further work that needs to be done, is the hardware implementation of the image processing and classification algorithm before this technique can be implemented at the industry level. With the availability of several commercial image processing routines, DSP technology based vision processing hardware boards, and tools to convert the classifiers such as neural networks into a dynamically linked library (DLL) file or a C++ code, the task of hardware implementation can be done in a very short duration.

The dual conveyor belt system along with the vibratory feed mechanism facilitates grain sample presentation to the line scan camera in a non-touching fashion on a continuous basis. The current design consists of a single motor creating a differential speed using a gear mechanism. Future design recommendations include separate motors for primary and secondary conveyor belts with adjustable speeds for both to facilitate taking not just the single kernel but also bulk sample images. The primary belt, running at a faster speed than the secondary belt, would ensure creation of a grain heap on the secondary belt for bulk imaging. The flow rate would have to be increased to ensure a naturally packed layer of grain without the background being visible in the camera's field of view.

The machine vision technology, in its present state, is just a few steps away from where it can be fully applied at the commercial level in the grain industry. To attain that level of sophistication in technology, further research needs to be done in the following specialized areas:

- techniques such as fractal geometry, fractal dimension, and wavelet transforms can be investigated to extract new characteristic features from images that can help in classification of unknown kernels;
- classification techniques such as pattern recognition, fuzzy set theory and fuzzy logic need to be studied for object recognition; and
- algorithms need to be implemented on hardware using parallel or pipeline processing techniques to attain the maximum data rate while handling and processing images.

6. REFERENCES

Al-Janobi, A.A. and G. Kranzler. 1994. Machine vision inspection of date fruits. ASAE Paper No. 94-3575. St. Joseph, MI: ASAE.

Ballard, D.H. and C.M. Brown. 1982. *Computer Vision*. Englewood Cliffs, NJ: Prentice - Hall Inc.

Barker, D.A., T.A. Vouri, M.R. Hegedus, and D.G. Myers. 1992a. The use of ray parameters for the discrimination of Australian wheat varieties. *Plant Varieties and Seeds* 5(1):35-45.

Barker, D.A., T.A. Vouri, and D.G. Myers. 1992b. The use of slice and aspect ratio parameters for the discrimination of Australian wheat varieties. *Plant Varieties and Seeds* 5(1):47-52.

Barker, D.A., T.A. Vouri, and D.G. Myers. 1992c. The use of Fourier descriptors for the discrimination of Australian wheat varieties. *Plant Varieties and Seeds* 5(2):93-102.

Barker, D.A., T.A. Vouri, M.R. Hegedus, and D.G. Myers. 1992d. The use of Chebychev coefficients for the discrimination of Australian wheat varieties. *Plant Varieties and Seeds* 5(2):103-111.

Brogan, W.L. and A.R. Edison.1974. Automatic classifications of grains via pattern recognition techniques. *Pattern Recognition* 6: 97-103.

Brown, G.K. and E.J. Timm. 1992. Lighting for fruit and vegetable sorting. ASAE Paper No. 93-6069. St. Joseph, MI: ASAE.

Canada Grains Council. 1994. *Statistical Handbook.* Winnipeg, MB: Canada Grains Council.

Casady, W.W. and M.R. Paulsen. 1988. An automated kernel positioning device for computer vision analysis of grain. ASAE Paper No. 88-7003. St. Joseph, MI: ASAE.

Crowe, T.G., X.Y. Luo, D.S. Jayas, and N.R. Bulley. 1997. Color line-scan imaging of cereal grain kernels. *Applied Engineering in Agriculture* 13(5):689-694.

Dowell, F.E. 1993. Neural network classification of undamaged and damaged peanut kernels using spectral data. ASAE Paper No. 93-3050. St. Joseph, MI: ASAE.

Draper, S.R. and A.J. Travis. 1984. Preliminary observations with a computer based system for analysis of the shape of seeds and vegetative structures. *Journal of the National Institute of Agricultural Botany* 16(3):387-395.

El-Faki, M.S., N.Q. Zhang, and D.E. Peterson. 2000. Weed detection using color machine vision. *Transactions of the ASAE* 43 (6):1969-1978.

Ghazanfari, A., D. Wulfsohn, and J. Irudayaraj. 1998. Machine vision grading of pistachio nuts using gray-level histogram. *Canadian Agricultural Engineering* 40(1):61-66.

Gonzalez, R.C. and R.E. Woods. 1992. *Digital Image Processing*. Reading, MA: Addison-Wesley Publishing Co.

Guyer,D.E., G.E. Miles, L.D. Gaultney, and M.M. Schreiber. 1993. Application of machine vision to shape analysis in leaf and plant identification. *Transactions of the ASAE* 36(1):163-171.

Han,Y.J. and J.C. Hayes. 1990. Soil cover determination using color image analysis. *Transactions of the ASAE* 33(4):1402-1408.

Haralick, R.M. and L. Shapiro. 1992. *Computer and robot vision*. Reading, MA: Addison-Wesley Publishing Co.

Howerth, M.S., J.R. Brandon, S.W. Searcy, and N. Kehtarnavaz. 1992. Estimation of tip shape for carrot classification by machine vision. *Journal of Agricultural Engineering Research* 53(2):123-139.

Humburg, D.S. and J. Srinivasan. 1994. A structured light and camera system for scanning mushroom trays. ASAE Paper No. 94-3509. St. Joseph, MI: ASAE.

Jain, A.K. 1988. *Fundamentals of Digital Image Processing*. Englewood Cliffs , NJ: Prentice Hall Inc.

Jayas,D.S., C.E. Murray, and N.R. Bulley. 1999. An automated seed presentation device for use in machine vision identification of grain. *Canadian Agricultural Engineering* 41(2):113-118.

Jayas, D.S., J. Paliwal, and N.S. Visen. 2000. Multi-layer neural networks for image analysis of agricultural products. *Journal of Agricultural Engineering Research.* 77(2):119-128.

Karunakaran, C., N.S. Visen, J. Paliwal, G. Zhang, D.S. Jayas, and N.D.G White. 2002. Machine Vision Systems for Agricultural Products. CSAE Paper No. 01-305. Masonville, PQ: CSAE.

Keefe, P.D. 1992. A dedicated wheat grain image analyser. *Plant Varieties and Seeds* 5(1):27-33.

Keefe, P.D. and S.R. Draper. 1988. An automated machine vision system for the morphometry of new cultivars and plant genebank accessions. *Plant Varieties and Seeds* 1(1):1-11.

Keefe, P.D. and S.R. Draper. 1986. The measurement of new characters for cultivar identification in wheat using machine vision. *Seed Science and Technology.* 14(3):715-724.

Kranzler, G.A. 1985. Applying digital image processing in agriculture. *Agricultural Engineering* 66(3):11-13.

Lai, F.S., I. Zayas, and Y. Pomeranz. 1986. Application of pattern recognition techniques in the analysis of cereal grains. *Cereal chemistry* 63(2):168-172.

Langford, M., G.E. Taylor, and J.R. Flenley. 1990. Computerized identification of pollen grains by texture analysis. *Review of Palaeobotany and Palynology* 64(1990): 197-203.

Luo, X., D.S. Jayas, T.G. Crowe, and N.R. Bulley. 1997. Evaluation of light sources for machine vision. *Canadian Agricultural Engineering* 39(4):309-315.

Luo, X.Y., D.S. Jayas, and S.J. Symons. 1999a. Identification of damaged kernels in wheat using a color machine vision system. *Journal of Cereal Science* 30(1):49-59.

Luo, X.Y., D.S. Jayas, and S.J. Symons. 1999b. Comparison of statistical and neural network methods for classifying cereal grains using machine vision. *Transactions of the ASAE* 42(2): 413-419.

Majumdar, S., D.S. Jayas, J.L. Hehn, and N.R. Bulley. 1996. Classification of various grains using optical properties. *Canadian Agricultural Engineering* 38(2):139-144.

Majumdar, S. and D.S. Jayas. 1999. Single-kernel mass determination for grain inspection using machine vision. *Applied Engineering in Agriculture* 15(4):357-362.

Majumdar, S. and D.S. Jayas. 1999. Classification of bulk samples of cereal grains using machine vision. *Journal of Agricultural Engineering Research.* 73(1):35-47.

Majumdar, S. and D.S. Jayas. 2000a. Classification of cereal grains using machine vision. I. Morphology models. *Transactions of the ASAE.* 43(6):1669-1675.

Majumdar, S. and D.S. Jayas. 2000b. Classification of cereal grains using machine vision. II. Color models. *Transactions of the ASAE.* 43(6):1677-1680.

Majumdar, S. and D.S. Jayas. 2000c. Classification of cereal grains using machine vision. III. Texture models. *Transactions of the ASAE.* 43(6):1681-1687.

Majumdar, S. and D.S. Jayas. 2000d. Classification of cereal grains using machine vision. IV. Combined morphology, color, and texture models. *Transactions of the ASAE.* 43(6):1689-1694.

Majumdar, S., D.S. Jayas, S.J. Symons, and N.R. Bulley. 1996. Textural features for automated grain identification. CSAE Paper No. 96-602. Saskatoon, SK: CSAE.

Miller, B.K. and M.J. Delwiche. 1989. A color vision system for peach grading. *Transactions of the ASAE* 32(4):1484-1490.

Murase, H., Y. Nishiura, and N. Honami. 1994. Textural features/neural network for plant growth monitoring. ASAE Paper No. 94-4016. St. Joseph, MI: ASAE.

Myers, D.G. and K.J. Edsall. 1989. The application of image processing techniques to the identification of Australian wheat varieties. *Plant Varieties and Seeds.* 2(2):109-116.

Neuman, M., H.D. Sapirstein, E. Shwedyk, and W. Bushuk. 1987. Discrimination of wheat class and variety by digital image analysis of whole grain samples. *Journal of Cereal Science* 6(2):125-132.

Neuman, M., H.D. Sapirstein, E. Shwedyk, and W. Bushuk. 1989a. Wheat grain color analysis by digital image processing: I. Methodology. *Journal of Cereal Science* 10(3):175-182.

Neuman, M., H.D. Sapirstein, E. Shwedyk, and W. Bushuk. 1989b. Wheat grain color analysis by digital image processing: II. Wheat class determination. *Journal of Cereal Science* 10(3):183-182.

Paliwal, J., N.S. Shashidhar, and D.S. Jayas. 1999. Grain kernel identification using kernel signature. *Transactions of the ASAE* 42(6): 1921-1924.

Paliwal, J., N.S. Visen, and D.S. Jayas. 1998. Determination of physical properties of different grain types using machine vision. ASAE Paper No. 98-3060, St. Joseph, MI: ASAE.

Paliwal, J., N.S. Visen, and D.S. Jayas. 2001. Evaluation of neural network architectures for cereal grain classification using morphological features. *Journal of Agricultural Engineering Research*. 79(4):361-370.

Panigrahi, S. and R. Marsh. 1996. Neural network techniques for color classification of french fries. ASAE Paper No. 96-3004. St. Joseph, MI: ASAE.

Patel,V.C., R.W. McClendon, and J.W. Goodrum. 1996. Detection of blood spots and dirt stains in eggs using computer vision and neural networks. *Applied Engineering in Agriculture* 12(2):253-258.

Paulsen, M.R. and W.F. McClure. 1986. Illumination for computer vision systems. *Transactions of the ASAE* 29(5):1398-1404.

Putnam, D.F. and R.G. Putnam. 1970. *Canada: A Regional Analysis*. Toronto, ON: J.M. Dent and Sons, Inc.

Precetti, C.J. and G.W. Krutz. 1993a. Building a color classification system. ASAE Paper No. 93-3003. St. Joseph, MI: ASAE.

Precetti, C.J. and G.W. Krutz. 1993b. Real-time color classification system. ASAE Paper No. 93-3002. St. Joseph, MI: ASAE.

Precetti, C.J. and G.W. Krutz. 1993c. A new seed corn husk deduction system using color machine vision. ASAE Paper No. 93-1012. St. Joseph, MI: ASAE.

Sapirstein, H.D. and J.M. Kohler. 1995. Physical uniformity of graded railcar and vessel shipments of Canada Western Red Spring wheat determined by digital image analysis. *Canadian Journal of Plant Science* 75(2):363-369.

Sapirstein, H.D., Neuman, M., Wright, E.H., Shwedyk, E. and W. Bushuk. 1987. An instrumental system for cereal grain classification using digital image analysis. *Journal of Cereal Science*. 6(1):3-14.

Sapirstein, H.D. and W. Bushuk. 1989. Quantitative determination of foreign material and vitreosity in wheat by digital image analysis. In *ICC'89 Symposium: Wheat End-Use Properties*. H. Salovaara (ed.). Lahiti, Finland.

Sarkar, N.R. 1986. Machine vision in the food industry. In *ASAE Food Engineering News*, October, 3-5. St. Joseph, MI: ASAE.

Segerlind, L. and B. Weinberg. 1972. Grain kernel identification by profile analysis. ASAE Paper No. 72-314. St. Joseph, MI: ASAE.

Shahin, M.A. and S.J. Symons. 1999. A machine vision system for color classification of lentils. ASAE Paper No. 99-3202. St. Joseph, MI: ASAE.

Shaw, W.E. 1990. Machine vision for detecting defects on fruit and vegetables. In *Food Processing Automation I - Proceedings of the 1990 conference*, 50-59. St. Joseph, MI: ASAE.

Shearer, S.A., T.F. Burks, P.T. Jones, and W.Qiu. 1994. One dimensional image texture analysis for maturity assessment of broccoli. ASAE Paper No. 94-3017. St. Joseph, MI: ASAE.

Simonton,W. and J. Pease. 1993. Orientation independent machine vision classification of plant parts. *Journal of Agricultural Engineering Research* 54(3):231-243.

Spewak, R. 1995. An automated seed singulation device for presenting grains to an image processing system. Unpublished B.Sc. thesis, University of Manitoba.

Strachan N.J.C. and P. Nesvadba. 1990. Fish species recognition by shape analysis of images. Pattern recognition 23(5):539-544.

Symons, S.J. and R.G. Fulcher. 1988a. Relationship between oat kernel weight and milling yield. *Journal of Cereal Science*. 7(3):215-217.

Symons, S.J. and R.G. Fulcher. 1988b. Determination of variation in oat kernel morphology by digital image analysis. *Journal of Cereal Science*. 7(3):219-228.

Tillet, R.D. 1990. Image analysis for agricultural processes. Div. Note DN 1585, AFRC Institute of Engineering Research, Silsoe, UK.

Tillet, R.D. 1991. Image analysis for agricultural processes: A review of potential opportunities. *Journal of Agricultural Engineering Research* 50:247-258.

Travis, A.J. and S.R. Draper. 1985. A computer based system for the recognition of seed shape. *Seed Science and Technology* 13:813-820.

Visen, N.S., J. Paliwal, D.S. Jayas, and N.D.G. White. 2002. Specialist neural networks for cereal grain classification. (Accepted for publication in *Journal of Agricultural Engineering Research*).

Visen, N.S., N.S. Shashidhar, J. Paliwal, and D.S. Jayas. 2001. Identification and segmentation of groups of touching kernels. *Journal of Agricultural Engineering Research*. 79(2):159-166.

Vooren,J.G.van de, G. Polder, and G.W.A.M. van der Heijden. 1992. Identification of mushroom cultivars using image analysis. *Transactions of the ASAE* 35 (1):357-350.

Wigger, W.D., M.R. Paulsen, J.B. Litchfield, and J.B. Sinclair. 1988. Classification of fungal-damaged soybeans using color-image processing. ASAE Paper No. 88-3053. St. Joseph, MI: ASAE.

Wilhoit, J.R., R.K. Byler, M.B. Koslav, and D.H. Vaughan. 1990. Broccoli head sizing using image textural analysis. *Transactions of the ASAE* 33(5):1736-1740.

Ying, J.P., M.D. Evans, S.R. Ghate, and P.Y. Jia. 1996. Catfish feature identification via computer vision. *Transactions of the ASAE* 39(5):1923-1931.

Zayas, I., F.S. Lai, and Y. Pomeranz. 1986. Discrimination between wheat classes and varieties by image analysis. *Cereal Chemistry* 63(1):52-56.

Zayas, I., H. Converse, and J. Steele. 1990. Discrimination of whole from broken corn kernels with image analysis. *Transactions of the ASAE* 35(5):1642-1646.

Zayas, I., Y. Pomeranz, and F.S. Lai. 1985. Discrimination between Arthur and Arcan wheats by image analysis. *Cereal Chemistry* 62(6):478-480.

Zayas, I., Y. Pomeranz, and F.S. Lai. 1989. Discrimination of wheat and non-wheat components in grain samples by digital image analysis. *Cereal Chemistry* 66(3):233-237.

Zhang, N., Y. Yang, and M. El-Faki. 1994. Neural network application in weed identification using color digital images. ASAE Paper No. 94-3511. St. Joseph, MI: ASAE.

Appendix A

CONFIGURATION FILES USED WITH AREA AND LINE SCAN CAMERAS

A.1 Digitizer configuration files (DCF) created using Matrox Intellicam utility for area scan camera

[CAMERA_NAME]
RS-170A compatible
[CONFIG_FILE]
50CF
CORONA
Tue Aug 14 13:35:14 2001
[INFO_FILE_REV]
0002.0033.0000
METEOR-II/MC
[GENERAL_PARAMETERS]
GEN_MATCH_HW 0x1
GEN_SAVED_W_ERR 0x0
CT_LS 0x0
CT_FS 0x1
CT_CONV_INVERTED 0x0
CT_TAPS 0x0
CT_CAMERA 0x0
VDC_DIG 0x0
VDC_ANA 0x1
VDC_MONO 0x0
VDC_RGB_ALPHA 0x0
VDC_SVID 0x0
VDC_YUVVID 0x0
VDC_TTL 0x0
VDC_422 0x0
VDT_SER 0x0
VDT_EQU 0x0
VDT_CLP_SYN 0x0
VDT_CLP_BPO 0x1
VDT_CLP_FPO 0x0
PCK_CAM_GEN 0x0
PCK_CAM_REC 0x0
PCK_CAM_R&G 0x0
PCK_OTH_REC 0x0
PCK_USE_OUT 0x0
PCK_CAM_XCHG 0x0
PCK_ITTL 0x0
PCK_I422 0x0
PCK_IPOS 0x0
PCK_INEG 0x0
PCK_FREQ 0xbb43d8
PCK_INTDVED 0x0
PCK_OFREQDV 0xbb43d8
PCK_OTTL 0x0
PCK_O422 0x0
PCK_OPOS 0x0
PCK_ONEG 0x0
PCK_IDELAY 0x0
SYC_DIG 0x0
SYC_ANA 0x1
SYC_C_IPOS 0x0
SYC_C_INEG 0x0
SYC_C_OTTL 0x0
SYC_C_O422 0x0
SYC_C_OPOS 0x0
SYC_C_ONEG 0x0
SYC_BLK 0x0
SYC_COMP 0x0
SYC_SEP 0x1
SYC_IN_CH 0x0
EXP_SYN_CLK 0x0
EXP_ASY_CLK 0x0
EXP_CLK_FREQ 0xbb43d8
EXP_CLK_DVED 0x0
EXP_CLK_DIVF 0x0
EXP_MD_PERD 0x0
EXP_MD_W_TRG 0x0
EXP_MD_SW 0x0
EXP_TRG_TTL 0x0
EXP_TRG_422 0x0
EXP_TRG_POS 0x0
EXP_TRG_NEG 0x0
EXP_OUT_DLYD 0x0
EXP_OUT_T0 0x0
EXP_OUT_T1 0x0

EXP_CLK_FREQ_2 0x0

EXP_CLK_DVED_2 0x0

EXP_CLK_DIVF_2 0x0

EXP_MD_PERD_2 0x0

EXP_MD_W_TRG_2 0x0

EXP_MD_EXT_2 0x0

EXP_MD_HSY_2 0x0

EXP_MD_VSY_2 0x0

EXP_MD_SW_2 0x0

EXP_TRG_TTL_2 0x0

EXP_TRG_422_2 0x0

EXP_TRG_POS_2 0x0

EXP_TRG_NEG_2 0x0

EXP_OUT_DLYD_2 0x0

EXP_OUT_T0_2 0x0

EXP_OUT_T1_2 0x0

EXP_OUT_TTL_2 0x0

EXP_OUT_422_2 0x0

EXP_OUT_POS_2 0x0

EXP_OUT_NEG_2 0x0

GRB_RGB_PATH_FORCED 0x0

TAP_CONFIG 0x1

VDC_VID_WIDTH_10 0x0

VDC_VID_WIDTH_12 0x0

VDC_VID_WIDTH_14 0x0

GRB_TRG_SIGNAL_APORT 0x0

GRB_TRG_SIGNAL_DPORT 0x0

GRB_TRG_SIGNAL_HSDPORT 0x0

GRB_TRG_SIGNAL_VSDPORT 0x0

GRB_TRG_SIGNAL_TIMER1 0x0

GRB_TRG_SIGNAL_TIMER2 0x0

EXP_CLOCK_HSYNC 0x0

EXP_CLOCK_VSYNC 0x0

DEF_DIG_SYNCPIPE 0x3

DEF_DIG_VIDPIPE 0x1

DEF_PSG_HSPLLFB 0x1

DEF_HSYNC_TRAILS_VSYNC 0x2

DEF_NTSC_HSYNC_TO_COLOR_BURST 0x7

DEF_NTSC_COLOR_BURST_LENGTH 0x1f

DEF_SYSCLK_FREQ 0x17d7840

DEF_SYSCLK_SEL 0x2

DEF_SYSCLK156MZ_MULT 0x2

DEF_HFPORCH_60HZ 0x16

DEF_HSYNC_60HZ 0x3a

DEF_HBPORCH_60HZ 0x3c

DEF_HACTIVE_60HZ 0x280

DEF_HTOTAL_60HZ 0x30c

DEF_HFPORCH_50HZ 0x16

DEF_HSYNC_50HZ 0x45

DEF_HBPORCH_50HZ 0x55

DEF_HACTIVE_50HZ 0x300

DEF_HTOTAL_50HZ 0x3b0

DEF_DIG_HVNEG_VALUE 0x0

DEF_DAC8800_DEFAULT 0x3b

DEF_KS_CHIP_DELAY 0x3c

DEF_KS_HAVB_60HZ_DEFAULT 0xa7

DEF_KS_HAVE_60HZ_DEFAULT 0x1d

DEF_KS_HS1B_60HZ_DEFAULT 0x20

DEF_KS_HS1E_60HZ_DEFAULT 0x6e

DEF_KS_HAVB_50HZ_DEFAULT 0xcf

DEF_KS_HAVE_50HZ_DEFAULT 0x1d

DEF_KS_HS1B_50HZ_DEFAULT 0x20

DEF_KS_HS1E_50HZ_DEFAULT 0x87

DEF_NTSC_PORCH 0x52

DEF_EXP_OUT_T0 0x0

DEF_EXP_OUT_T0_2 0x0

DEF_TAP_VALID 0x1

DEF_CLAMP_WIDTH 0x17

DEF_CLAMP_BORDER 0x12

DEF_HBPORCH_MIN 0x0

DEF_0,15_HBPORCH 0x9

DEF_VS_SAMPLING_MIN 0x0

DEF_HSPVAL_MIN 0x0

DEF_VIDEO_GAIN 0xaf0

DEF_PCK_IDLY_SEL 0x0

[REG_DIGIT]

INFO_XSIZE 0x280

INFO_YSIZE 0x1e0

INFO_MODE 0x2c

INFO_TYPE 0x2

INFO_DEPTH 0x8

INFO_BAND 0x3

INFO_INPUT 0x0

INFO_PIXCLK 0xbb43d8

INFO_PIPELINE 0x0

INFO_MODULE_422 0x0

INFO_CHANNEL 0x30

INFO_XTAPSPERCH 0x1

INFO_YTAPSPERCH 0x1

INFO_XTAPSPERCHADJ 0x1

INFO_YTAPSPERCHADJ 0x1

BT254_BTCOMMAND 0x0

BT254_BTIOOUT0 0x0

BT254_BTIOOUT1 0x0

BT254_BTIOOUT2 0x0

BT254_BTIOOUT3 0x0

BT254_BTIOOUT4 0x0

A.2 CCA file containing acquisition parameters describing the camera's video signal characteristics

[General]

Camera Name = Dalsa TR-31-2K

Version = 200

Company Name = No Name

Model Name = No Name

[Signal Description]

Channel = 1

Frame = 2

Interface = 2

Scan = 2

Signal = 2

Video = 8

Pixel Depth = 8

Video Standard = 1

Field Order = 4

Coupling = 2

Taps = 1

Tap Output = 2

Tap 1 Direction = 1

Tap 2 Direction = 1

Tap 3 Direction = 1

Tap 4 Direction = 1

Tap 5 Direction = 1

Tap 6 Direction = 1

Tap 7 Direction = 1

Tap 8 Direction = 1

Channels Order = 4

Video Level Minimum = 0

Video Level Maximum = 0

[Signal Timings]

Horizontal Active = 2048

Horizontal Sync = 16

Vertical Active = 0

Vertical Sync = 0

Horizontal Front Porch = 0

Horizontal Back Porch = 0

Vertical Front Porch = 0

Vertical Back Porch = 0

Horizontal Front Invalid = 0

Horizontal Back Invalid = 0

Vertical Front Invalid = 0

Vertical Back Invalid = 0

[Pixel Clock]

Pixel Clock Source = 2

Pixel Clock Frequency Internal = 0

Pixel Clock Frequency 1:1 = 25000000

Pixel Clock Frequency External = 25000000

Pixel Clock Detection = 4

[Synchronization Signals]

Synchronization Source = 4

Horizontal Sync Polarity = 1

Vertical Sync Polarity = 1

[Control Signals]

Frame Integrate Method = 0

Frame Integrate Polarity = 1

Time Integrate Method = 1

Time Integrate Polarity = 2

Camera Trigger Method = 1

Camera Trigger Polarity = 2

Camera Trigger Duration = 200

Camera Trigger/Exposure Signal = 1

Camera Reset Method = 0

Camera Reset Polarity = 2

Camera Reset Duration = 0

Line Integrate Method = 4

Line Integrate Polarity = 2

Line Integrate Delay = 0

Line Trigger Method = 0

Line Trigger Polarity = 2

Line Trigger Delay = 0

Line Trigger Duration = 0

LineScan Direction = 1

LineScan Direction Polarity = 2

Camera Line Trigger Frequency Minimum = 0

Camera Line Trigger Frequency Maximum = -1

Camera Time Integrate Duration Minimum = 0

Camera Time Integrate Duration Maximum = -1

Time Integrate Pulse 1 Polarity = 2

Time Integrate Pulse 1 Delay = 0

Time Integrate Pulse 1 Duration = 0

Time Integrate Pulse 0 Polarity = 2

Time Integrate Pulse 0 Delay = 0

Time Integrate Pulse 0 Duration = 0

Line Integrate Pulse 1 Polarity = 1

Line Integrate Pulse 1 Delay = 0

Line Integrate Pulse 1 Duration = 0

Line Integrate Pulse 0 Polarity = 1

Line Integrate Pulse 0 Delay = 0

Line Integrate Pulse 0 Duration = 0

Trigger/Exposure Signal = 1

Time Integrate Pulse Polarity = 1

Time Integrate Pulse Delay = 0

Time Integrate Pulse Duration = 0

[Connector Description]

HD Input = 0x0

VD Input = 0x0

Reset/Trigger Input = 0x0

Exposure Input = 0x0

[Custom Camera IO Control Signals]

Max Control = 0

A.3 CVI file containing acquisition parameters describing the frame grabber's characteristics

[General]
Version = 200
Vic Name = Dalsa TR-31-2K

[Input]
Camera Selector = 0
Bit Ordering = 1

[Signal Conditioning]
Brightness = 0
Brightness Red = 0
Brightness Green = 0
Brightness Blue = 0
Contrast = 100000
Contrast Red = 100000
Contrast Green = 100000
Contrast Blue = 100000
Hue = 0
Saturation = 100000
DC Restoration Mode = 1
DC Restoration Start = 0
DC Restoration Width = 0
Fix Filter Enable = 0
Fix Filter Selector = 0
Programmable Filter Enable = 0
Programmable Filter Frequency = 0

[Stream Conditioning]
Crop Left = 0
Crop Top = 0
Crop Width = 2048
Crop Height = 512
Scale Horizontal = 2048
Scale Vertical = 512
Scale Horizontal Method = 1
Scale Vertical Method = 1
Decimate Method = 1
Decimate Count = 1
Lut Enable = 0
Lut Number = 0

Pixel Mask = 255
Horizontal Sync Reference = 2
Vertical Sync Reference = 2
Snap Count = 1
External Trigger Frame Count = 1

[Control Signals]
Strobe Enable = 0
Strobe Method = 1
Strobe Polarity = 1
Strobe Duration = 10
Strobe Delay = 0
Strobe Delay 2 = 0
Strobe Level = 2
Frame Integrate Enable = 0
Frame Integrate Count = 0
Time Integrate Enable = 0
Time Integrate Duration = 0
Camera Trigger Enable = 0
Camera Reset Enable = 0
External Trigger Detection = 4
External Trigger Level = 2
Line Integrate Enable = 1
Line Integrate Duration = 1024
Line Trigger Enable = 0
External Frame Trigger Enable = 0
External Frame Trigger Detection = 4
External Frame Trigger Level = 2
External Line Trigger Enable = 0
External Line Trigger Detection = 4
External Line Trigger Level = 2
Internal Line Trigger Enable = 1
Internal Line Trigger Freq = 2700
LineScan Direction Output = 1
Master Mode = 0
Master Mode Horizontal Sync Polarity = 1
Master Mode Vertical Sync Polarity = 1
Shaft Encoder Pulse Drop = 0
Shaft Encoder Enable = 0
Internal Frame Trigger Enable = 0
Internal Frame Trigger Freq = 10

[Output]
Output Format = 13

Output Enable = 1

[Shared Control Signals]
External Trigger = -1
Camera Reset = -1
Camera Trigger = -1
Time Integrate = -1
Frame Integrate = -1
Strobe = -1

Appendix B

MORPHOLOGICAL, COLOR, AND TEXTURAL FEATURES EXTRACTED BY THE PROGRAM

Table B.1 List of morphological features extracted using the program.

Feature Number	Feature name
1	Area
2	Perimeter
3	Maximum radius
4	Minimum radius
5	Mean radius
6	Major axis length
7	Minor axis length
8 - 11	Shape moments 1 through 4
12 - 31	Radial Fourier descriptors 1 through 20
32 - 51	Boundary Fourier descriptors 1 through 20

Table B.2 List of color features extracted using the program.

Feature Number	Feature name
1	Red mean
2	Green mean
3	Blue mean
4	Red range
5	Green range
6	Blue range
7	Red variance
8	Green variance
9	Blue variance
10	Hue mean
11	Saturation mean
12	Intensity mean
13	Hue range
14	Saturation range
15	Intensity range
16 - 19	Red moments 1 through 4
20 - 23	Green moments 1 through 4
24 - 27	Blue moments 1 through 4
28 - 59	Red histogram ranges 1 through 32
60 - 91	Green histogram ranges 1 through 32
92 - 123	Blue histogram ranges 1 through 32

Table B.3 List of textural features extracted using the program.

Feature Number	Feature name	Code
1	Gray level co-occurrence matrix mean for gray band	Gray GLCM mean
2	Gray level co-occurrence matrix variance for gray band	Gray GLCM variance
3	Gray level co-occurrence matrix uniformity for gray band	Gray GLCM uniformity
4	Gray level co-occurrence matrix correlation for gray band	Gray GLCM correlation
5	Gray level co-occurrence matrix cluster shade for gray band	Gray GLCM cluster shade
6	Gray level co-occurrence matrix entropy for gray band	Gray GLCM entropy
7	Gray level co-occurrence matrix homogeneity for gray band	Gray GLCM homogeneity
8	Gray level co-occurrence matrix inertia for gray band	Gray GLCM inertia
9	Gray level co-occurrence matrix mean for red band	Red GLCM mean
10	Gray level co-occurrence matrix variance for red band	Red GLCM variance
11	Gray level co-occurrence matrix uniformity for red band	Red GLCM uniformity
12	Gray level co-occurrence matrix correlation for red band	Red GLCM correlation
13	Gray level co-occurrence matrix cluster shade for red band	Red GLCM cluster shade
14	Gray level co-occurrence matrix entropy for red band	Red GLCM entropy
15	Gray level co-occurrence matrix homogeneity for red band	Red GLCM homogeneity

. . . continued . . .

. . . continued Table B.3 . . .

Feature Number	Feature name	Code
16	Gray level co-occurrence matrix inertia for red band	Red GLCM inertia
17	Gray level co-occurrence matrix mean for green band	Green GLCM mean
18	Gray level co-occurrence matrix variance for green band	Green GLCM variance
19	Gray level co-occurrence matrix uniformity for green band	Green GLCM uniformity
20	Gray level co-occurrence matrix correlation for green band	Green GLCM correlation
21	Gray level co-occurrence matrix cluster shade for green band	Green GLCM cluster shade
22	Gray level co-occurrence matrix entropy for green band	Green GLCM entropy
23	Gray level co-occurrence matrix homogeneity for green band	Green GLCM homogeneity
24	Gray level co-occurrence matrix inertia for green band	Green GLCM inertia
25	Gray level co-occurrence matrix mean for blue band	Blue GLCM mean
26	Gray level co-occurrence matrix variance for blue band	Blue GLCM variance
27	Gray level co-occurrence matrix uniformity for blue band	Blue GLCM uniformity
28	Gray level co-occurrence matrix correlation for blue band	Blue GLCM correlation
29	Gray level co-occurrence matrix cluster shade for blue band	Blue GLCM cluster shade
30	Gray level co-occurrence matrix entropy for blue band	Blue GLCM entropy

. . . continued . . .

. . . continued Table B.3 . . .

Feature Number	Feature name	Code
31	Gray level co-occurrence matrix homogeneity for blue band	Blue GLCM homogeneity
32	Gray level co-occurrence matrix inertia for blue band	Blue GLCM inertia
33	Gray level run length matrix short run for gray band	Gray GLRM short run
34	Gray level run length matrix long run for gray band	Gray GLRM long run
35	Gray level run length matrix color non-uniformity for gray band	Gray GLRM color non-uniformity
36	Gray level run length matrix run length non-uniformity for gray band	Gray GLRM run length non-uniformity
37	Gray level run length matrix entropy for gray band	Gray GLRM entropy
38	Gray level run length matrix runpercent for gray band	Gray GLRM runpercent
39	Gray level run length matrix short run for red band	Red GLRM short run
40	Gray level run length matrix long run for red band	Red GLRM long run
41	Gray level run length matrix color non-uniformity for red band	Red GLRM color non-uniformity
42	Gray level run length matrix run length non-uniformity for red band	Red GLRM run length non-uniformity
43	Gray level run length matrix entropy for red band	Red GLRM entropy
44	Gray level run length matrix runpercent for red band	Red GLRM runpercent
45	Gray level run length matrix short run for green band	Green GLRM short run

. . . continued . . .

. . . continued Table B.3 . . .

Feature Number	Measurement	Code
46	Gray level run length matrix long run for green band	Green GLRM long run
47	Gray level run length matrix color non-uniformity for green band	Green GLRM color non-uniformity
48	Gray level run length matrix run length non-uniformity for green band	Green GLRM run length non-uniformity
49	Gray level run length matrix entropy for green band	Green GLRM entropy
50	Gray level run length matrix runpercent for green band	Green GLRM runpercent
51	Gray level run length matrix short run for blue band	Blue GLRM short run
52	Gray level run length matrix long run for blue band	Blue GLRM long run
53	Gray level run length matrix color non-uniformity for blue band	Blue GLRM color non-uniformity
54	Gray level run length matrix run length non-uniformity for blue band	Blue GLRM run length non-uniformity
55	Gray level run length matrix entropy for blue band	Blue GLRM entropy
56	Gray level run length matrix runpercent for blue band	Blue GLRM runpercent

Appendix C

ANALYSIS FOR SELECTION OF REDUCED GRAY LEVEL

C.1 Output from SAS software for statistical analysis to determine the best reduced gray level

The SAS System

The GLM Procedure

Class Level Information

Class	Levels	Values
type	5	Barley CWAD CWRS Oats Rye
treat	6	8 16 32 64 128 256

Number of observations 90

Dependent Variable: levels

Source	DF	Sum of Squares	Mean Square	F Value	Pr > F
Model	29	970.204232	33.455318	12.18	<.0001
Error	60	164.808800	2.746813		
Corrected Total	89	1135.013032			

R-Square	Coeff Var	Root MSE	levels Mean
0.854796	1.801597	1.657351	91.99344

Source	DF	Type I SS	Mean Square	F Value	Pr > F
Type	4	884.1355933	221.0338983	80.47	<.0001
Treat	5	17.9002722	3.5800544	1.30	0.2747
Type*Treat	20	68.1683667	3.4084183	1.24	0.2552

Duncan's Multiple Range Test for levels

NOTE: This test controls the Type I comparisonwise error rate, not the experiment-wise error rate.

Alpha	0.05
Error Degrees of Freedom	60
Error Mean Square	2.746813

Number of Means	2	3	4	5
Critical Range	1.105	1.163	1.200	1.228

Means with the same letter are not significantly different.

Duncan Grouping	**Mean**	**N**	**Type**
A	96.1906	18	Oats
B	94.5928	18	Rye
C	91.9856	18	CWAD
D	89.5222	18	Barley
E	87.6761	18	CWRS

Duncan's Multiple Range Test for levels

NOTE: This test controls the Type I comparisonwise error rate, not the experiment-wise error rate.

Alpha	0.05
Error Degrees of Freedom	60
Error Mean Square	2.746813

Number of Means	2	3	4	5	6
Critical Range	1.211	1.273	1.315	1.345	1.368

Means with the same letter are not significantly different.

Duncan Grouping		Mean	N	Treat
	A	92.7733	15	64
B	A	92.1733	15	32
B	A	92.1067	15	16
B	A	91.8073	15	128
B	A	91.7867	15	256
B		91.3133	15	8

Table C.1 Classification accuracies of various grain types using 8 gray levels.

Grain type	Classification accuracies for three trials, %			
	1	2	3	Mean
Barley	85.9	89.3	90.3	88.5
CWAD	91.3	93.6	94.6	93.2
CWRS	87.5	87.2	86.8	87.2
Oats	93.5	95.7	94.7	94.6
Rye	93.3	93.5	92.5	93.1

Table C.2 Classification accuracies of various grain types using 16 gray levels.

Grain type	Classification accuracies for three trials, %			
	1	2	3	Mean
Barley	89.0	89.8	89.5	89.4
CWAD	90.1	93.1	89.7	91.0
CWRS	89.0	88.8	90.3	89.4
Oats	95.2	96.5	94.7	95.4
Rye	95.7	94.5	95.7	95.3

Table C.3 Classification accuracies of various grain types using 32 gray levels.

Grain type	Classification accuracies for three trials, %			
	1	2	3	Mean
Barley	87.9	89.1	91.0	89.3
CWAD	87.5	95.5	92.1	91.7
CWRS	86.8	88.3	90.5	88.6
Oats	96.7	97.7	96.0	96.8
Rye	95.8	91.5	96.2	94.5

Table C.4 Classification accuracies of various grain types using 64 gray levels.

Grain type	Classification accuracies for three trials, %			
	1	2	3	Mean
Barley	90.0	89.0	92.5	90.5
CWAD	89.1	94.4	92.9	92.1
CWRS	88.7	88.2	88.5	88.4
Oats	96.8	98.2	95.7	96.9
Rye	96.5	94.3	96.8	95.9

Table C.5 Classification accuracies of various grain types using 128 gray levels.

Grain type	Classification accuracies for three trials, %			
	1	2	3	Mean
Barley	89.8	87.8	90.1	89.2
CWAD	90.7	93.4	90.1	91.4
CWRS	87.0	87.5	89.2	87.9
Oats	96.8	97.8	95.2	96.6
Rye	95.8	91.2	94.7	93.9

Table C.6 Classification accuracies of various grain types using 256 gray levels.

Grain type	Classification accuracies for three trials, %			
	1	2	3	Mean
Barley	90.1	89.5	90.8	90.1
CWAD	92.4	93.9	91.3	92.5
CWRS	84.2	82.7	87.0	84.6
Oats	98.2	96.7	95.3	96.7
Rye	94.2	95.0	95.5	94.9

Appendix D

CONFUSION MATRICES FOR BPN, STATISTICAL, SPNN, AND MODIFIED SPNN CLASSIFIERS

Table D.1 Confusion matrix for morphological features model using a BPN.

Types	Barley	CWAD	CWRS	Oats	Rye	Total
Barley	21709 96.48	66 0.29	0 0.00	594 2.64	131 0.58	22500 100
CWAD	83 0.37	20106 89.36	847 3.76	75 0.33	1389 6.17	22500 100
CWRS	0 0.00	326 1.45	22119 98.31	0 0.00	55 0.24	22500 100
Oats	309 1.37	210 0.93	0 0.00	21379 95.02	602 2.68	22500 100
Rye	118 0.52	1142 5.08	76 0.34	281 1.25	20883 92.81	22500 100
Total	22219 19.75	21850 19.42	23042 20.48	22329 19.85	23060 20.50	112500 100

Table D.2 Confusion matrix for morphological features model using a statistical classifier.

Types	Barley	CWAD	CWRS	Oats	Rye	Total
Barley	20960 93.16	181 0.80	6 0.02	851 3.78	502 2.23	22500 100
CWAD	73 0.32	20395 90.65	774 3.44	23 0.10	1235 5.49	22500 100
CWRS	0 0.00	621 2.76	21815 96.96	0 0.00	64 0.28	22500 100
Oats	188 0.83	533 2.37	7 0.03	20562 91.39	1210 5.37	22500 100
Rye	65 0.29	1739 7.73	37 0.17	103 0.46	20556 91.36	22500 100
Total	21286 18.92	23469 20.86	22639 20.13	21539 19.15	23567 20.95	112500 100

Table D.3 Confusion matrix for morphological features model using a SPNN.

Types	Barley	CWAD	CWRS	Oats	Rye	Total
Barley	11870	463	26	651	490	13500
	87.93	3.43	0.19	4.82	3.63	100
CWAD	51	11019	1670	86	674	13500
	0.38	81.62	12.37	0.64	4.99	100
CWRS	2	463	12951	7	77	13500
	0.01	3.43	95.93	0.05	0.57	100
Oats	174	466	13	12257	590	13500
	1.29	3.45	0.10	90.79	4.37	100
Rye	223	1125	94	232	11826	13500
	1.65	8.33	0.70	1.72	87.60	100
Total	12320	13536	14754	13233	13657	67500
	18.25	20.05	21.86	19.60	20.23	100

Table D.4 Confusion matrix for color features model using a BPN.

Types	Barley	CWAD	CWRS	Oats	Rye	Total
Barley	21105	529	24	708	134	22500
	93.80	2.35	0.11	3.15	0.60	100
CWAD	477	20909	598	169	347	22500
	2.12	92.93	2.66	0.75	1.54	100
CWRS	14	136	22278	1	71	22500
	0.06	0.60	99.01	0.00	0.32	100
Oats	516	262	20	20903	799	22500
	2.29	1.16	0.09	92.90	3.55	100
Rye	139	556	99	450	21256	22500
	0.62	2.47	0.44	2.00	94.47	100
Total	22251	22392	23019	22231	22607	112500
	19.78	19.90	20.46	19.76	20.10	100

Table D.5 Confusion matrix for color features model using a statistical classifier.

Types	Barley	CWAD	CWRS	Oats	Rye	Total
Barley	16091 71.52	1289 5.73	62 0.28	4927 21.90	131 0.58	22500 100
CWAD	2304 10.24	17792 79.07	1224 5.44	890 3.96	290 1.29	22500 100
CWRS	51 0.22	349 1.55	20766 92.29	88 0.39	1246 5.54	22500 100
Oats	3021 13.43	1419 6.31	1110 4.93	15028 66.79	1922 8.54	22500 100
Rye	282 1.25	576 2.56	1538 6.84	359 1.59	19745 87.76	22500 100
Total	21749 19.33	21425 19.05	24700 21.96	21292 18.93	23334 20.74	112500 100

Table D.6 Confusion matrix for color features model using a SPNN.

Types	Barley	CWAD	CWRS	Oats	Rye	Total
Barley	12139 89.92	809 5.99	82 0.61	197 1.46	273 2.02	13500 100
CWAD	642 4.76	10812 80.09	1593 11.80	43 0.32	410 3.04	13500 100
CWRS	71 0.53	298 2.21	12766 94.56	63 0.47	302 2.24	13500 100
Oats	962 7.13	590 4.37	329 2.44	10114 74.92	1505 11.15	13500 100
Rye	153 1.13	351 2.60	726 5.38	127 0.94	12143 89.95	13500 100
Total	13967 20.69	12860 19.05	15496 22.96	10544 15.62	14633 21.68	67500 100

Table D.7 Confusion matrix for textural features model using a BPN.

Types	Barley	CWAD	CWRS	Oats	Rye	Total
Barley	21199 94.22	248 1.10	0 0.00	1018 4.52	35 0.16	22500 100
CWAD	209 0.93	20594 91.53	1198 5.32	280 1.24	219 0.97	22500 100
CWRS	0 0.00	448 1.99	21341 94.85	77 0.34	634 2.82	22500 100
Oats	1327 5.90	500 2.22	145 0.64	20425 90.78	103 0.46	22500 100
Rye	12 0.05	254 1.13	737 3.28	89 0.40	21408 95.15	22500 100
Total	22747 20.22	22044 19.59	23421 20.82	21889 19.46	22399 19.91	112500 100

Table D.8 Confusion matrix for textural features model using a statistical classifier.

Types	Barley	CWAD	CWRS	Oats	Rye	Total
Barley	20563 91.39	599 2.66	0 0.00	1296 5.76	42 0.19	22500 100
CWAD	125 0.56	20814 92.51	1186 5.27	92 0.41	283 1.26	22500 100
CWRS	6 0.02	281 1.25	21500 95.56	1 0.00	712 3.17	22500 100
Oats	1300 5.78	513 2.28	53 0.23	20490 91.07	144 0.64	22500 100
Rye	80 0.35	321 1.43	440 1.95	21 0.09	21638 96.17	22500 100
Total	22074 19.62	22528 20.03	23179 20.6	21900 19.47	22819 20.28	112500 100

Table D.9 Confusion matrix for textural features model using a SPNN.

Types	Barley	CWAD	CWRS	Oats	Rye	Total
Barley	12001	645	56	706	92	13500
	88.90	4.78	0.41	5.23	0.68	100
CWAD	337	10960	1756	144	303	13500
	2.50	81.19	13.01	1.07	2.24	100
CWRS	10	773	11683	77	957	13500
	0.07	5.73	86.54	0.57	7.09	100
Oats	1520	774	331	10725	150	13500
	11.26	5.73	2.45	79.44	1.11	100
Rye	85	168	1035	24	12188	13500
	0.63	1.24	7.67	0.18	90.28	100
Total	13953	13320	14861	11676	13690	67500
	20.67	19.73	22.02	17.30	20.28	100

Table D.10 Confusion matrix for all features model using a BPN.

Types	Barley	CWAD	CWRS	Oats	Rye	Total
Barley	22102	58	7	318	15	22500
	98.23	0.26	0.03	1.41	0.07	100
CWAD	44	20460	1834	57	105	22500
	0.20	90.93	8.15	0.25	0.47	100
CWRS	39	210	22179	5	67	22500
	0.17	0.93	98.57	0.02	0.30	100
Oats	165	141	20	22129	45	22500
	0.73	0.63	0.09	98.35	0.20	100
Rye	10	121	36	55	22278	22500
	0.04	0.54	0.16	0.24	99.01	100
Total	22360	20990	24076	22564	22510	112500
	19.88	18.66	21.40	20.06	20.01	100

Table D.11 Confusion matrix for all features model using a statistical classifier.

Types	Barley	CWAD	CWRS	Oats	Rye	Total
Barley	19142 85.08	87 0.39	14 0.06	3042 13.52	215 0.96	22500 100
CWAD	157 0.70	19995 88.87	2237 9.94	11 0.05	100 0.45	22500 100
CWRS	12 0.05	571 2.54	21809 96.93	0 0.00	108 0.48	22500 100
Oats	391 1.74	329 1.46	205 0.91	21366 94.96	209 0.93	22500 100
Rye	221 0.98	195 0.87	251 1.12	139 0.62	21694 96.42	22500 100
Total	19923 17.71	21177 18.82	24516 21.79	24558 21.83	22326 19.85	112500 100

Table D.12 Confusion matrix for all features model using a SPNN.

Types	Barley	CWAD	CWRS	Oats	Rye	Total
Barley	12820 94.96	293 2.17	14 0.10	240 1.78	133 0.99	13500 100
CWAD	40 0.30	11908 88.21	1423 10.54	16 0.12	113 0.84	13500 100
CWRS	3 0.02	166 1.23	13302 98.53	3 0.02	26 0.19	13500 100
Oats	177 1.31	238 1.76	36 0.27	12787 94.72	262 1.94	13500 100
Rye	41 0.30	97 0.72	119 0.88	17 0.13	13226 97.97	13500 100
Total	13081 19.38	12702 18.82	14894 22.07	13063 19.35	13760 20.39	67500 100

Table D.13 Confusion matrix for combined 60 features model using a BPN.

Types	Barley	CWAD	CWRS	Oats	Rye	Total
Barley	22072 98.10	64 0.28	5 0.02	331 1.47	28 0.12	22500 100
CWAD	52 0.23	20372 90.54	1864 8.28	47 0.21	165 0.73	22500 100
CWRS	41 0.18	186 0.83	22199 98.66	5 0.02	69 0.31	22500 100
Oats	185 0.82	113 0.50	19 0.08	22132 98.36	51 0.23	22500 100
Rye	14 0.06	110 0.49	47 0.21	70 0.31	22259 98.93	22500 100
Total	22364 19.88	20845 18.53	24134 21.45	22585 20.08	22572 20.06	112500 100

Table D.14 Confusion matrix for combined 60 features model using a statistical classifier.

Types	Barley	CWAD	CWRS	Oats	Rye	Total
Barley	20328 90.35	145 0.65	7 0.03	1815 8.07	205 0.91	22500 100
CWAD	74 0.33	20315 90.29	1797 7.99	74 0.33	240 1.07	22500 100
CWRS	97 0.43	435 1.93	21837 97.05	0 0.00	131 0.58	22500 100
Oats	246 1.09	485 2.15	74 0.33	21549 95.77	146 0.65	22500 100
Rye	84 0.37	204 0.91	64 0.28	93 0.41	22055 98.02	22500 100
Total	20829 18.51	21584 19.19	23779 21.13	23531 20.92	22777 20.25	112500 100

Table D.15 Confusion matrix for combined 60 features model using a SPNN.

Types	Barley	CWAD	CWRS	Oats	Rye	Total
Barley	12682	313	15	372	118	13500
	93.94	2.32	0.11	2.76	0.87	100
CWAD	35	12010	1316	35	104	13500
	0.26	88.96	9.75	0.26	0.77	100
CWRS	8	164	13283	3	42	13500
	0.06	1.21	98.39	0.02	0.31	100
Oats	130	219	16	12950	185	13500
	0.96	1.62	0.12	95.93	1.37	100
Rye	109	106	74	37	13174	13500
	0.81	0.79	0.55	0.27	97.59	100
Total	12964	12812	14704	13397	13623	67500
	19.21	18.98	21.78	19.85	20.18	100

Table D.16 Confusion matrix for combined 30 features model using a BPN.

Types	Barley	CWAD	CWRS	Oats	Rye	Total
Barley	22038	73	5	365	19	22500
	97.95	0.32	0.02	1.62	0.08	100
CWAD	71	20271	1894	67	197	22500
	0.32	90.09	8.42	0.30	0.88	100
CWRS	23	197	22158	27	95	22500
	0.10	0.88	98.48	0.12	0.42	100
Oats	234	156	15	22005	90	22500
	1.04	0.69	0.07	97.80	0.40	100
Rye	13	237	95	98	22057	22500
	0.06	1.05	0.42	0.44	98.03	100
Total	22379	20934	24167	22562	22458	112500
	19.89	18.61	21.48	20.06	19.96	100

Table D.17 Confusion matrix for combined 30 features model using a statistical classifier.

Types	Barley	CWAD	CWRS	Oats	Rye	Total
Barley	21393 95.08	186 0.83	6 0.03	786 3.49	129 0.57	22500 100
CWAD	88 0.39	20389 90.62	1756 7.80	70 0.31	197 0.88	22500 100
CWRS	87 0.39	1114 4.95	21056 93.58	0 0.00	243 1.08	22500 100
Oats	323 1.44	564 2.51	29 0.13	21303 94.68	281 1.25	22500 100
Rye	24 0.11	279 1.24	63 0.28	51 0.22	22083 98.15	22500 100
Total	21915 19.48	22532 20.03	22910 20.36	22210 19.74	22933 20.39	112500 100

Table D.18 Confusion matrix for combined 30 features model using a SPNN.

Types	Barley	CWAD	CWRS	Oats	Rye	Total
Barley	12648 93.69	252 1.87	14 0.10	416 3.08	170 1.26	13500 100
CWAD	60 0.44	11880 88.00	1317 9.76	58 0.43	185 1.37	13500 100
CWRS	16 0.12	141 1.04	13275 98.33	3 0.02	65 0.48	13500 100
Oats	124 0.92	241 1.79	28 0.21	12798 94.80	309 2.29	13500 100
Rye	87 0.64	187 1.39	130 0.96	32 0.24	13064 96.77	13500 100
Total	12935 19.16	12701 18.82	14764 21.87	13307 19.71	13793 20.43	67500 100

Table D.19 Confusion matrix obtained using a modified SPNN.

Types	Barley	CWAD	CWRS	Oats	Rye	Total
Barley	12682 93.94	312 2.31	16 0.12	372 2.76	118 0.87	13500 100
CWAD	35 0.26	12429 92.07	897 6.64	35 0.26	104 0.77	13500 100
CWRS	8 0.06	171 1.27	13276 98.34	3 0.02	42 0.31	13500 100
Oats	130 0.96	221 1.64	14 0.10	12950 95.93	185 1.37	13500 100
Rye	109 0.81	106 0.79	74 0.55	37 0.27	13174 97.59	13500 100
Total	12964 19.21	13239 19.61	14277 21.15	13397 19.85	13623 20.18	67500 100